Spring 2026 – Systems Biology of Reproduction
Discussion Outline – Gonadal Developmental Systems Biology
Eric Nilsson – Biol 475/575
10:35-11:50 am, Tuesday & Thursday
February 19, 2026
Week 6

Gonadal Developmental Systems Biology

Primary Papers:

1. Soto and Ross (2021) Reproduction 161:239-253
2. Real, et al. (2023) J Exp Zool B Mol Dev Evol. 340(3):231-244
3. Nilsson, et al. (2013) BMC Genomics 14:496

Discussion

Student 17: Reference #1 above

- What is the technical approach?
- What specific transcriptome observations were made?
- Why is there such similarity in cow and human germline development?

Student 18: Reference# 2 above

- What are the technologies used and objectives?
- What environmental exposures were compared?
- What impacts on testis are observed in seasonal breeders?

Student 2: Reference #3 above

- What is the experimental and systems approach?
- What is a cluster analysis?
- What gene networks were identified for primordial follicle assembly?

REPRODUCTION
RESEARCH

Similarities between bovine and human germline development revealed by single-cell RNA sequencing

Delia Alba Soto and Pablo Juan Ross

Department of Animal Science, University of California, Davis, California, USA

Correspondence should be addressed to P J Ross; Email: pross@ucdavis.edu

Abstract

The germ cell lineage ensures the creation of new individuals and perpetuates the genetic information across generations. Primordial germ cells are pioneers of gametes and exist transiently during development until they differentiate into oogonia in females, or spermatogonia in males. Little is known about the molecular characteristics of primordial germ cells in cattle. By performing single-cell RNA-sequencing, quantitative real-time PCR, and immunofluorescence analyses of fetal gonads between 40 and 90 days of fetal age, we evaluated the molecular signatures of bovine germ cells at the initial stages of gonadal development. Our results indicate that at 50 days of fetal age, bovine primordial germ cells were in the early stages of development, expressing genes of early primordial germ cells, including transcriptional regulators of human germline specification (e.g. *SOX17*, *TFAP2C,* and *PRDM1*). Bovine and human primordial germ cells also share expression of *KIT*, *EPCAM*, *ITGA6*, and *PDPN* genes coding for membrane-bound proteins, and an asynchronous pattern of differentiation. Additionally, the expression of members of Notch, Nodal/Activin, and BMP signaling cascades in the bovine fetal ovary, suggests that these pathways are involved in the interaction between germ cells and their niche. Results of this study provide insights into the mechanisms involved in the development of bovine primordial germ cells and put in evidence similarities between the bovine and human germline.

Reproduction (2021) **161** 239–253

Introduction

The specification of primordial germ cells (PGCs), the progenitors of sperm and eggs, occurs around the onset of gastrulation by the inductive signaling of bone morphogenetic proteins (BMP) on a group of cells that are initially destined toward a somatic mesodermal fate (Lawson *et al.* 1999, Saitou *et al.* 2002, Kobayashi *et al.* 2017, Chen *et al.* 2019). Even though the signaling pathways that operate during PGC specification are conserved across mammals (Nikolic *et al.* 2016), the origin of the signaling molecules, the key transcriptional regulators, and their hierarchy are divergent between species (Kojima *et al.* 2017).

In mice, the period of PGC development lasts around 7 days. This process is initiated by BMP4 signaling on WNT-primed cells, which activates PRDM1 (also known as BLIMP1) and PRDM14. Together with TFAP2C, a direct target of PRDM1, these genes act in combination to induce PGC fate (Ohinata *et al.* 2005, Yamaji *et al.* 2008). The PRDM1-PRDM14-TFAP2C tripartite genetic network acts to repress the somatic mesodermal program, induce re-expression of pluripotency genes, initiate expression of PGC genes, and prompt genome-wide epigenetic reprogramming (Saitou *et al.* 2002, Yabuta *et al.* 2006, Seki *et al.* 2007); all key events involved in the specification of PGCs. After specification, PGCs follow guidance cues that will ultimately lead them to the genital anlage. Upon colonization of the undifferentiated developing gonad, PGCs undergo synchronous mitotic divisions with incomplete cytokinesis, forming nests of interconnected germ cells (Pepling & Spradling 1998). The PGC development period ends when female PGCs enter meiotic prophase or male PGCs enter mitotic quiescence (McLaren & Southee 1997). In the ovary, meiosis initiation is triggered by retinoic acid signaling which in the testis is antagonized by the cytochrome P450 activity of Sertoli cells (Bowles *et al.* 2006, Koubova *et al.* 2006).

In humans, the period of PGC development lasts around 7 weeks (from week 2 to week 9 of fetal development) (Tang *et al.* 2015). Activation of BMP signaling leads to upregulation of PRDM1, which in primates and pigs, is triggered by SOX17, a key regulator of PGC specification (Irie *et al.* 2015, Kobayashi *et al.* 2017, Kojima *et al.* 2017). BMP signaling initially upregulates TFAP2C independently from SOX17, which in combination with PRDM1 establish the gene expression program of human PGCs (Kojima *et al.* 2017). Upon specification, human PGCs migrate and colonize the genital ridge to extensively proliferate until they enter meiosis asynchronously in females (Anderson *et al.* 2007) or enter mitotic quiescence and undergo meiosis after puberty in males (Tang *et al.* 2015).

ISSN 1470–1626 (paper) 1741–7899 (online)
https://doi.org/10.1530/REP-20-0313
Online version via https://rep.bioscientifica.com

Despite the advances in mice and humans, PGC specification and development in livestock species are largely unknown. Similar to humans, the period of bovine PGC development lasts around 6 weeks (from week 2 to week 8 of fetal development) (Lavoir *et al.* 1994, Wrobel & Süß 1998). At 40 days of fetal development, the undifferentiated bovine gonad undergoes sexual differentiation, and then female germ cells initiate meiosis between 70 and 80 days of fetal age (Erickson 1966). At the molecular level, bovine PGCs are characterized by nonspecific alkaline phosphatase (AP) activity (Wrobel & Süß 1998), expression of well-conserved germline markers such as the tyrosine-kinase receptor KIT (also known as cKIT) (Kritzenberger & Wrobel 2004), and the RNA-binding proteins NANOS3 (Ideta *et al.* 2016), DDX4 (also known as VASA) (Pennetier *et al.* 2004, Bartholomew & Parks 2007, Luo *et al.* 2013) and DAZL (Hummitzsch *et al.* 2013). However, the molecular signatures that characterize the bovine germline during early gonadal development have not been elucidated, due in part to the challenges associated with studying PGCs. During their initial development, PGCs are embedded in the developing embryo in small numbers (Barton *et al.* 2016, Cantú & Laird 2017) and even though human and mice PGCs can be purified by cell sorting, antibodies to successfully target and isolate bovine PGCs are not commercially available. To overcome this limitation and elucidate the molecular signatures that characterize the bovine germline during early gonadal development, we performed single-cell RNA-sequencing (scRNA-seq), quantitative real-time PCR (RT-qPCR), and immunofluorescence analyses of fetal gonads between 40 and 90 days of age. At day 50 bovine PGCs were in early stages of development and shared with the human germline expression of transcriptional regulators and surface markers, and an asynchronous progression of differentiation.. Bovine PGCs and their somatic counterparts expressed members of the BMP, Activin/Nodal, and Notch signaling cascades, suggesting that these pathways may have roles in coordinating the events of gonad development in cattle.

Materials and methods

Tissue collection and processing

Bovine fetuses were obtained from a local abattoir and transported on ice to the laboratory within 3 h of retrieval. Fetuses were inspected for normal development and the crown-rump length (CRL) was measured to estimate gestational age (DesCôteaux *et al.* 2009). Gonads were identified based on their location within the abdominal cavity, anatomy, and relationship with neighboring organs (mesonephros and/or kidneys). Tissues retrieved for histology were fixed in 4% paraformaldehyde for 24 h at 4°C and stepwise dehydrated through an ethanol gradient and processed in a VIP Tissue Tech processor (Sakura Finetek). Tissue was then embedded in paraffin, sectioned at 5 µm thickness and stained with hematoxylin and eosin (H&E). Gonads collected for immunostaining analyses were fixed in 4% paraformaldehyde for 5 h at 4°C, washed and transferred to 30% sucrose until embedding in Tissue-Tek optimal cutting temperature (OCT) compound (4883, Sakura Finetek). Cryoblocks were sectioned at 10 µm thickness and tissue sections were stored at −20°C until staining. Gonads retrieved for scRNA-seq were washed in ice-cold PBS and slow frozen in DMEM containing 20% FBS and 10% DMSO using a freezing device (5100-0001, Thermo Scientific). Fetal ovaries and testes harvested for quantitative RT-PCR were snap-frozen in liquid nitrogen and stored at −80°C until RNA was extracted. Samples utilized in this study are listed in Table 1.

Immunofluorescence analysis

Cryosections were washed to remove the OCT compound before unmasking for 10 min in a steamer in 10 mM sodium citrate buffer, pH 6.0. Blocking was performed by incubating the tissue sections with 0.3 mM glycine and 10% normal donkey serum for 1 h, at room temperature. Tissue sections were then incubated overnight at 4°C with the following primary antibodies: anti-PRDM1 (1:50; 14-5963-80, Invitrogen), anti-OCT4 (1:500; sc-8628, Santa Cruz Biotechnology), anti-DAZL (1:500; Ab34139, Abcam), anti-DDX4 (1:500; Ab13840, Abcam). Secondary antibody incubation was performed for 1 h at room temperature and Hoechst 33342 was used for counterstaining. Tissue sections were mounted using ProLong Gold Antifade (P36934, Invitrogen) and images captured using

Table 1 List of bovine fetuses harvested for this study.

CRL (cm)	**Sex**	**Estimated fetal age** (days)	**Analysis**
2	N/A	40	H&E
2	Male	40	IMF
2.5	Male	45	IMF
3	Female	45–50	IMF
3	Male	45–50	RT-qPCR
3.5	Female	50	AP
3.5	Female	50	RT-qPCR
4	Female	50	scRNA-seq
4	Female	50	scRNA-seq
4.5	Female	50	H&E
4.5	Female	50	RT-qPCR
5.5	Female	50–60	RT-qPCR
5.5	Male	50–60	RT-qPCR
6	Female	60	IMF
6.3	Male	60	IMF & AP
8	Male	60–70	RT-qPCR
8.3	Female	60–70	RT-qPCR
11	Female	80	RT-qPCR
11	Male	80	RT-qPCR
12	Male	80	IMF & AP
14	Female	90	RT-qPCR
14	Male	90	RT-qPCR
15.5	Female	90	IMF
16	Female	90	IMF

AP, detection of alkaline phosphatase activity; CRL, crown-rump length; H&E, hematoxylin and eosin staining; IMF, immunofluorescence staining; N/A, not available; RT-qPCR, quantitative real-time PCR; scRNA-seq: single-cell RNA-sequencing.

a Leica TCS SP8STED 3X laser-scanning confocal microscope. Image processing was performed using ImageJ (v2.0.0-rc-69/1.52n). Immunostaining of mesonephros was utilized as negative control when germline-specific proteins were detected.

Alkaline phosphatase staining

Detection of AP activity was performed using the Alkaline Phosphatase Staining Kit II (00-0055; Stem-gent) adapting the manufacturer's protocol for tissue sections. Briefly, cryosections were washed in PBS supplemented with 0.05% Tween 20 and incubated with freshly prepared AP Substrate Solution (provided with the kit) in the dark at room temperature for 15 min. The reaction was stopped by washing tissue sections in PBS and stained sections were mounted in ClearMount mounting medium (MMC0112, American MasterTech). Imaging was performed using a Q Imaging camera on an Olympus BH2 microscope.

Sex determination by polymerase chain reaction

Fetuses less than 50 days of fetal age (4 cm CRL) were sexed by PCR targeting the DEAD box helicase 3 gene (*DDX3X/DDX3Y*), which allows discrimination between X and Y chromosomes based on amplicon size (Gokulakrishnan *et al.* 2012). DNA extraction was performed using the DNeasy Blood and Tissue Kit (69504, Qiagen) according to manufacturer's protocol. DNA was quantified using a NanoDrop 2000C Spectrophotometer (Thermo Scientific) and amplified using the Go Taq Hot Start Green Master Mix. Amplicons were observed by agarose gel electrophoresis stained with ethidium bromide. Genomic DNA from adult testes and ovaries were used as controls.

cDNA preparation and quantitative RT-PCR

Total RNA was extracted using the RNeasy Mini Kit (74104, Qiagen) and DNase treated with the RNase-Free DNase Set (79254, Qiagen). After extraction, RNA was quantified using the Qubit RNA BR Assay Kit (Q10211, Invitrogen) and reverse transcribed using SuperScript III Reverse Transcriptase (18080044, Invitrogen) according to the manufacturer's protocols.

Evaluation of gene expression was performed using PowerUp SYBR Green Master Mix (A25742, Applied Biosystems) on a QuantStudio 3 Real-Time PCR System (A28137, Applied Biosystems). The Primer Quest tool (Integrated DNA Technologies) was used to design primers (Table 2) spanning an exon–exon junction. Samples were run in technical duplicates and relative expression was calculated by the delta Ct method, normalizing values to the HMBS housekeeping gene. cDNA from adult testes and ovaries were used as controls.

Fetal gonad dissociation for single cell RNA-sequencing

Slow-frozen gonads from two independent replicates of approximately 50 days of fetal age (4 cm CRL) were removed from liquid nitrogen and thawed at 37°C in a water bath. Gonads were then rinsed in ice-cold PBS, minced into ~0.1 mm pieces and incubated in Collagenase Type IV (800 U/mL) (LS004186, Worthington) supplemented with DNase I (6 U/mL) (04536282001, Roche Applied Science) at 37°C in a prewarmed orbital shaker for 10 min at 150 rpm. After dissociation, the cell suspension was filtered and dead cells were removed by magnetic bead sorting using a Dead Cell Removal Kit (13009010, Miltenyi) following the manufacturer's protocol. Viable cells resuspended in 0.4% BSA were submitted on ice to the UC Davis DNA Technologies & Expression Analysis Core for library preparation and sequencing.

10× Genomics library preparation and sequencing

Cells were captured using a 10× Chromium controller targeting 10,000 cells per sample. Libraries were prepared using the Chromium Single Cell 3′ v2 chemistry for sample 1 and v3 chemistry for sample 2 according to the manufacturer's protocol. Sequencing was performed in an Illumina HiSeq 4000 platform as 150 base paired-end.

Mapping, cell quality control and downstream analyses

Demultiplexing of raw reads and mapping to the bovine reference genome (ARS-UCD1.2.96) was performed using the Cell Ranger software (v3.0.2). Reads were filtered and counted through the Cell Ranger Count pipeline. The R package Seurat (v3.1.0.9003) was used for sample integration, quality control,

Table 2 Sequence of primer sets used for qPCR.

Gene	Forward primer sequence	Reverse primer sequence	Tm (°C)	Amplicon size (bp)
DDX4	GAAGGTGATAGCTCTGGTTTCT	GTCTTGATAACCGCCTCTCTT	62	99
HMBS	CTTCACCATTGGAGCTGTCT	TAGTTCCTACCACACTCTTCTCT	62	116
NANOS3	TGTGCAGGTTCCAAAGGT	GTCTCCTTAGGCAGAAGTTGAG	62	81
PRDM1	CCACATGAATGCCAGGTTTG	TGCACTGGTAAGGTTTCTCTC	62	97
PRDM14	GGACAAGGGTGACAGGAAAT	TCCCGCATGTAGAACACTTG	62	128
POU5F1	AACGAGAATCTGCAGGAGATATG	TCTCACTCGGTTCTCGATACT	62	87
SOX2	CATTAACGGCACACTGCCCC	TGAAAATGTCTCCCCCGCCC	62	76
SOX17	AAGATGCTGGGCAAGTCG	CGGTACTTGTAGTTGGGATGG	62	116
TFAP2C	CGACATGGCACACCAGAT	GGAAATAGGACCTTTGCGAATAAC	62	94
DDX3	AGGAAGCCAGGAAAGTAA	CATCCACGTTCTAAGTCT	58	184 and 208

Tm, melting temperature.

and secondary analyses (Stuart *et al.* 2019). Quality check of datasets and cell filtering was based on 4 criteria: number of detected genes, number of unique molecular identifiers, percentage of mitochondrial genes, and percentage of ribosomal genes. Cells that passed the selection criteria (cells containing 200 to 6000 reads and <5% of mitochondrial genes) were used for downstream analysis (Supplementary Fig. 1A, see section on supplementary materials given at the end of this article). Integration and normalization of the two replicates was performed by identifying 'anchors' across datasets. Dimensionality reduction was performed by uniform manifold approximation and projection (UMAP) and differential gene expression was performed using non-parametric Wilcoxon rank sum test, which is part of the standard Seurat pipeline. Functional clustering of gene ontology (GO) term enrichment of differentially expressed genes was performed using DAVID (Huang *et al.* 2009). The integration of bovine and human data sets was performed using the human UMI count data from http://github.com/zorrodong/germcell (Li *et al.* 2017). Only female cells expressing 2000 to 10,000 genes and 100,000 to 1,100,000 transcripts were kept for integration, resulting in 970 total cells. Integration of the bovine and human datasets was also performed by the identification of 'anchors' using R package Seurat (v3.1.5.9003) (Stuart *et al.* 2019) and variations due cell cycle heterogeneity were regressed out. The identification of candidate surface marker genes was performed using the computational framework COMET (Delaney *et al.* 2019) using their stand-alone software package.

Data availability

Accession numbers for the 10×X Genomics single cell RNA-seq data that support the findings of this study are openly available at https://www.ncbi.nlm.nih.gov/geo/, GEO accession: GSE162952. Code availability of the custom scripts used can be found on GitHub at https://github.com/deliasoto/Bovine_scRNA-seq.

Results

Morphology and alkaline phosphatase activity of bovine fetal gonads

We evaluated the anatomical relationship of the developing gonad with the mesonephros between 40 and 50 days of fetal age (2–4.5 cm CRL) by H&E staining. At 40 days of fetal age (Supplementary Fig. 2A and B), the gonads were identified by their ventral location to the mesonephros, one of the biggest organs in the abdominal cavity at this stage. Around 10 days later (Supplementary Fig. 2C and D), gonads had tripled in size and grown out from the mesonephros. Similar to other mammals, bovine PGCs possess temporary AP activity that is lost upon differentiation (Gropp & Ohno 1966, Lavoir *et al.* 1994). We detected nonspecific AP activity throughout the fetal gonad in ovaries and testes (Supplementary Fig. 2E, F and G). In ovaries at 50 days of fetal age (3.5 cm CRL), AP positive cells were detected throughout the whole organ, but the surface epithelium seemed to be AP negative. In testes, positive cells in the seminiferous tubules progressively lost AP activity between 60 and 80 days of development (6-12 cm CRL), whereas somatic cells in the interstitium remained AP positive. Thus, in female and male fetal gonads, germ cells were masked by the positive AP reaction of the surrounding cells, confirming the lack of specificity of AP staining that others have described (Gropp & Ohno 1966, Lavoir *et al.* 1994, Wrobel & Süß 1998). Even though bovine fetal gonads can be easily identified after 40 days of development, AP activity is not an appropriate germ cell marker as it is unspecific and germ cells lose AP expression over time.

Single-cell RNA-sequencing of 50 days old bovine fetal ovaries

Since specific surface markers and antibodies to sort the different cell populations of the bovine fetal gonad are not available, we performed scRNA-seq on dissociated fetal gonads to capture the molecular signatures of the bovine germline and its niche. A total of 19,499 cells from two independent replicates of approximately 50 days of fetal age (4 cm CRL) were sequenced obtaining 564,587,528 sequence reads, with 64,039 and 22,332 mean reads per cell in sample 1 and 2, respectively (Supplementary Fig. 1A). After filtering out cell doublets and low-quality cells, 15,548 cells were used for clustering. We identified 11 cell clusters with all clusters being represented in each replicate (Supplementary Fig. 1B). Cluster identity was assigned based on the expression of well-conserved marker genes (Fig. 1A and B) and functional GO term enrichment (Supplementary Table 1). Cells allocated to cluster 5 were identified as PGCs based on the expression of pluripotency and germline-specific genes such as *NANOG*, *OCT4* (also known as POU5F1), *NANOS3*, and *EPCAM* (Fig. 1B and C). PGCs represented 10.8% of the cells present in the fetal gonad. Clusters 0, 1, and 2 expressed genes associated with stromal (*NR5A1* and *COL1A2)* and epithelial (*KRT19* and *MSLN*) cell populations of the fetal ovary (Jameson *et al.* 2012, Mork *et al.* 2012, Hummitzsch *et al.* 2013), and respectively represented 51.7, 20.1, 17.5% of the cells restricted to the somatic and germ cell compartment. GO analysis indicated that clusters 0, 1, and 2 showed specific enrichment for terms such as collagen and extracellular matrix, translation and cell–cell adhesion, and cell proliferation, respectively (Supplementary Table 1). Thus, we identified clusters 0, 1, and 2 as stromal cells, quiescent epithelial cells and proliferative epithelial cells, respectively (Fig. 1B and C). Clusters 3, 4, 6, 7, 8, 9, and 10 represented 29.7% of the total cells analyzed and corresponded to endothelial cells, erythrocytes,

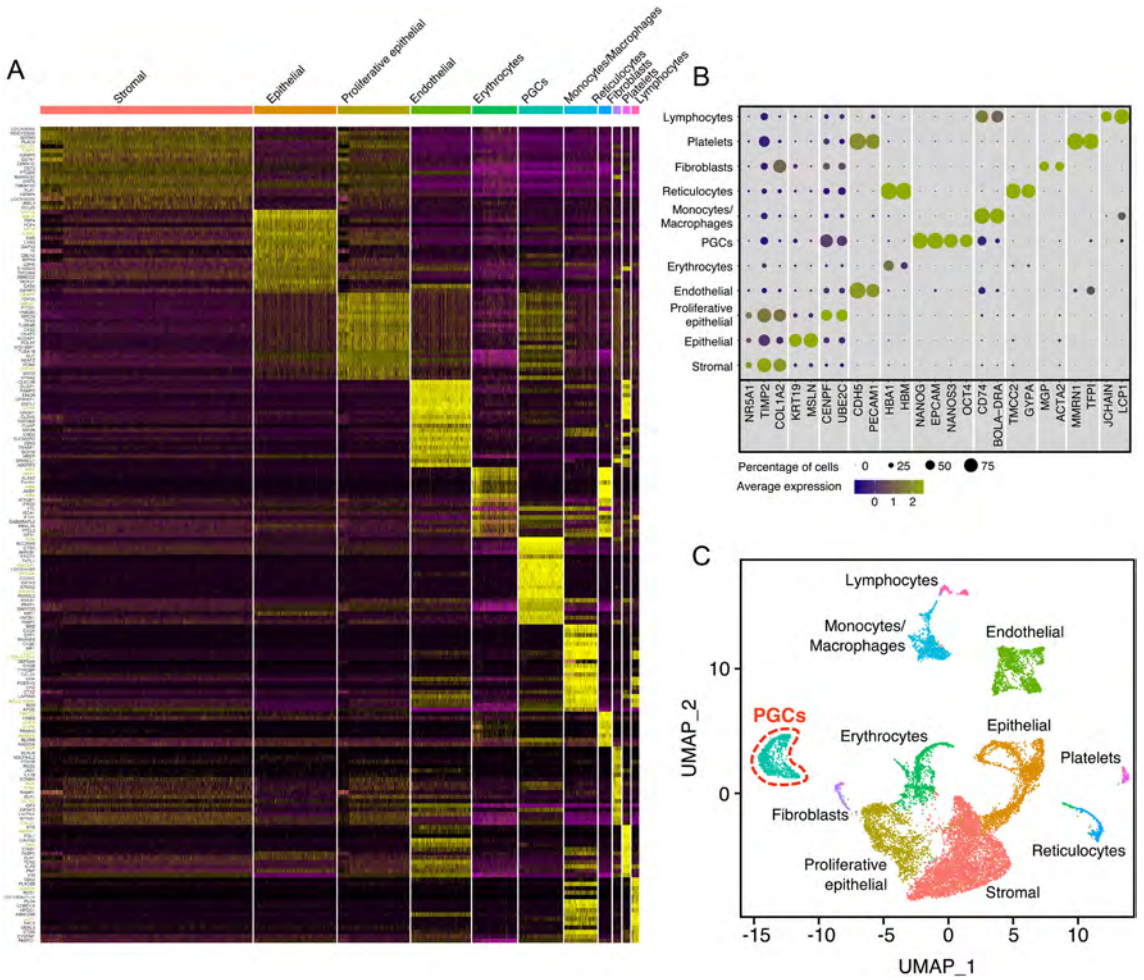

Figure 1 Cell populations detected by scRNA-seq in the bovine fetal ovary at 50 days of fetal age. (A) Heatmap of differentially expressed genes in each cell cluster. Genes used for cluster identification are colored in yellow. (B) Dot plot of the average level of expression (dot color) and percentage of positive cells (dot size) expressing specific marker genes in each cell cluster. (C) Identity of cell populations in UMAP projection.

monocytes/macrophages, reticulocytes, fibroblasts, platelets, and lymphocytes, respectively (Fig. 1C). This analysis demonstrated that different cell populations, including PGCs, can be identified in the bovine fetal gonad by scRNA-seq.

Evaluation of the gene expression profile of the somatic compartment (clusters 0, 1 and 2) (Supplementary Fig. 3) showed high expression of genes involved in the development of the genital ridge (*WT1*, *GATA4*, *SF1*, *EMX2* and *LHX9*) (Luo *et al.* 1994, Miyamoto *et al.* 1997, Birk *et al.* 2000, Hammes *et al.* 2001, Kusaka *et al.* 2010, Hu *et al.* 2013). On the other hand, genes associated with pre-granulosa cells (*LGR5*, *RSP01*, *WNT4*, *FOXL2* and *FST*) (Jorgez *et al.* 2004, Mork *et al.* 2012, Rastetter *et al.* 2014, Zheng *et al.* 2014) presented only low expression in around 5.5% of the cells. These results indicate that the somatic cells of 50 days old (4 cm CRL) bovine fetal gonads are largely undifferentiated and starting the transition toward supportive cells.

Molecular profiling of the bovine germline during early fetal development

scRNA-seq data indicated that at 50 days of fetal age (4 cm CRL) most of the cells in the PGC cluster (98.7%) expressed at least one marker of pluripotency including *OCT4* (72.5%), *NANOG* (95.2%), and *SALL4* (47.2%), or at least one marker of early PGCs development (95.5%) including *NANOS3* (80.2%), *KIT* (69%), and *AP* (57.6%). A smaller subset of cells (21.1%) expressed genes that characterize pre-meiotic late-stage PGCs including *DAZL* (6.3%), *DDX4* (16%), and *STRA8* (0.5%) (Fig. 2A and Table 3). Marker co-expression analysis showed that 76% of the cells allocated to the PGC cluster shared expression of pluripotency and early markers, with 21% also co-expressing late PGCs markers (Fig. 2B), indicating that most PGCs in day 50 fetuses are still in early stages of differentiation, with a subset of cells transitioning toward a more advanced stage.

To confirm the early stage of bovine PGCs at 50 days of fetal age (4 cm CRL) and assess the developmental

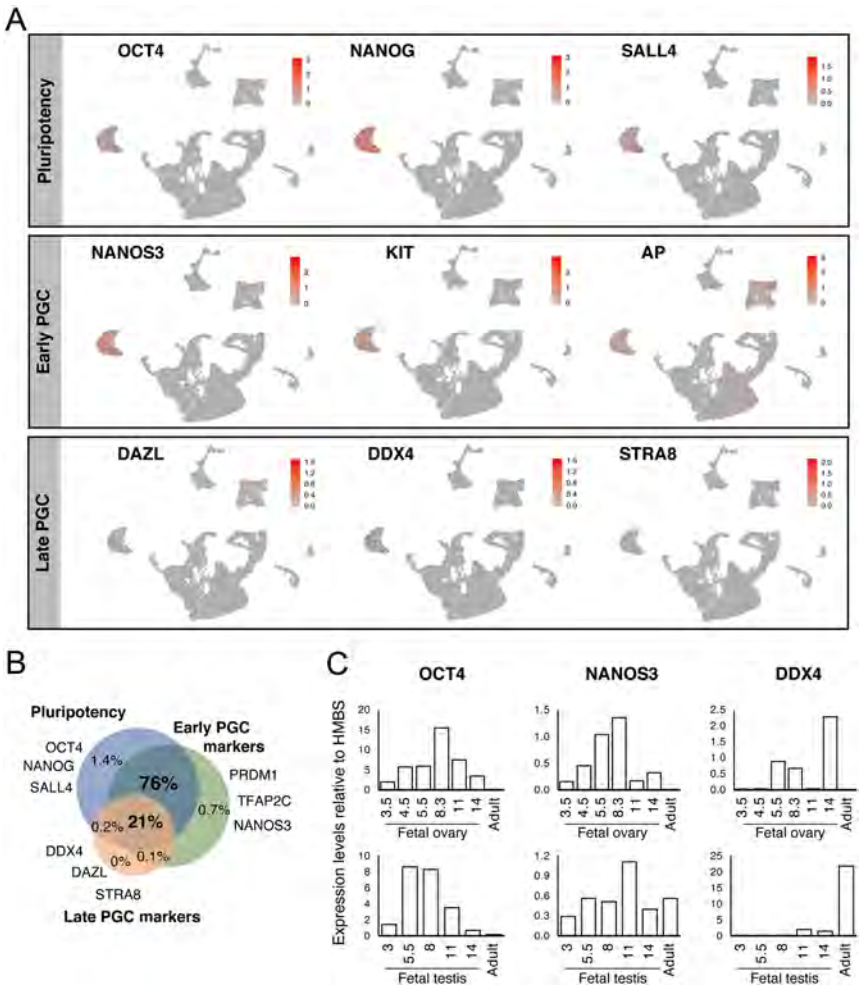

Figure 2 Gene expression profile of bovine PGCs. (A) Level of expression of pluripotency, early and late markers of PGC development in cells of the bovine gonad. (B) Venn diagram of the co-expression of pluripotency, early, and late markers of PGCs development in bovine PGCs. (C) Relative expression of *OCT4*, *NANOS3* and *DDX4* in fetal gonads between 45 and 90 days of fetal age and adult testes and ovaries. Numbers in fetal samples represent crown-rump length in cm.

timeline of the bovine germline, we analyzed expression of well-known markers of early and late PGC at different stages of development by RT-qPCR and immunofluorescence (Figs 2C and 3). Detection of *OCT4, NANOS3,* and *DDX4* in fetal gonads by RT-qPCR (Fig. 2C) corroborated the findings from scRNA-seq. *OCT4* and *NANOS3* presented a similar pattern of expression, characterized by a progressive increase during the first 2–3 months of gonad development, likely reflecting PGC proliferation. *OCT4* and *NANOS3* expression decreased after this period (Fig. 2C). *NANOS3* was not detected in adult ovaries, but was expressed in the adult testes, which is consistent with its role during spermatogenesis (Lolicato *et al.* 2008). Expression of *DDX4* increased after 50 days of development (4 cm CRL) reaching its highest expression in the adult testis (Fig. 2C). Immunofluorescence analyses (Figs 3 and 6) indicated that PRDM1 and OCT4 were equally expressed in female and male PGCs early in development (40–70 days or 2–7 cm CRL). Upon progression of differentiation, PRDM1 and OCT4 were first downregulated in males while in females their expression persisted in germ cells located at the ovarian cortex. DAZL protein was first detected at 60 days (6 cm CRL) of development and rapidly became broadly expressed in the germline, especially in males. DAZL detection persisted at 80-90 days (12–16 cm CRL), in spermatogonia and oogonia inside the seminiferous tubules and ovigerous cords, respectively. DDX4 was only detected in the fetal gonads after day 80 of fetal development (12 cm CRL), following DAZL upregulation. Overall, RT-qPCR and immunofluorescence analyses confirmed scRNA-seq results indicating that at day 50 of fetal age (4 cm CRL), bovine PGCs are mostly in early stages of development.

Similarities between bovine and human germline development

Given the early developmental stage of day 50 bovine PGCs, we evaluated the presence of known transcriptional regulators involved in human germline commitment. The signaling cascade that triggers specification of the human germline has been well studied. *PRDM1*, *PRDM14*, and *TFAP2C* form a key

Table 3 Gene expression profile of female bovine PGCs at 50 days of fetal age.

Genes	PGC cluster	
	Number of positive cells	Percentage of positive cells
Pluripotency		
OCT4	854	72.5
NANOG	1121	95.2
SALL4	556	47.2
KLF4	128	10.9
LIN28A	59	5.0
DPPA3	0	0.0
SOX2	0	0.0
Early PGCs		
PRDM1	794	67.4
PRDM14	44	3.7
TFAP2C	1006	85.4
SOX17	1116	94.7
SOX15	1008	85.6
NANOS3	945	80.2
ALPL	679	57.6
DND1	3	0.3
Late PGCs		
DDX4	188	16.0
DAZL	74	6.3
PIWIL2	23	2.0
Meiosis		
STRA8	6	0.5
SYCP1	5	0.4
SYCP2	261	22.2
SYCP3	479	40.7
REC8	29	2.5
STAG3	9	0.8
Oocyte		
NOBOX	1	0.1
FIGLA	1	0.1
ZP3	57	4.8
GDF9	4	0.3
Surface proteins		
KIT	813	69.0
EPCAM	1133	96.2
PDPN	1110	94.2
ITGA6	409	34.7

transcriptional network that commands specification of the germline in different species (Ohinata *et al.* 2005, Yamaji *et al.* 2008, Kobayashi *et al.* 2017, Sybirna *et al.* 2020). Specifically in humans, the SRY-Box proteins SOX17 and SOX15 also play an important role in germline development (Guo *et al.* 2015, Tang *et al.* 2015, Kobayashi *et al.* 2017, Kojima *et al.* 2017, Chen *et al.* 2018, 2019). Bovine PGCs expressed *PRDM1*, *TFAP2C*, *SOX17*, and *SOX15* transcription factors (Fig. 4A). *PRDM14* was only detected in a few cells, which is consistent with observations in human PGCs (Guo *et al.* 2015, Irie *et al.* 2015, Tang *et al.* 2015, Kobayashi *et al.* 2017) and *SOX2*, which is only re-activated in mouse PGCs (Western *et al.* 2005, Perrett *et al.* 2008, Campolo *et al.* 2013), was not detected. We confirmed expression of *PRDM1*, *TFAP2C*, *SOX17*, *SOX2,* and *PRDM14* by RT-qPCR in fetal gonads (Fig. 4B). Levels of *PRDM1*, *TFAP2C,* and *SOX17* increased until days 60–70 of development (approximately 8 cm CRL) and then decreased steadily. Interestingly, *PRDM14* shared a similar pattern of expression with *PRDM1*, *TFAP2C*, and *SOX17*, especially in fetal ovaries. Expression of SOX2 was almost undetectable in all the fetal samples evaluated, confirming results of scRNA-seq analysis.

Integration of our dataset with a publicly available single-cell transcriptome of human fetal gonadal cells (FGCs) of 5–26 weeks of development (Li *et al.* 2017), showed that 50 days old bovine PGCs clustered together with early human germ cells (Mitotic) (Fig. 5A). Bovine PGCs and human mitotic FGCs had a similar gene expression profile, especially for genes involved in germline specification and pluripotency, and genes that characterize early and late PGC development (Fig. 5B). Our scRNA-seq results also revealed that bovine PGCs expressed genes coding for the surface proteins *EPCAM* (96.2%), *PDPN* (94.2%), *KIT* (69%), and *ITGA6* (34.7%) (Table 3), which are also present in human FGCs (Fig. 5C) (Sasaki *et al.* 2016, Chen *et al.* 2018). These findings further confirm the similar germline-specific molecular profiles between these two species.

We performed prediction of marker panels by COMET which ranks single or multiple marker genes for identification of cell populations of interest. In line with previous results, *EPCAN, KIT* and *PDPN* appeared among the top ranked markers to identify bovine PGCs (Supplementary Fig. 4A and Supplementary Table 3). Interestingly *CD9*, which has a role during fertilization (Umeda *et al.* 2020) and is present in 99.7% of the cells in the PGC cluster and ranked the fifth best marker for PGC identification and isolation. Reliable approaches for the isolation of gonadal somatic cells could be possible using single marker genes (Supplementary Fig. 4B) or by positive and negative selection of marker pairs (Supplementary Fig. 4C).

Exploring the distribution of OCT4 and DAZL in whole ovaries from 40- to 90 day-old fetuses (Fig. 6), we found a progressive loss of OCT4 expression from the center of the ovary outwards to the periphery, while DAZL expression persisted during differentiation, as others have described (Hummitzsch *et al.* 2013). At 40 days of age, few OCT4-positive cells were detected in the ovary. OCT4-positive cells dramatically increased 20 days later and at day 90 OCT4 was only expressed in cells confined to the vicinity of the surface epithelium. Expression of DAZL was first detected at 60 days of age in cells of the medulla and ovarian cortex. DAZL-positive cells localized in the same pattern of cells expressing OCT4; in fact, all the DAZL-positive cells detected at 60 days co-expressed OCT4. Overall, the expression pattern of germline transcriptional regulators, germline-specific, pluripotency, and cell surface markers, and the asynchronous pattern of differentiation detected in the bovine germline, revealed important similarities in the development of bovine and human germ cells.

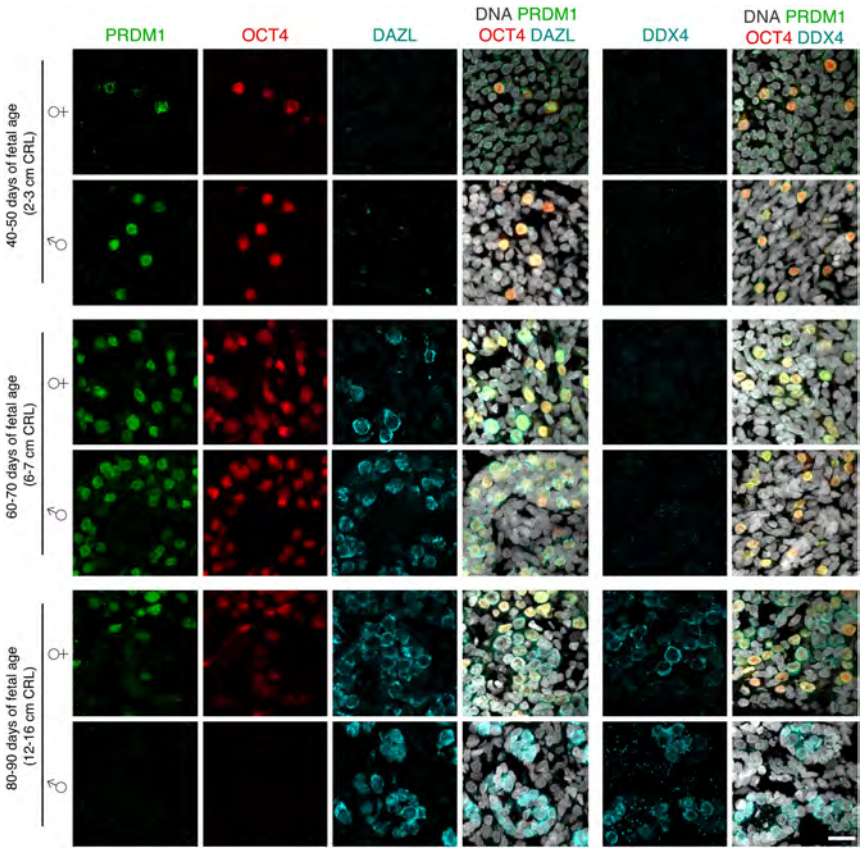

Figure 3 Expression of well-conserved germ cell markers in bovine fetal gonads. Immunofluorescence for PRDM1, OCT4, DAZL, and DDX4 in gonads from 40 to 90 days of fetal age. Nuclear staining was performed using Hoechst 33342. Scale bar 20 µm. OCT4 and PRDM1 detection was confined to the nuclei of PGCs, and DAZL and DDX4 to the cytoplasm. This is in agreement with their roles as transcriptional regulators and RNA-binding proteins, respectively.

Expression of mediators of different signaling pathways in the bovine fetal ovary

Our data confirmed that bovine PGCs express the *KIT* receptor (Kritzenberger & Wrobel 2004), while gonadal somatic cells expressed the *KIT* ligand (KITLG, also known as SCF) (Fig. 7), consistent with previous findings (reviewed by Driancourt *et al.* 2000).

It has been suggested that bone morphogenetic protein (BMP), Nodal, and Notch signaling cascades have roles in the initial development of the human germline (Li *et al.* 2017). We identified expression of *BMP2* and *BMP4* ligands in different cell populations, particularly in PGCs (Fig. 7). *BMP4* was more broadly expressed than *BMP2*, and it was among the top differentially expressed genes detected in the PGC cluster (Supplementary Table 2). Receptors (*ACVR1*, *BMPR1A*) and effector (*SMAD5)* of BMP signaling were detected in several cell groups at different levels of expression. Notably, most of the cells expressing *ACVR1*, *BMPR1A* or *SMAD5* corresponded to stromal cells, epithelial cells, and PGCs.

The *Nodal* ligand was detected only in a few PGCs, but receptors (*ACVR1C*, *ACVR2A*) and nuclear effectors (*SMAD2* and *SMAD3*) of the Nodal cascade, were present in several cell clusters with a higher number of positive cells in the stromal, epithelial, and PGC clusters. Since Nodal and Activin are both members of the TGFβ superfamily of signaling molecules, and signal through the same mediators (reviewed by Pauklin & Vallier 2015), we evaluated the expression of the subunits I*INHA*, *INHBA*, and *INHBB*) (Fig. 7) that form Activins (A, B, and AB), as well as Inhibins (A, B, and AB). We detected expression of the three Inhibin subunits in our dataset, with specific enrichment in stromal cells and epithelial cells.

Members of notch signaling members were found at varying levels of expression in many of the cell populations analyzed (Fig. 7). The Notch ligand *DLL3* was mostly detected in PGCs, and the receptors *NOTCH2*, *NOTCH3*, the effector *RBPJ* (also known as CBF1), which cooperates with Notch intracellular domain to promote transcription, and the target gene *HES1*, were abundant in stromal and/or epithelial cells. The consistent expression of mediators of KIT, BMP, Nodal/Activin, and Notch signaling in PGCs and supporting somatic cells of the bovine fetal gonad, suggest that these pathways may be involved in the interaction between bovine PGCs and their niche.

Discussion

Obtaining a pure population of PGCs for molecular profiling is challenging. Previous means used to identify bovine PGCs included AP activity, KIT expression, detection of specific lectins, and histological features. AP activity and KIT expression are unspecific methods

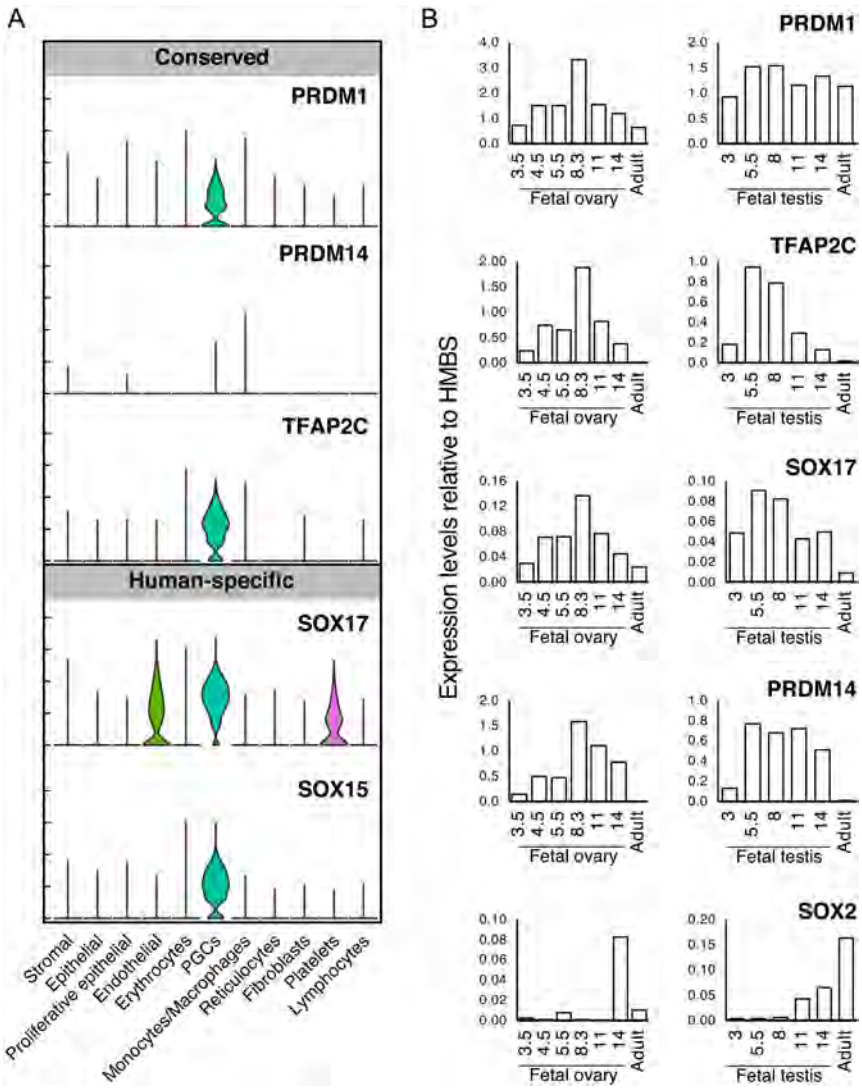

Figure 4 Expression of transcriptional regulators of germline development in bovine PGCs. (A) Violin plots of common (*PRDM1, PRDM14* and *TFAP2C*), and species-specific genes with a function in human (*SOX15* and *SOX17*) germline development. (B) Relative expression of *PRDM1*, *TFAP2C*, *SOX17*, *SOX2*, and *PRDM14* in fetal gonads between 45 and 90 days of fetal age, and adult testes and ovaries. Numbers in fetal samples represent crown-rump length in cm.

to identify germ cells, as they are also present in hematopoietic cells and gonadal somatic cells (Ohno & Gropp 1965, Lavoir *et al.* 1994, Kritzenberger & Wrobel 2004). Similar to other species, bovine PGCs have a characteristic morphology that allows their identification (Leichthammer *et al.* 1990, Wrobel & Süß 1998); however, identification of cells by morphology is impractical, considering the time required for tissue dissociation and manual cell selection. Targeting specific lectins on bovine PGCs does not offer a great advantage either, as glycan-binding antibodies have weak affinity for their target, leading to poor sensitivity (Haab 2012). DDX4 is a germline-specific marker frequently used for sorting human germ cells, but since the expression of a membrane-bound isoform of DDX4 in pre-meiotic germ cells is debatable, the use of commercially available anti-DDX4 antibodies for sorting purposes has shown conflicting outcomes (Woods & Tilly 2013, Zarate-Garcia *et al.* 2016, Wagner *et al.* 2020). Therefore, by performing scRNA-seq, we overcame the limiting step of cell sorting and obtained the transcriptional landscape of bovine PGCs and of different cell groups within the fetal ovary.

The relatively undifferentiated state of bovine PGCs captured by scRNA-seq and the positive expression of master regulators of human germline commitment suggest that the signaling network governing bovine PGC specification might be similar to what has been described in humans. Our scRNA-seq data indicated that at 50 days of fetal age, the transcriptional profile of bovine PGCs is characterized by the expression of *PRDM1*, *TFAP2C*, *SOX17*, *SOX15*, *SALL4*, *LIN28A*, *KLF4*, and *ITGA6* (Table 3), with *SOX17* being one of the top differentially expressed genes (Supplementary Table 2), and lacking *SOX2* expression (Fig. 5B). Therefore, bovine PGCs seem to possess a transcriptional network similar to human PGCs. It has been postulated that SOX17 exerts its critical function in the development of the human germline by regulating gene expression as a binding partner of OCT4 (Tang *et al.* 2016). Expression of SOX17 and SOX2 are mutually exclusive in human

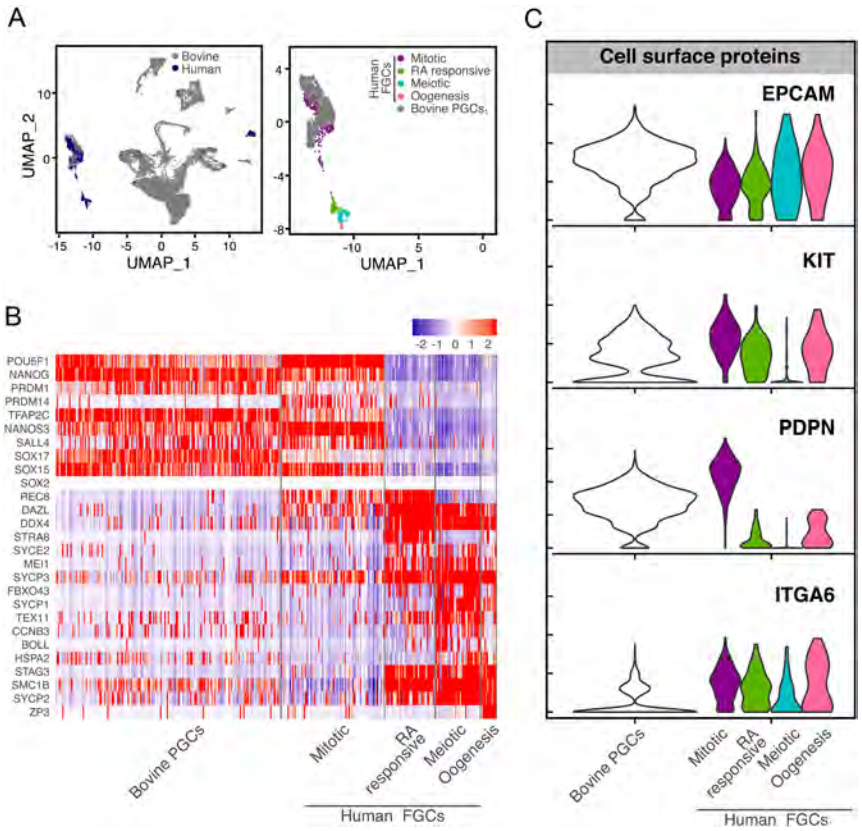

Figure 5 Similarities between bovine and human PGCs transcriptional profile. (A) Integration of scRNA-seq data from bovine (50 days) and human (5–26 weeks) fetal germ cells at different stages of differentiation (Li *et al.* 2017). (B) Comparison of the expression of germline-specific genes between bovine PGCs and human fetal germ cells (Li *et al.* 2017). (C) Expression of *EPCAM*, *KIT*, *PDPN*, and *ITGA6* genes coding for membrane-bound proteins in bovine PGCs and human fetal germ cells (Li *et al.* 2017). FGCs, fetal germ cells; RA, retinoic acid.

PGCs and downregulation of SOX2 is required for PGC-like cell differentiation *in vitro* (Lin *et al.* 2014). OCT4 switches binding partners from SOX2 to SOX17, and regulates the expression of endoderm genes during mouse primitive endoderm differentiation (Aksoy *et al.* 2013). Interestingly, targets of the SOX17-OCT4 partnership are PRDM1 and SALL4 (Aksoy *et al.* 2013), which are both also expressed in bovine PGCs (Table 3). Therefore, our data support the notion that there might be a correspondence between embryonic structure and usage of transcription factors, and that SOX17 may be critical in determining PGC fate in species that develop as bilaminar discs, such as pigs, primates and cattle (Kobayashi & Surani 2018). It will be of interest in the future to evaluate the requirement for SOX17 in the development of the bovine germline.

Unlike PRDM1, which seems to have a conserved role in PGC fate across mammals, PRDM14 function seems to be less explicit. In mouse PGCs, PRDM14 is involved in repressing the somatic program, upregulating germline-specific genes, and promoting epigenetic reprogramming (Saitou *et al.* 2002, Yabuta *et al.* 2006, Seki *et al.* 2007). Instead in human PGCs the role of PRDM14 is less understood. Since in fetal gonads PRDM14 has a cytoplasmic location (Irie *et al.* 2015) and its knockdown did not affect PGC-like cell specification (Sugawa *et al.* 2015) it has been suggested that PRDM14 is dispensable for human PGC fate. However, a recent report put in evidence the crucial role of PRDM14 in the differentiation of human PGC-like cells by inducing a rapid and comprehensive loss of endogenous PRDM14 protein (Sybirna *et al.* 2020). Thus, we compared the expression profile of *PRDM14* in bovine and human PGCs and interestingly, only a small group of bovine PGCs expressed PRDM14. This difference could be attributed to a different role of PRDM14 in bovine PGC fate, or possible to the different scRNA-seq platform used between datasets.

The transcriptome of bovine PGCs revealed the expression of genes coding for membrane-bound proteins that could be of utility for cell sorting. Besides the *KIT* receptor (Kritzenberger & Wrobel 2004), bovine PGCs also expressed *PDPN*, *EPCAM*, and *ITGA6*. Even though these markers do not seem to be specific to the germline, they may be a good alternative to the also unspecific KIT receptor, especially if they are targeted simultaneously. KIT, AP, PDPN, EPCAM, and ITGA6 have also been used to sort or quantify gonadal and *in vitro* generated germ cells in humans (Guo *et al.* 2015, Irie *et al.* 2015, Sasaki *et al.* 2015, Kobayashi *et al.* 2017, Li *et al.* 2017, Yokobayashi *et al.* 2017, Chen *et al.* 2018).

Different signaling pathways have roles in regulating the delicate interaction between PGCs and gonadal somatic cells. BMP signaling has a well-known role in determining germline fate and regulating follicular development (reviewed by Rossi *et al.* 2016). BMP4 and BMP7, secreted from theca and granulosa cells, are important for the primordial to primary follicle

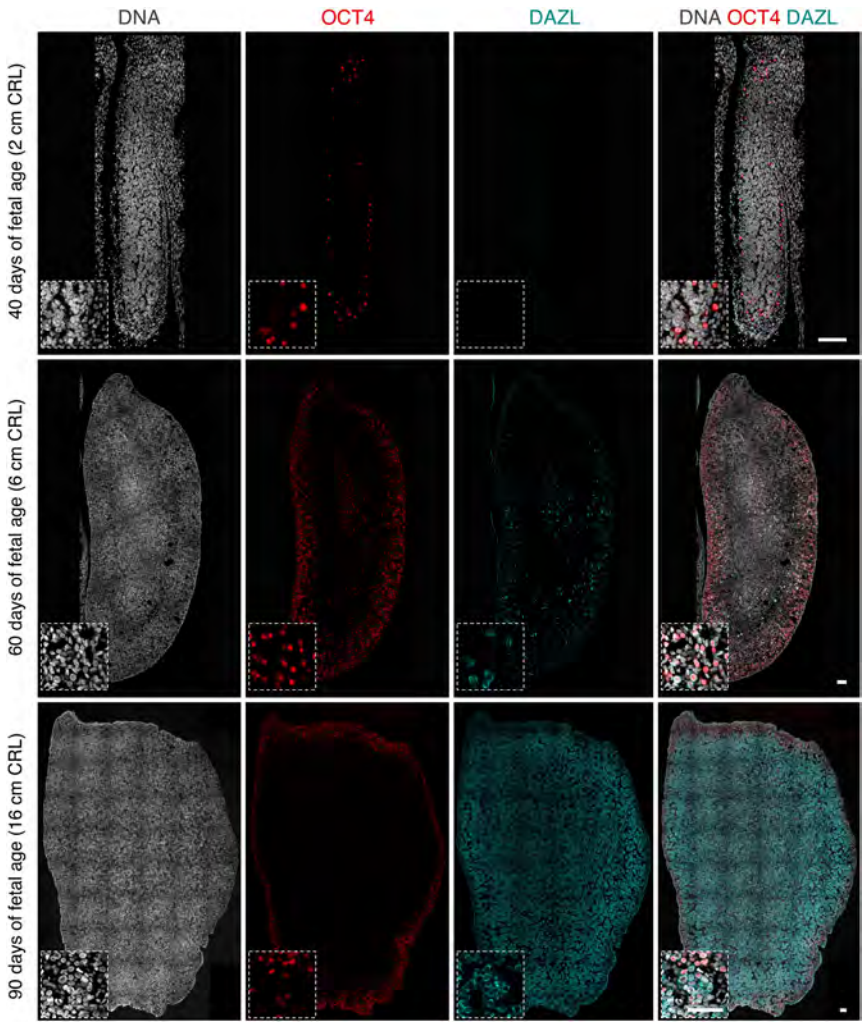

Figure 6 Expression of germ cell markers in whole bovine ovaries. Immunofluorescence for OCT4 and DAZL in the developing ovary. Histological sections were imaged at 20× and pictures were merged to inspect a complete section of the ovary. Nuclear staining was performed using Hoechst 33342. Scale bars 100 µm.

transition (Lee *et al.* 2001, Nilsson & Skinner 2003). Granulosa cells of human fetal ovaries are characterized by having high expression of BMP2, which possibly plays a role during the mitosis-meiosis transition of germ cells (Li *et al.* 2017). In the bovine fetal gonad, we detected *BMP2* and *BMP4* ligands in germ cells, and *BMP7* highly expressed in a small group of cells in the somatic compartment. Receptors and mediators of BMP signaling were present in stromal cells, epithelial cells, and PGCs. These results suggest that BMP signaling operates two-ways between PGCs and the somatic compartment in the bovine fetal ovary. Human PGCs might induce differentiation of other germ cells through activation of the Nodal/Activin signaling pathway (Li *et al.* 2017). Our results indicate that Nodal/Activin signaling may also be active in different cell populations of the fetal ovary, but mainly in stromal cells, epithelial cells, and PGCs. We hypothesize that neither Activins nor Nodal ligands are the main drivers of activation of the cascade, but rather, that Inhibins are the ligands that trigger activation of Activin/Nodal pathway in the bovine fetal ovary. Recently the role of the Notch pathway in the development of the mammalian ovary has begun to be elucidated (Vanorny & Mayo 2017). Notch activation in somatic cells of the mouse fetal ovary is required for germ cell nest breakdown, follicle assembly (Xu & Gridley 2013, Vanorny *et al.* 2014), and meiosis entry (Feng *et al.* 2014). Our scRNA-seq results show high expression of the *DLL3* ligand in PGCs, and expression of the *NOTCH2* receptor and the target gene *HES1* in somatic cells, in agreement with findings in the human fetal gonad (Li *et al.* 2017). Therefore, these results suggest that Notch signaling plays an important role during gonad development, which is conserved among the mouse, human, and cow.

Another difference between mouse and human germ cells development is the pattern by which differentiation proceeds. In the mouse fetal ovary, meiosis progresses in a rostro-caudal wave (Bowles *et al.* 2006, Koubova *et al.* 2006) while in the human fetal ovary meiosis occurs radially (Anderson *et al.* 2007). Interestingly, our data indicate similarities between the bovine and human germline in terms of spatio-temporal differentiation. In fetal ovaries, we

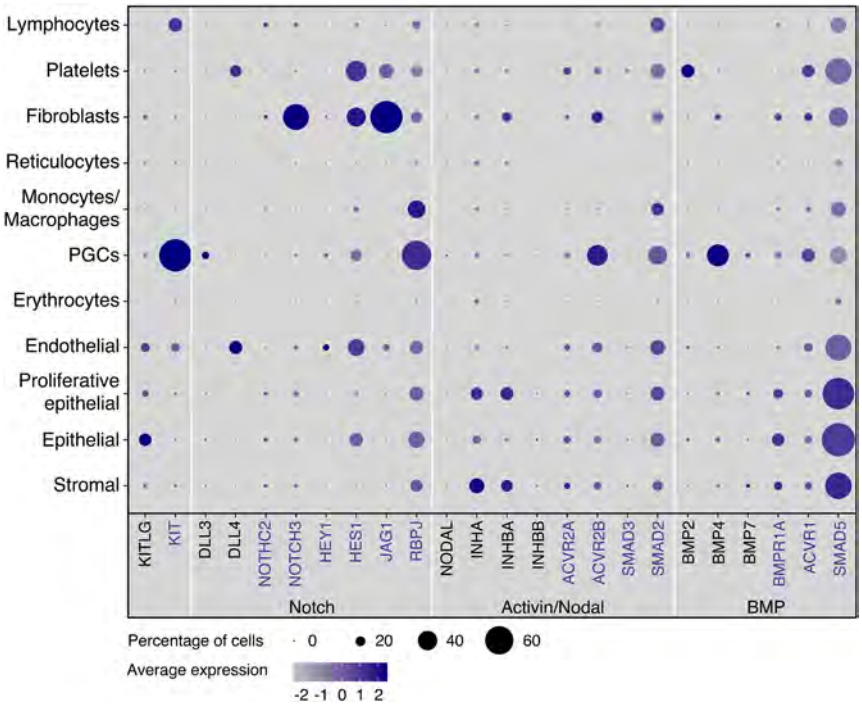

Figure 7 Gene expression of members of different signaling pathways in the bovine fetal ovary. Dot plot of the average level of expression (dot color) and percentage of positive cells in each cell cluster (dot size). Genes in black represent ligands. Genes in purple represent receptors, effectors, or targets of each signaling cascade.

detected a progressive downregulation of OCT4 from the center to the periphery. Germ cells in seminiferous tubules also progressively lost expression of OCT4, and only few OCT4-positive cells remained among DAZL/DDX4-positive cells at day 80 of development. This is in agreement with characterizations of the developing human testis, where differentiation is asynchronous and germ cells expressing early and late markers coexist inside the same seminiferous tubule (Anderson *et al.* 2007, Sohni *et al.* 2019). These results may indicate that the progression of bovine PGC differentiation is asynchronous and that germ cells at different stages of differentiation coexist in the fetal gonad, similar to what has been reported for the human ovary (Anderson *et al.* 2007).

Conclusions

Results from this work offer new insights into the mechanisms that govern gonadal and germline development in cattle. The data we report here is a useful resource to understand the different cell compartments of the developing gonad, the reciprocal relationship between germ cells and their niche, and the factors that may affect germ cell development. Further, results from this study may provide the basis for developing approaches for *in vitro* differentiation of bovine gametes from pluripotent stem cells. The similarities we found in the transcriptional profile of human and bovine PGCs confirm that mouse biology can only be partially extrapolated to other mammalian species and indicate that cattle may be a suitable model to study the specification and commitment of PGCs in humans.

Supplementary materials

This is linked to the online version of the paper at https://doi.org/10.1530/REP-20-0313.

Declaration of interest

The authors declare that there is no conflict of interest that could be perceived as prejudicing the impartiality of the research reported.

Funding

This work was supported by UC Davis Chancellor's Fellowship to P J R and USDA program W-4171 and NRSP8. D A S was supported by a doctoral scholarship from CONICYT within the funding program Becas Chile.

Author contribution statement

D A S was involved in the conception and design, performing experiments, data collection, data analysis, bioinformatics, data interpretation, and manuscript writing. P J R contributed to teh conception and design, financial support, data interpretation, and manuscript writing.

Acknowledgements

The authors thank the UC Davis DNA Tech Core for support with single cell sample preparation, Prof Anna Denicol for technical recommendations, Carly Guiltinan for proofreading and Ingrid Brust-Mascher for assistance with confocal microscopy.

References

Aksoy I, Jauch R, Chen J, Dyla M, Divakar U, Bogu GK, Teo R, Leng Ng CK, Herath W, Lili S *et al.* 2013 Oct4 switches partnering from Sox2 to Sox17 to reinterpret the enhancer code and specify endoderm. *EMBO Journal* **32** 938–953. (https://doi.org/10.1038/emboj.2013.31)

Anderson RA, Fulton N, Cowan G, Coutts S & Saunders PTK 2007 Conserved and divergent patterns of expression of DAZL, VASA and OCT4 in the germ cells of the human fetal ovary and testis. *BMC Developmental Biology* **7** 136. (https://doi.org/10.1186/1471-213X-7-136)

Bartholomew RA & Parks JE 2007 Identification, localization, and sequencing of fetal bovine VASA homolog. *Animal Reproduction Science* **101** 241–251. (https://doi.org/10.1016/j.anireprosci.2006.09.017)

Barton LJ, LeBlanc MG & Lehmann R 2016 Finding their way: themes in germ cell migration. *Current Opinion in Cell Biology* **42** 128–137. (https://doi.org/10.1016/j.ceb.2016.07.007)

Birk OS, Caslano DE, Wassif CA, Cogilatl T, Zhaos L, Zhao Y, Grinberg A, Huang SP, Kreidberg JA, Parker KL et al. 2000 The LIM homeobox gene Lhx9 is essential for mouse gonad formation. *Nature* **403** 909–913. (https://doi.org/10.1038/35002622)

Bowles J, Knight D, Smith C, Wilhelm D, Richman J, Mamiya S, Yashiro K, Chawengsaksophak K, Wilson MJ, Rossant J *et al.* 2006 Retinoid signaling determines germ cell fate in mice. *Science* **312** 596–600. (https://doi.org/10.1126/science.1125691)

Campolo F, Gori M, Favaro R, Nicolis S, Pellegrini M, Botti F, Rossi P, Jannini EA & Dolci S 2013 Essential role of Sox2 for the establishment and maintenance of the germ cell line. *Stem Cells* **31** 1408–1421. (https://doi.org/10.1002/stem.1392)

Cantú AV. & Laird DJ 2017 A pilgrim's progress: seeking meaning in primordial germ cell migration. *Stem Cell Research* **24** 181–187. (https://doi.org/10.1016/j.scr.2017.07.017)

Cao J, Spielmann M, Qiu X, Huang X, Ibrahim DM, Hill AJ, Zhang F, Mundlos S, Christiansen L, Steemers FJ *et al.* 2019 The single-cell transcriptional landscape of mammalian organogenesis. *Nature* **566** 496–502. (https://doi.org/10.1038/s41586-019-0969-x)

Chen D, Liu W, Zimmerman J, Pastor WA, Kim R, Hosohama L, Ho J, Aslanyan M, Gell JJ, Jacobsen SE *et al.* 2018 The TFAP2C-regulated OCT4 naive enhancer is involved in human germline formation. *Cell Reports* **25** 3591.e5–3602.e5. (https://doi.org/10.1016/j.celrep.2018.12.011)

Chen D, Sun N, Hou L, Kim R, Faith J, Aslanyan M, Tao Y, Zheng Y, Fu J, Liu W *et al.* 2019 Human primordial germ cells are specified from lineage-primed progenitors. *Cell Reports* **29** 4568.e5–4582.e5. (https://doi.org/10.1016/j.celrep.2019.11.083)

Delaney C, Schnell A, Cammarata LV, Yao-Smith A, Regev A, Kuchroo VK & Singer M 2019 Combinatorial prediction of marker panels from single cell transcriptomic data. *Molecular Systems Biology* **15** e9005. (https://doi.org/10.15252/msb.20199005)

DesCôteaux L, Gnemmi G & Colloton J 2009 *Practical Atlas of Ruminant and Camelid Reproductive Ultrasonography*. Ames, Iowa: Wiley-Blackwell. (https://doi.org/10.1002/9781119265818)

Driancourt MA, Reynaud K, Cortvrindt R & Smitz J 2000 Roles of KIT and KIT LIGAND in ovarian function. *Reviews of Reproduction* **5** 143–152. (https://doi.org/10.1530/ror.0.0050143)

Erickson BH 1966 Development and radio-response of the prenatal bovine ovary. *Reproduction* **11** 97–105. (https://doi.org/10.1530/jrf.0.0110097)

Feng YM, Liang GJ, Pan B, Qin XS, Zhang XF, Chen CL, Li L, Cheng SF, De Felici M & Shen W 2014 Notch pathway regulates female germ cell meiosis progression and early oogenesis events in fetal mouse. *Cell Cycle* **13** 782–791. (https://doi.org/10.4161/cc.27708)

Gokulakrishnan P, Kumar RR, Sharma BD, Mendiratta SK & Sharma D 2012 Sex determination of cattle meat by polymerase chain reaction amplification of the DEAD box protein (DDX3X/DDX3Y) gene. *Asian-Australasian Journal of Animal Sciences* **25** 733–737. (https://doi.org/10.5713/ajas.2012.12003)

Gropp A & Ohno S 1966 The presence of a common embryonic blastema for ovarian and testicular parenchymal (follicular, interstitial and tubular) cells in cattle, Bos taurus. *Zeitschrift für Zellforschung und Mikroskopische Anatomie* **74** 505–528. (https://doi.org/10.1007/BF00496841)

Guo F, Yan L, Guo H, Li L, Hu B, Zhao Y, Yong J, Hu Y, Wang X, Wei Y *et al.* 2015 The transcriptome and DNA methylome landscapes of human primordial germ cells. *Cell* **161** 1437–1452. (https://doi.org/10.1016/j.cell.2015.05.015)

Haab BB 2012 Using lectins in biomarker research: addressing the limitations of sensitivity and availability. *Proteomics: Clinical Applications* **6** 346–350. (https://doi.org/10.1002/prca.201200014)

Hammes A, Guo JK, Lutsch G, Leheste JR, Landrock D, Ziegler U, Gubler MC & Schedl A 2001 Two splice variants of the Wilms' tumor 1 gene have distinct functions during sex determination and nephron formation. *Cell* **106** 319–329. (https://doi.org/10.1016/s0092-8674(01)00453-6)

Huang da W, Sherman BT & Lempicki RA 2009 Systematic and integrative analysis of large gene lists using DAVID bioinformatics resources. *Nature Protocols* **4** 44–57. (https://doi.org/10.1038/nprot.2008.211)

Hummitzsch K, Irving-Rodgers HF, Hatzirodos N, Bonner W, Sabatier L, Reinhardt DP, Sado Y, Ninomiya Y, Wilhelm D & Rodgers RJ 2013 A new model of development of the mammalian ovary and follicles. *PLoS ONE* **8** e55578. (https://doi.org/10.1371/journal.pone.0055578)

Hu YC, Okumura LM & Page DC 2013 Gata4 Is Required for Formation of the Genital Ridge in Mice. *PLoS Genetics* **9** 1003629. (https://doi.org/10.1371/journal.pgen.1003629)

Ideta A, Yamashita S, Seki-Soma M, Yamaguchi R, Chiba S, Komaki H, Ito T, Konishi M, Aoyagi Y & Sendai Y 2016 Generation of exogenous germ cells in the ovaries of sterile NANOS3-null beef cattle. *Scientific Reports* **6** 24983. (https://doi.org/10.1038/srep24983)

Irie N, Weinberger L, Tang WWC, Kobayashi T, Viukov S, Manor YS, Dietmann S, Hanna JH & Surani MA 2015 SOX17 is a critical specifier of human primordial germ cell fate. *Cell* **160** 253–268. (https://doi.org/10.1016/j.cell.2014.12.013)

Jameson SA, Natarajan A, Cool J, DeFalco T, Maatouk DM, Mork L, Munger SC & Capel B 2012 Temporal transcriptional profiling of somatic and germ cells reveals biased lineage priming of sexual fate in the fetal mouse gonad. *PLoS Genetics* **8** e1002575. (https://doi.org/10.1371/journal.pgen.1002575)

Jorgez CJ, Klysik M, Jamin SP, Behringer RR & Matzuk MM 2004 Granulosa Cell-Specific Inactivation of Follistatin Causes Female Fertility Defects. *Molecular Endocrinology* **18** 953–967. (https://doi.org/10.1210/me.2003-0301)

Kobayashi T & Surani MA 2018 On the origin of the human germline. *Development* **145** dev150433. (https://doi.org/10.1242/dev.150433)

Kobayashi T, Zhang H, Tang WWC, Irie N, Withey S, Klisch D, Sybirna A, Dietmann S, Contreras DA, Webb R *et al.* 2017 Principles of early human development and germ cell program from conserved model systems. *Nature* **546** 416–420. (https://doi.org/10.1038/nature22812)

Kojima Y, Sasaki K, Yokobayashi S, Sakai Y, Nakamura T, Yabuta Y, Nakaki F, Nagaoka S, Woltjen K, Hotta A *et al.* 2017 Evolutionarily distinctive transcriptional and signaling programs drive human germ cell lineage specification from pluripotent stem cells. *Cell Stem Cell* **21** 517.e5–532.e5. (https://doi.org/10.1016/j.stem.2017.09.005)

Koubova J, Menke DB, Zhou Q, Cape B, Griswold MD & Page DC 2006 Retinoic acid regulates sex-specific timing of meiotic initiation in mice. *PNAS* **103** 2474–2479. (https://doi.org/10.1073/pnas.0510813103)

Kritzenberger M & Wrobel KH 2004 Histochemical in situ identification of bovine embryonic blood cells reveals differences to the adult haematopoietic system and suggests a close relationship between haematopoietic stem cells and primordial germ cells. *Histochemistry and Cell Biology* **121** 273–289. (https://doi.org/10.1007/s00418-004-0629-5)

Kusaka M, Katoh-Fukui Y, Ogawa H, Miyabayashi K, Baba T, Shima Y, Sugiyama N, Sugimoto Y, Okuno Y, Kodama R et al. 2010 Abnormal epithelial cell polarity and ectopic Epidermal Growth Factor Receptor (EGFR) expression induced in Emx2 KO Embryonic Gonads. *Endocrinology* **151** 5893–5904. (https://doi.org/10.1210/en.2010-0915)

Lavoir MC, Basrur PK & Betteridge KJ 1994 Isolation and identification of germ cells from fetal bovine ovaries. *Molecular Reproduction and Development* **37** 413–424. (https://doi.org/10.1002/mrd.1080370408)

Lawson KA, Dunn NR, Roelen BAJ, Zeinstra LM, Davis AM, Wright CVE, Korving JPWFM & Hogan BLM 1999 Bmp4 is required for the generation of primordial germ cells in the mouse embryo. *Genes and Development* **13** 424–436. (https://doi.org/10.1101/gad.13.4.424)

Lee WS, Otsuka F, Moore RK & Shimasaki S 2001 Effect of bone morphogenetic protein-7 on folliculogenesis and ovulation in the rat1. *Biology of Reproduction* **65** 994–999. (https://doi.org/10.1095/biolreprod65.4.994)

Leichthammer F, Baunack E & Brem G 1990 Behavior of living primordial germ cells of livestock in vitro. *Theriogenology* **33** 1221–1230. (https://doi.org/10.1016/0093-691X(90)90040-Z)

Li L, Dong J, Yan L, Yong J, Liu X, Hu Y, Fan X, Wu X, Guo H, Wang X *et al.* 2017 Single-cell RNA-seq analysis maps development of human germline cells and gonadal niche interactions. *Cell Stem Cell* **20** 858. e4–873.e4. (https://doi.org/10.1016/j.stem.2017.03.007)

Lin IY, Chiu FL, Yeang CH, Chen HF, Chuang CY, Yang SY, Hou PS, Sintupisut N, Ho HN, Kuo HC *et al.* 2014 Suppression of the SOX2 neural effector gene by PRDM1 promotes human germ cell fate in embryonic stem cells. *Stem Cell Reports* **2** 189–204. (https://doi.org/10.1016/j.stemcr.2013.12.009)

Lolicato F, Marino R, Paronetto MP, Pellegrini M, Dolci S, Geremia R & Grimaldi P 2008 Potential role of Nanos3 in maintaining the undifferentiated spermatogonia population. *Developmental Biology* **313** 725–738. (https://doi.org/10.1016/j.ydbio.2007.11.011)

Luo X, Ikeda Y & Parker KL 1994 A cell-specific nuclear receptor is essential for adrenal and gonadal development and sexual differentiation. *Cell* **77** 481–490. (https://doi.org/10.1016/0092-8674(94)90211-9)

Luo H, Zhou Y, Li Y & Li Q 2013 Splice variants and promoter methylation status of the bovine vasa homology (Bvh) gene may be involved in bull spermatogenesis. *BMC Genetics* **14** 58. (https://doi.org/10.1186/1471-2156-14-58)

McLaren A & Southee D 1997 Entry of mouse embryonic germ cells into meiosis. *Developmental Biology* **187** 107–113. (https://doi.org/10.1006/dbio.1997.8584)

Miyamoto N, Yoshida M, Kuratani S, Matsuo I & Aizawa S 1997 Defects of urogenital development in mice lacking Emx2. Development 124 1653–1664.

Mork L, Maatouk D, McMahon JA, Guo JJ, Zhang P, McMahon AP, McMahon JA & Capel B 2012 Temporal differences in granulosa cell specification in the ovary reflect distinct follicle fates. *Biology of Reproduction* **87** 128–128. (https://doi.org/10.1095/biolreprod.111.095208)

Nikolic A, Volarevic V, Armstrong L, Lako M & Stojkovic M 2016 Primordial germ cells: current knowledge and perspectives. *Stem Cells International* **2016** 1741072. (https://doi.org/10.1155/2016/1741072)

Nilsson EE & Skinner MK 2003 Bone morphogenetic protein-4 acts as an ovarian follicle survival factor and promotes primordial follicle development. *Biology of Reproduction* **69** 1265–1272. (https://doi.org/10.1095/biolreprod.103.018671)

Ohinata Y, Payer B, O'Carroll D, Ancelin K, Ono Y, Sano M, Barton SC, Obukhanych T, Nussenzweig M, Tarakhovsky A *et al.* 2005 Blimp1 is a critical determinant of the germ cell lineage in mice. *Nature* **436** 207–213. (https://doi.org/10.1038/nature03813)

Ohno S & Gropp A 1965 Embryological basis for germ cell chimerism in mammals. *Cytogenetics* **4** 251–261. (https://doi.org/10.1159/000129862)

Pauklin S & Vallier L 2015 Activin/nodal signalling in stem cells. *Development* **142** 607–619. (https://doi.org/10.1242/dev.091769)

Pennetier S, Uzbekova S, Perreau C, Papillier P, Mermillod P & Dalbiès-Tran R 2004 Spatio-temporal expression of the germ cell marker genes MATER, ZAR1, GDF9, BMP15,andVASA in adult bovine tissues, oocytes, and preimplantation embryos1. *Biology of Reproduction* **71** 1359–1366. (https://doi.org/10.1095/biolreprod.104.030288)

Pepling ME & Spradling AC 1998 Female mouse germ cells form synchronously dividing cysts. *Development* **125** 3323–3328.

Perrett RM, Turnpenny L, Eckert JJ, O'Shea M, Sonne SB, Cameron IT, Wilson DI, Meyts ER-D & Hanley NA 2008 The early human germ cell lineage does not express SOX2 during in vivo development or upon in vitro culture1. *Biology of Reproduction* **78** 852–858. (https://doi.org/10.1095/biolreprod.107.066175)

Rastetter RH, Bernard P, Palmer JS, Chassot AA, Chen H, Western PS, Ramsay RG, Chaboissier MC & Wilhelm D 2014 Marker genes identify three somatic cell types in the fetal mouse ovary. *Developmental Biology* **394** 242–252. (https://doi.org/10.1016/j.ydbio.2014.08.013)

Rossi RODS, Costa JJN, Silva AWB, Saraiva MVA, Van Den Hurk R & Silva JRV 2016 The bone morphogenetic protein system and the regulation of ovarian follicle development in mammals. *Zygote* **24** 1–17. (https://doi.org/10.1017/S096719941400077X)

Saitou M, Barton SC & Surani MA 2002 A molecular programme for the specification of germ cell fate in mice. *Nature* **418** 293–300. (https://doi.org/10.1038/nature00927)

Sasaki K, Yokobayashi S, Nakamura T, Okamoto I, Yabuta Y, Kurimoto K, Ohta H, Moritoki Y, Iwatani C, Tsuchiya H *et al.* 2015 Robust in vitro induction of human germ cell fate from pluripotent stem cells. *Cell Stem Cell* **17** 178–194. (https://doi.org/10.1016/j.stem.2015.06.014)

Sasaki K, Nakamura T, Okamoto I, Yabuta Y, Iwatani C, Tsuchiya H, Seita Y, Nakamura S, Shiraki N, Takakuwa T *et al.* 2016 The germ cell fate of cynomolgus monkeys is specified in the nascent amnion. *Developmental Cell* **39** 169–185. (https://doi.org/10.1016/j.devcel.2016.09.007)

Seki Y, Yamaji M, Yabuta Y, Sano M, Shigeta M, Matsui Y, Saga Y, Tachibana M, Shinkai Y & Saitou M 2007 Cellular dynamics associated with the genome-wide epigenetic reprogramming in migrating primordial germ cells in mice. *Development* **134** 2627–2638. (https://doi.org/10.1242/dev.005611)

Sohni A, Tan K, Song HW, Burow D, de Rooij DG, Laurent L, Hsieh TC, Rabah R, Hammoud SS, Vicini E *et al.* 2019 The neonatal and adult human testis defined at the single-cell level. *Cell Reports* **26** 1501.e4–1517.e4. (https://doi.org/10.1016/j.celrep.2019.01.045)

Stuart T, Butler A, Hoffman P, Hafemeister C, Papalexi E, Mauck WM, Hao Y, Stoeckius M, Smibert P & Satija R 2019 Comprehensive integration of single-cell data. *Cell* **177** 1888.e21–1902.e21. (https://doi.org/10.1016/j.cell.2019.05.031)

Sugawa F, Araúzo Bravo MJ, Yoon J, Kim KP, Aramaki S, Wu G, Stehling M, Psathaki OE, Hübner K & Schöler HR 2015 Human primordial germ cell commitment in vitro associates with a unique PRDM14 expression profile. *EMBO Journal* **34** 1009–1024. (https://doi.org/10.15252/embj.201488049)

Sybirna A, Tang WWC, Pierson Smela M, Dietmann S, Gruhn WH, Brosh R & Surani MA 2020 A critical role of PRDM14 in human primordial germ cell fate revealed by inducible degrons. *Nature Communications* **11** 1282. (https://doi.org/10.1038/s41467-020-15042-0)

Tang WWC, Dietmann S, Irie N, Leitch HG, Floros VI, Bradshaw CR, Hackett JA, Chinnery PF & Surani MA 2015 A unique gene regulatory network resets the human germline epigenome for development. *Cell* **161** 1453–1467. (https://doi.org/10.1016/j.cell.2015.04.053)

Tang WWC, Kobayashi T, Irie N, Dietmann S & Surani MA 2016 Specification and epigenetic programming of the human germ line. *Nature Reviews: Genetics* **17** 585–600. (https://doi.org/10.1038/nrg.2016.88)

Umeda R, Satouh Y, Takemoto M, Nakada-Nakura Y, Liu K, Yokoyama T, Shirouzu M, Iwata S, Nomura N, Sato K *et al.* 2020 Structural insights into tetraspanin CD9 function. *Nature Communications* **11** 1606. (https://doi.org/10.1038/s41467-020-15459-7)

Vanorny DA & Mayo KE 2017 The role of Notch signaling in the mammalian ovary. *Reproduction* **153** R187–R204. (https://doi.org/10.1530/REP-16-0689)

Vanorny DA, Prasasya RD, Chalpe AJ, Kilen SM & Mayo KE 2014 Notch signaling regulates ovarian follicle formation and coordinates follicular growth. *Molecular Endocrinology* **28** 499–511. (https://doi.org/10.1210/me.2013-1288)

Wagner M, Yoshihara M, Douagi I, Damdimopoulos A, Panula S, Petropoulos S, Lu H, Pettersson K, Palm K, Katayama S *et al.* 2020 Single-cell analysis of human ovarian cortex identifies distinct cell populations but no oogonial stem cells. *Nature Communications* **11** 1147. (https://doi.org/10.1038/s41467-020-14936-3)

Western P, Maldonado-Saldivia J, van den Bergen J, Hajkova P, Saitou M, Barton S & Surani MA 2005 Analysis of Esg1 expression in pluripotent cells and the germline reveals similarities with Oct4 and Sox2 and differences between human pluripotent cell lines. *Stem Cells* **23** 1436–1442. (https://doi.org/10.1634/stemcells.2005-0146)

Woods DC & Tilly JL 2013 Isolation, characterization and propagation of mitotically active germ cells from adult mouse and human ovaries. *Nature Protocols* **8** 966–988. (https://doi.org/10.1038/nprot.2013.047)

Wrobel KH & Süß F 1998 Identification and temporospatial distribution of bovine primordial germ cells prior to gonadal sexual differentiation. *Anatomy and Embryology* **197** 451–467. (https://doi.org/10.1007/s004290050156)

Xu J & Gridley T 2013 Notch2 is required in somatic cells for breakdown of ovarian germ-cell nests and formation of primordial follicles. *BMC Biology* **11** 13. (https://doi.org/10.1186/1741-7007-11-13)

Yabuta Y, Kurimoto K, Ohinata Y, Seki Y & Saitou M 2006 Gene expression dynamics during germline specification in mice identified by quantitative single-cell gene expression profiling1. *Biology of Reproduction* **75** 705–716. (https://doi.org/10.1095/biolreprod.106.053686)

Yamaji M, Seki Y, Kurimoto K, Yabuta Y, Yuasa M, Shigeta M, Yamanaka K, Ohinata Y & Saitou M 2008 Critical function of Prdm14 for the establishment of the germ cell lineage in mice. *Nature Genetics* **40** 1016–1022. (https://doi.org/10.1038/ng.186)

Yokobayashi S, Okita K, Nakagawa M, Nakamura T, Yabuta Y, Yamamoto T & Saitou M 2017 Clonal variation of human induced pluripotent stem cells for induction into the germ cell fate. *Biology of Reproduction* **96** 1154–1166. (https://doi.org/10.1093/biolre/iox038)

Zarate-Garcia L, Lane SIR, Merriman JA & Jones KT 2016 FACS-sorted putative oogonial stem cells from the ovary are neither DDX4-positive nor germ cells. *Scientific Reports* **6** 27991. (https://doi.org/10.1038/srep27991)

Zheng W, Zhang H, Gorre N, Risal S, Shen Y & Liu K 2014 Two classes of ovarian primordial follicles exhibit distinct developmental dynamics and physiological functions. *Human Molecular Genetics* **23** 920–928. (https://doi.org/10.1093/hmg/ddt486)

Received 5 June 2020
First decision 8 July 2020
Revised manuscript received 11 November 2020
Accepted 1 December 2020

Received: 29 October 2021 | Revised: 22 March 2022 | Accepted: 9 April 2022

DOI: 10.1002/jez.b.23142

RESEARCH ARTICLE

JEZ-B MOLECULAR AND DEVELOPMENTAL EVOLUTION WILEY

Cell adhesion and immune response, two main functions altered in the transcriptome of seasonally regressed testes of two mammalian species

Francisca M. Real[1,2] | Miguel Lao-Pérez[1] | Miguel Burgos[1] | Stefan Mundlos[2] | Darío G. Lupiáñez[3] | Rafael Jiménez[1] | Francisco J. Barrionuevo[1]

[1]Departamento de Genética e Instituto de Biotecnología, Lab. 127, Centro de Investigación Biomédica, Universidad de Granada, Granada, Spain

[2]RG Development & Disease, Max Planck Institute for Molecular Genetics, Berlin, Germany

[3]Epigenetics and Sex Development Group, Max-Delbrück Center for Molecular Medicine, Berlin Institute for Medical Systems Biology, Berlin, Germany

Correspondence
Rafael Jiménez and Francisco J. Barrionuevo, Departamento de Genética e Instituto de Biotecnología, Centro de Investigación Biomédica, Universidad de Granada, Avenida del Conocimiento S/N, Granada 18016, Spain.
Email: rjimenez@ugr.es and fjbarrio@go.ugr.es

Funding information
Consejería de Economía, Conocimiento, Empresas y Universidad, Junta de Andalucía, Grant/Award Number: BIO109; Helmholtz-Gemeinschaft, Grant/Award Number: ERC-RA-0033; Deutsche Forschungsgemeinschaft, Grant/Award Numbers: MU 880/15-1, MU 880/27-1; Secretaría de Estado de Investigación, Desarrollo e Innovación, Grant/Award Number: CGL-2015-67108-P

Abstract

In species with seasonal breeding, male specimens undergo substantial testicular regression during the nonbreeding period of the year. However, the molecular mechanisms that control this biological process are largely unknown. Here, we report a transcriptomic analysis on the Iberian mole, *Talpa occidentalis*, in which the desquamation of live, nonapoptotic germ cells is the major cellular event responsible for testis regression. By comparing testes at different reproductive states (active, regressing, and inactive), we demonstrate that the molecular pathways controlling the cell adhesion function in the seminiferous epithelium, such as the MAPK, ERK, and TGF-β signaling, are altered during the regression process. In addition, inactive testes display a global upregulation of genes associated with immune response, indicating a selective loss of the "immune privilege" that normally operates in sexually active testes. Interspecies comparative analyses using analogous data from the Mediterranean pine vole, a rodent species where testis regression is controlled by halting meiosis entry, revealed a common gene expression signature in the regressed testes of these two evolutionary distant species. Our study advances in the knowledge of the molecular mechanisms associated to gonadal seasonal breeding, highlighting the existence of a conserved transcriptional program of testis involution across mammalian clades.

KEYWORDS
cell adhesion, immune response, *Microtus duodecimcostatus*, seasonal reproduction, seasonal testis regression, *Talpa occidentalis*, testis transcriptome

Francisca M. Real and Miguel Lao-Pérez should be considered joint first author. Rafael Jiménez and Francisco J. Barrionuevo should be considered joint senior author.

1 | INTRODUCTION

In temperate zones of the Earth, most species reproduce during the season that offers the best conditions for breeding success. In the transition period between the reproductive and the nonreproductive seasons, the gonads of both sexes undergo substantial changes, whose nature is species-specific (Jiménez et al., 2015). In females, ovaries entry in anoestrus (Das & Khan, 2010) and sexual receptivity is either reduced or abolished, as shown in the musk shrew, *Suncus murinus* (Temple, 2004). In males of several species, a process of testis regression takes place by which gonad volume is remarkably reduced and spermatogenesis is arrested, as described in the Syriam hamster, *Mesocricetus auratus* (Martínez-Hernández et al., 2020; Seco-Rovira et al., 2015), the black bear, *Ursus americanus* (Tsubota et al., 1997), the Iberian mole, *Talpa occidentalis* (Dadhich et al., 2010, 2013), the large hairy armadillo *Chaetophractus villosus* (Luaces et al., 2013), the wood mouse, *Apodemus sylvaticus* (Massoud et al., 2021), and the Mediterranean pine vole, *Microtus duodecimcostatus* (Lao-Pérez et al., 2021), among others.

Seasonal breeding relies on circannual modulations of the main regulator of the reproductive system, the hypothalamic–pituitary–gonadal (HPG) axis. In sexually active males the gonadotropin-releasing hormone, GnRH, which is secreted by the hypothalamus, induces the hypophysis (pituitary) to produce and secrete gonadotropic hormones (luteinizing hormone, LH, and follicle-stimulating hormone, FSH) which, in turn, activates both the production of steroids by Leydig cells and the spermatogenic cycle. Environmental cues modulate the function of this axis, being the photoperiod by far the best known, although other factors, such as food and water availability, stress, and weather, can either modify or even overcome the influence of photoperiod (Bronson & Heideman, 1994; Martin et al., 1994; Nelson et al., 1995). In the nonreproductive season, these environmental cues alter the levels of HPG axis hormones, resulting in reduced levels of serum gonadotropins and circulating testosterone, leading to alterations of the spermatogenic cycle and, most frequently, to a halt in gamete production (Dardente et al., 2016).

For many years, germ cell apoptosis was considered to be the only cellular process responsible for germ cell depletion during seasonal testis regression (Pastor et al., 2011; Young & Nelson, 2001). However, more recently, alternative mechanisms have been reported, including germ cell desquamation (sloughing, detachment) (Dadhich et al., 2013; Luaces et al., 2014; Massoud et al., 2018), a combination of apoptosis and autophagy (González et al., 2018), and germ cell de-differentiation (Liu et al., 2016). Despite this, the genetic control of these testicular changes is poorly understood and insufficiently investigated. Expression profiling studies provide both an integrated view of the interacting molecular pathways operating in the testis and relevant information about which of them are altered during seasonal testis regression. The transcription profile of active and inactive testes of seasonal breeding males have been studied in some few mammalian species using either microarray, as in the Syriam hamster, *M. auratus* (Maywood et al., 2009) or RNA-seq technology, as in the European beaver, *Castor fiber* (Bogacka et al., 2017), the plateau pika, *Ochotona curzoniae* (X. Wang, Adegoke, et al., 2019; Y.-J. Wang, Jia, et al., 2019), and the Mediterranean pine vole, *M. duodecimcostatus* (Lao-Pérez et al., 2021). However, the number and identity of the deregulated genes vary substantially from study to study, a fact that might reflect gene expression differences among species, but it is also likely that these differences are due to the use of distinct profiling technologies and/or bioinformatic analysis. For instance, no data normalization was done in these studies to prevent over-representation of meiotic and postmeiotic germ-cell specific transcripts in the testes of active males (these cell types are absent in the inactive testes). In fact, these disproportionate gene expression differences between active and inactive testes are derived from their different cell contents and do not reflect regulatory changes related to seasonal testis regression. Hence, data must be normalized as these large differences would mask functionally relevant changes in gene expression produced in somatic cells, mainly Sertoli cells (SCs), which do actually regulate the spermatogenic cycle. More species have to be investigated to identify evolutionarily conserved transcriptomic alterations related to seasonal testis regression.

The Iberian mole, *T. occidentalis*, develop sexual features that are unique among mammals, as females consistently develop bilateral ovotestes (gonads with both ovarian and testicular tissue) instead of normal ovaries (Barrionuevo et al., 2004; Jimenez et al., 1993). In addition, moles are strict seasonal breeders. In southern Iberian Peninsula, reproduction occurs during the autumn-winter period (October–March) whereas spring-summer (April–September) is the quiescence season. In summer, circulating testosterone levels are reduced and the regressed (inactive) testis shrinks to one-fourth of their winter volume and mass. This testis regression is mediated by desquamation of live, nonapoptotic germ cells occurring in spring (April–May). In the regressed testes, spermatogonia continue entering meiosis, but spermatogenesis does not progress beyond the primary spermatocyte stage (pachytene), as meiotic cells are eliminated by apoptosis. Also, the expression and distribution of the cell-adhesion molecules in the seminiferous epithelium are altered, and the blood-testis barrier (BTB) becomes permeable (Dadhich et al., 2010, 2011, 2013).

We have recently sequenced and annotated the genome of *T. occidentalis*, shedding light on the genomic changes and molecular adaptations that lead to female ovotestis formation (Real et al., 2020). Using this resource, we have now explored the genetic control of the changes that the testis of the Iberian mole undergoes during the process of testicular regression. By performing a transcriptomic analysis of active, regressing, and inactive testes, we demonstrate that pathways such as extracellular matrix organization and cell junction assembly are derregulated during testis regression, as well as the molecular pathways that control these processes during normal testicular function, mainly the MAPK signaling pathway. We also found that inactive testes have lost the "immune privilege" (reduced immune response) that operates normally in active testes. Finally, we performed an inter-species comparative analysis against analogous

datasets we reported for the Mediterranean pine vole (Lao-Pérez et al., 2021), finding that a large number of genes are commonly deregulated in the inactive testes of both species. These genes are enriched in pathways such as the MAPK and regulation of the immune response, indicating the existence of common molecular mechanisms operating in the regressed testes of seasonal breeding mammals.

2 | RESULTS

2.1 | The expression of genes controlling cell adhesion and immune response is altered in the regressed testes of *T. occidentalis*

As we reported previously (Dadhich et al., 2010, 2013), the testes of Iberian mole males captured in the breeding period (autumn and winter) were four times larger than those of males captured in the nonbreeding period (spring and summer; Figure 1a). These inactive testes contained seminiferous tubules very reduced in diameter and lacked a well-developed germinative epithelium, as spermatogenesis was arrested at the primary spermatocyte stage (Supporting Information: Figure S1). To find differences in gene expression, we performed RNA-seq on active and inactive testes of *T. occidentalis*. Multidimensional scaling plot showed that replicate samples of the same breeding season clustered together, indicating consistent differences in the testis transcriptome between the breeding and the nonbreeding periods (Supporting Information: Figure S2). Before normalization for differences in germ cell contents between active and inactive testes, differential expression analysis of RNA-seq data revealed 7049 differentially expressed genes (DEGs) between the two breeding periods, from which 3365 were upregulated (up-DEGs) and 3684 downregulated (down-DEGs) in the regressed testes (FDR < 0.05 and $|\log_2 FC| > 1$; Supporting Information: Figure S3; Supporting Information: Table S1). GO analysis of these DEGs showed a significant enrichment (Padjust < 0.05) in a number of categories, many of them associated to biological processes occurring during spermatogenesis and spermiogenesis, including "cilium organization" (GO:0044782; Padjust = 1.9×10^{-6}), "microtubule-based movement" (GO:0007018; Padjust = 8×10^{-4}), spermatogenesis (GO:0007283; Padjust = 1.7×10^{-3}), and "sperm motility" (GO:0097722; Padjust = 6.8×10^{-3}) among others (Supporting Information: Figure S3; Supporting Information: Table S2). These results evidence the need for a normalization of the data, as most of these GO terms are related to cell contents differences between active and inactive testes, rather than to actual gene expression alterations during testis regression. After normalization, the distance between active and inactive samples was reduced in the multidimensional scaling plot (Supporting Information: Figure S2), indicating that our approach removed in fact differences derived from the distinct germ cell contents between active and inactive testes. In the normalized set of genes, we identified 4327 DEGs, from which 2055 were up-DEGs and 2272 were down-DEGs (Figure 1b; Supporting Information: Table S3). GO analysis of DEGs and down-DEGs showed very few significant categories (Padjust < 0.05; Supporting Information: Tables S4 and S5). In contrast, for the up-DEGs, we found terms related to the cell adhesion function of the seminiferous epithelium, including "regulation of cell adhesion" (GO:0030155; Padjust = 2×10^{-4}), "extracellular matrix organization" (GO:0030198; Padjust = 3×10^{-4}), "cell junction assembly" (GO:0034329; Padjust = 2.9×10^{-3}), and "cell-matrix adhesion" (GO:0007160; Padjust = 3×10^{-2}), among others (Figure 1c; Supporting Information: Table S6). We next searched for enriched GO terms related to molecular pathways and we found several GO terms related to SC signaling involved in the regulation of spermatogenesis and BTB dynamics, including "MAPK cascade" (GO:0000165; Padjust = 4×10^{-3}) (Ni et al., 2019) "positive regulation of small GTPase mediated signal transduction" (GO:0051057; Padjust = 3×10^{-2}; Lui et al., 2003a), "ERK1 and ERK2 cascade" (GO:0070371, Padjust = 2×10^{-3}; Zhang et al., 2014), "regulation of cytosolic calcium ion concentration" (GO:0051480; Padjust = 2×10^{-2}; Gorczynska & Handelsman, 1995), "response to transforming growth factor beta" (GO:0071559; Padjust = 9×10^{-3}; Ni et al., 2019), "Notch signaling pathway" (GO:0007219; Padjust = 1×10^{-3}; Garcia et al., 2013), and "canonical Wnt signaling pathway" (GO:0060070; Padjust = 4×10^{-2}; X. Wang, Adegoke, et al., 2019; Y.-J. Wang, Jia, et al., 2019) (Figure 1c; Supporting Information: -Table S6). Gene-concept analysis using these data resulted in a large network in which MAPK/ERK1/2 signaling occupied a central position sharing many genes with the other molecular pathways and with the biological process "cell-cell adhesion" (Figure 1d).

The GO analysis of up-DEGs also revealed an enrichment of genes participating in the immune response (Figure 1c; Supporting Information: Table S6) including "positive regulation of NF-kappaB transcription factor activity" (GO:0051092; Padjust = 2×10^{-3}), "macrophage activation" (GO:0042116; Padjust = 1×10^{-2})," response to tumor necrosis factor" (GO:0034612; Padjust = 4×10^{-2}), "positive regulation of leukocyte activation" (GO:0002696; Padjust = 3.9×10^{-2}), "regulation of inflammatory response" (GO:0050727; 1.6×10^{-3}), and "response to cytokine" (GO:0034097; Padjust = 3×10^{-8}). Gene-concept analysis using these data generated a network in which both TNF and NF-Kappa signaling share many genes with biological processes involved in the activation of the immune system (Figure 1e).

2.2 | Transcriptome alterations at the onset of testis regression in *T. occidentalis*

Our previous analysis revealed that several molecular pathways are altered in inactive testes when compared to the active ones. However, as these stages represent end-points of the activation-regression cycle, the results might not be indicative of the biological processes that are causative of testis regression. In the population we investigated, males of the Iberian mole undergo testis regression during the months of March and April, when seminiferous tubules

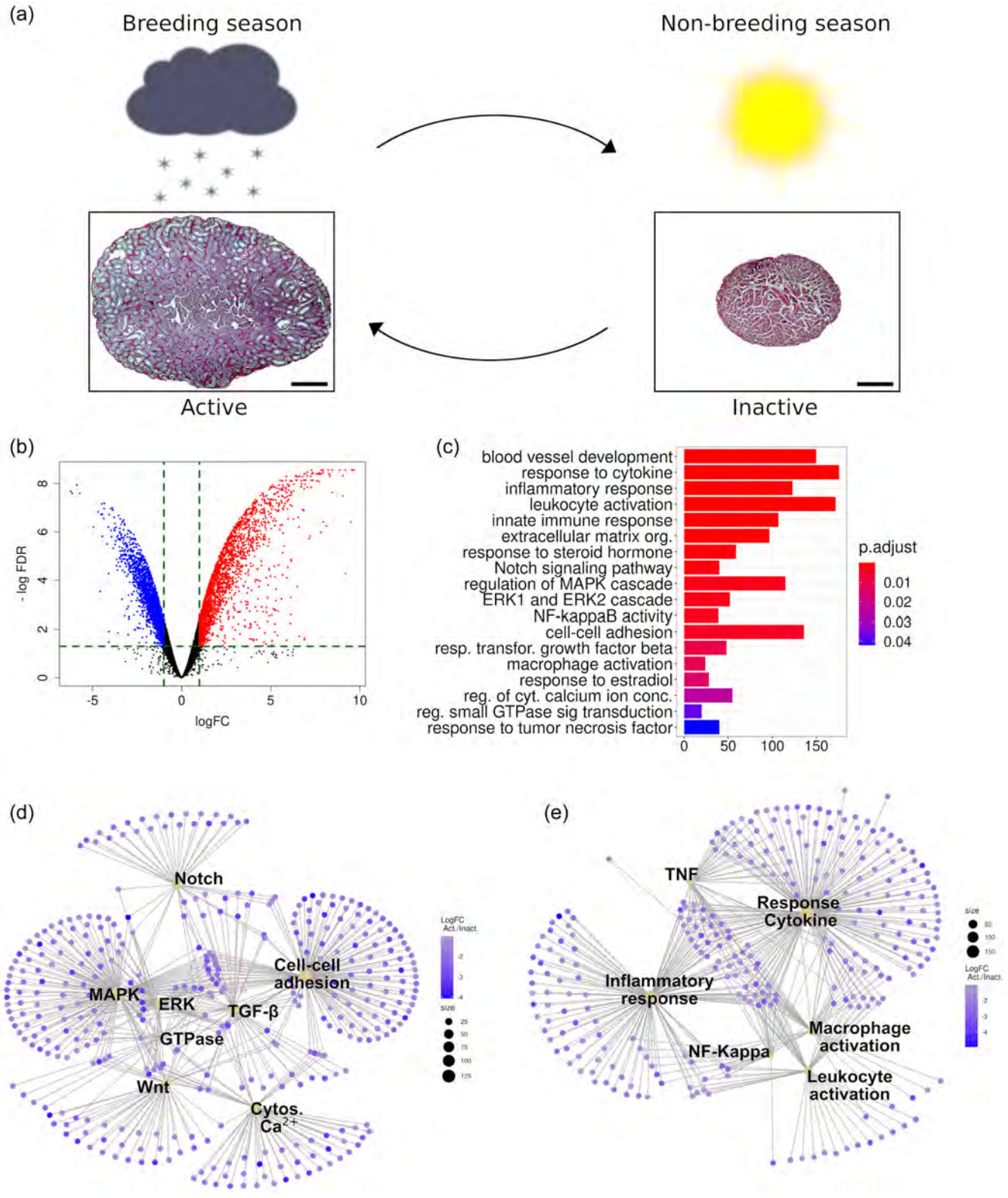

FIGURE 1 (See caption on next page)

shrink due to the germinative epithelium disorganization caused by a massive desquamation of live meiotic and post-meiotic germ cells (Figure 2a–c; Dadhich et al., 2010, 2013). Therefore, we also captured moles in April and generated transcriptomes from inactivating (regressing) testes. Multidimensional scaling plot showed that replicate samples of the same reproductive season clustered together, the inactivating samples being located between the active and the inactive ones. In this plot, the separation between active and inactivating testes was shorter than that between inactivating and inactive ones, confirming that we obtained transcriptomes corresponding to testes that were likely initiating the regression process (Figure 2d). Differential expression analysis between active and inactivating testes identified 452 DEGs, from which 207 were upregulated and 245 downregulated in the samples of the inactivating testes (FDR < 0.05 and $|\log_2 FC| > 1$; Figure 2e; Supporting Information: Table S7), a number much smaller than that of DEGs identified between active and inactive testes (see above). From these 452 DEGs, 446 were also differentially expressed between active and inactive testes. Almost all genes found to be downregulated in one comparison (active/inactivating) were also downregulated in the other one (active/inactive), and the same happened with the upregulated genes (Figure 2f; see $\log_2$FCs in Supporting Information: Table S8). In general, the amplitude of the changes in gene expression observed in the comparison active/inactive was greater than that in the active/inactivating one (Figure 2f, note that the $\log_2$FCs vary between −5 and 9 in the first case (*x*-axis), and between −3 and 3 in the second one (*y*-axis); Supporting Information: Table S8). Accordingly, the magnitude of the expression changes in most genes ($|\log_2 FC|$) was greater in the active/inactive comparison than in the active/inactivating one (red dots in Figure 2f; Supporting Information: Table S8). GO analysis using either all the DEGs or just the downregulated genes identified in the active/inactivating comparison testes revealed no significant enriched category. Contrarily, in the upregulated genes we found a significant enrichment (Padjust < 0.05) in a number of biological processes (Figure 2g; Supporting Information: Table S9), related to epithelium development, cell migration, wound healing and vasculogenesis (Figure 2g). We did not find any significantly enriched GO term associated to signaling pathways. So, we decided to search for DEGs between active and inactivating testes in the molecular pathways identified in the previous analysis (Figure 1e; Supporting Information: Table S4). We found 29 genes belonging to "MAPK cascade" (GO:0000165), 14 genes to the" ERK1 and ERK2 cascade" (GO:0070371), 11 to "response to transforming growth factor beta" (GO:0071559), 11 to "regulation of small GTPase mediated signal transduction" (GO:0051056; Supporting Information: Table S10), 7 to "regulation of cytosolic calcium ion concentration" (GO:0051480), and 6 to "Notch signaling pathway" (GO:0007219). In addition, we found 27 genes altered in the category "cell-cell adhesion" (GO:0098609). Gene-concept analysis using these data revealed an interacting network with many of these genes shared by several categories (Figure 2h). Altogether, these results suggest that the expression of genes belonging to several molecular pathways is altered at the beginning of testis regression, and that this alteration affects more genes (and probably more pathways) as the regression proceeds, thus ensuring the maintenance of the regressed status of the inactive testes of *T. occidentalis*. The MAPK/ERK1/2 pathway seems to play an essential role in this process.

2.3 | Transcriptomic analysis of early spermatogenesis in the regressed testis of *T. occidentalis*

We next investigate gene expression in the extant germ cells of the regressed testis. Consistent with our previous observations, double immunofluorescence for DMRT1, a marker of Sertoli and spermatogonial cells, and for DMC1, a marker for zygotene and early pachytene primary spermatocytes, revealed that spermatogonia maintain active proliferation in inactive testes and that a small number of spermatocytes reach the early pachytene stage (Figure 3a,b; Dadhich et al., 2011). Because of this, we decided to study the cell-specific expression profile of the early stages of spermatogenesis in active and inactive testes of the Iberian mole. For this, we used the gene expression signature of spermatogenic clusters reported by Hermann et al. (Hermann et al., 2018), assigning the genes we found to be differentially expressed between active and inactive testes to each of the early spermatogenic clusters, from undifferentiated spermatogonia to pachytene spermatocytes (Supporting Information: Table S11). Within these clusters, the number of downregulated genes increased as spermatogenesis progressed, being predominant at the pachytene stage (Figure 3c). However, this is probably a consequence of the much higher number of pachytene spermatocytes present in the active testis (see red cells in Figure 3a,b), rather than a reflection of actual changes in gene expression within cells. Biological theme comparison of downregulated genes in the inactive testes within these clusters

FIGURE 1 Transcriptomic analysis of seasonally active and inactive testes of *Talpa occidentalis*. Low magnification of hematoxylin and eosin-stained histological sections of seasonally active and inactive testes of the Iberian mole during the breeding (winter) and nonbreeding (summer) seasons (a). Note the pronounced reduction in testis size occurring during seasonal testis regression in this species. Scale bars represent 1 mm. (b) Volcano plot of the differential gene expression between active and inactive testes after normalization for different contents in germ cells. (c) Gene ontology analysis of the deregulated genes revealed a significant enrichment (Padjust < 0.05) in biological processes and molecular pathways associated to normal testicular functions. (d) Cnetplot of several significantly enriched molecular pathways identified in our GO analysis. (e) Gene-concept analysis of several significantly enriched GO terms associated with the activation of the immune system. In pictures (c–e), red color indicates downregulation and bluish color upregulation during testis regression. In figures (d, e), the size of sepia circles is proportional to the number of deregulated genes they represent.

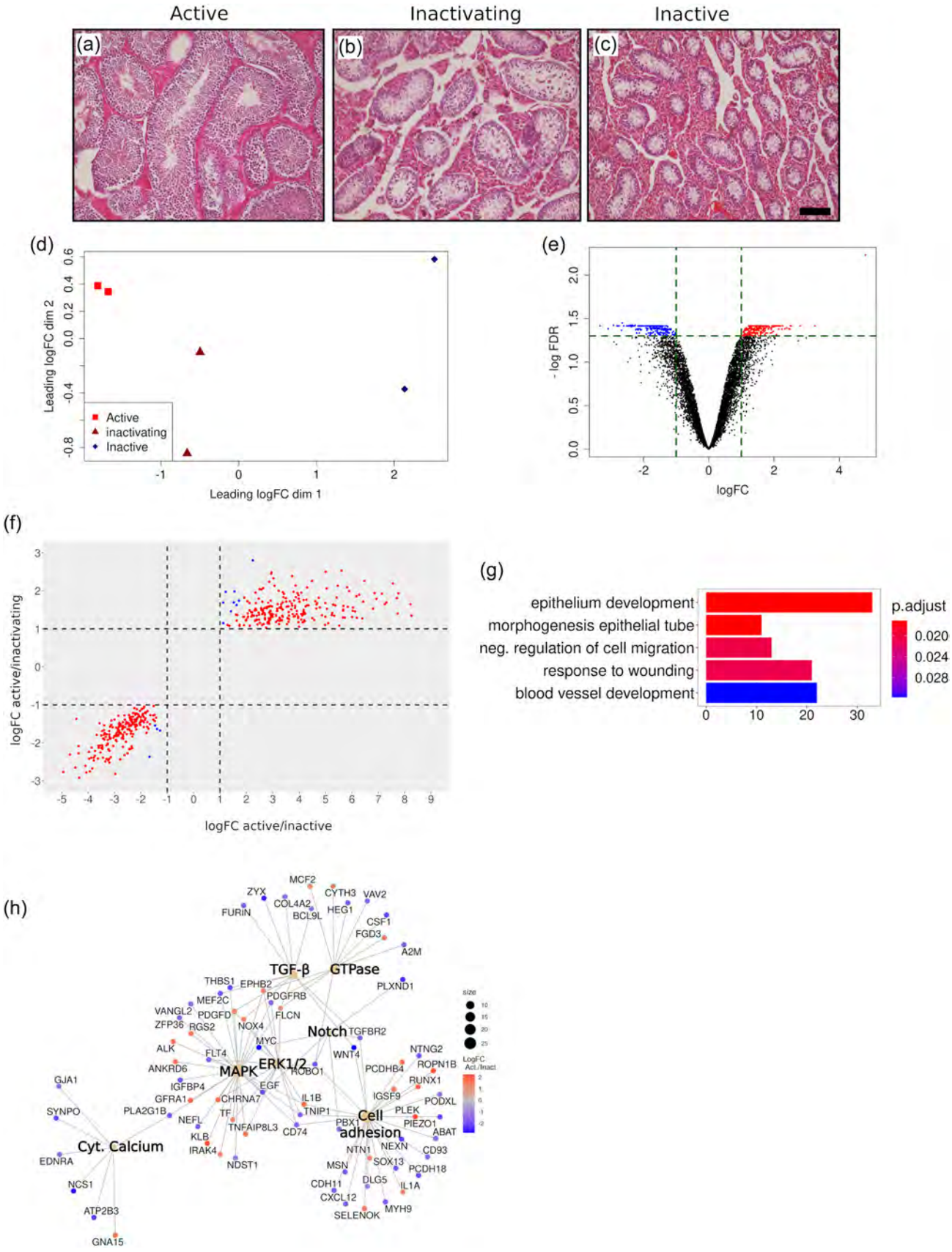

FIGURE 2 (See caption on next page)

(excluding the pachytene cluster) revealed in spermatogonial cells an enrichment of terms associated to "protein polyubiquitination" (GO:0000209), "covalent chromatin modification" (GO:0016569), "regulation of chromosome organization" (GO:0033044) and "DNA methylation" (GO:0006306). From the differentiated spermatogonia stage on, we identified GO categories associated to meiosis, including "nuclear chromosome segregation" (GO:0098813) and "meiotic nuclear division" (GO:0140013) among others (Figure 3d; Supporting Information: Table S12). As most of these latter biological processes are not completed in the inactive gonads, the differential expression detected for these genes is again probably a consequence of the different germ cell contents of active and inactive testes. Biological theme comparison of upregulated genes showed an enrichment in general biological processes such as "cotranslational protein targeting to membrane" (GO:0006613), "protein localization to endoplasmic reticulum" (GO:0070972), and "cellular respiration" (GO:0045333) among others (Figure 3e; Supporting Information: Table S13). Overall, these results clearly show that polyubiquitination seems to be a function affected in spermatogonial cells during testis regression. However, our findings at later stages (early meiotic prophase) are less consistent as the detected alterations could probably be derived from the different germ cell contents of seasonally active and inactive testes of *T. occidentalis*.

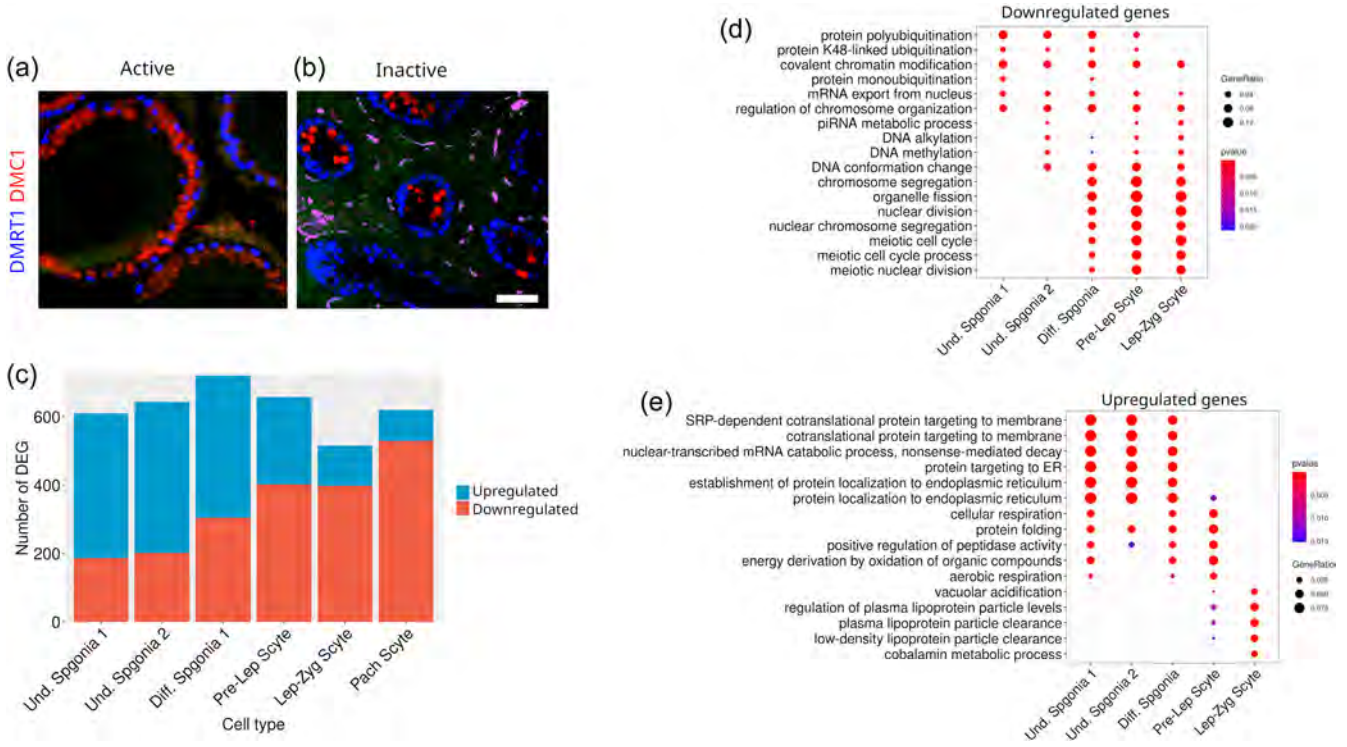

FIGURE 3 Transcriptomic analysis of early spermatogenesis in the inactive testis of *Talpa occidentalis*. Double immunofluorescence for DMRT1 (a marker for both Sertoli and spermatogonial cells) and for DMC1 (a marker for zygotene and early pachytene spermatocytes) in active (a) and inactive (b) testes. Note that the number of primary spermatocytes (red cells) is highly reduced in the inactive testis. (c) Number of genes predicted to be deregulated in each of the cell types of the early spermatogenic stages in the inactive testes of *T. occidentalis*. (d) Biological theme comparison of genes downregulated during testis regression in the early stages of spermatogenesis of the Iberian mole. (e) Biological theme comparison of genes upregulated during testis regression in the early stages of spermatogenesis of the Iberian mole. Scale bar in (b) represents 50 μm for (a, b). Original colors in (a, b) have been changed to make the figure accessible to color-blind readers.

FIGURE 2 Transcriptomic analysis of regressing (inactivating) testes of *Talpa occidentalis*. (a–c) Hematoxylin and eosin-stained histological sections of active (a), regressing (b), and inactive (c) testes of the Iberian mole. Note that seminiferous tubules of regressing testes have an intermediate size between those of active and inactive ones. (d) Multidimensional scaling plot of replicate samples of testes. Note that the regressing samples are placed between the active and inactive ones. (e) Volcano plot of the differentially expressed genes (DEGs) between active and regressing testes. (f) Log_2 fold change scatterplot representing the DEGs detected in the comparison between active and inactive testes against those observed in the comparison between active and regressing ones. (G) GO analysis of the deregulated genes identified in the comparison between active and regressing testes. (h) Gene-concept analysis of DEGs belonging to several molecular pathways. In pictures (e and h), red color indicates gene downregulation and bluish color upregulation during testis regression. In figure (h), the size of sepia circles is proportional to the number of deregulated genes they represent. Scale bar in (c) represents 100 μm for (a–c).

2.4 | Several biological processes are commonly affected in the regressed testes of both *T. occidentalis* and *M. duodecimcostatus*

We have recently reported the changes that the testicular transcriptome of the Mediterranean pine vole, *M. duodecimcostatus*, undergo during its seasonal reproductive cycle in southeastern Iberian Peninsula (Lao-Pérez et al., 2021). The inactive testes of this species show a clear difference with those of the Iberian mole: meiosis initiation is completely stopped, so that no zygotene or pachytene cells are present in the regressed seminiferous tubules. To explore the similarities of testicular regression between moles and voles, which are representative species of the Eulipotyphla and Rodentia orders, respectively, we decided to compare our testis transcriptomic datasets. We initially searched for genes that were either upregulated or downregulated in the regressed testes in both species (FDR < 0.05 and $|\log_2 FC| > 1$), and identified 1529 genes, 900 of which were upregulated and 629 downregulated (Figure 4a,b and Supporting Information: Table S14). For these genes, we plotted the $\log_2 FC$ of one species against the other one and found a linear correlation between both sets of data (Figure 4c; Pearson correlation test, cor. coeff = 0.85; $p < 2.2 \times 10^{-16}$), showing that many alterations in gene expression occur during the testis regression process of the two species. As expected, GO analysis of downregulated genes revealed a significant enrichment (Padjust < 0.05) in a reduced number of biological processes related to spermatogenesis and sperm differentiation (Supporting Information: Table S15). In contrast, in the group of upregulated genes, we identified many categories that were also detected in our previous analyses (Figure 4d; Supporting Information: Table S16), including "cell-cell adhesion (GO:0098609; Padjust = 1.7×10^{-3}) and "extracellular matrix organization" (GO:0030198; Padjust = 1.2×10^{-5}). This analysis also reported enriched GO terms associated to the same molecular pathways identified separately in both species, such as "regulation of MAPK cascade" (GO:0043408; Padjust = 9.3×10^{-6}), "response to transforming growth factor beta" (GO:0071559; Padjust = 3.9×10^{-4}), "ERK1 and ERK2 cascade" (GO:0070371; Padjust = 3.8×10^{-4}), and "regulation of cytosolic calcium ion concentration" (GO:0051480; Padjust = 2×10^{-2}) (Figure 4d; Supporting Information: Table S16). Gene-concept analysis revealed a complex interacting network with genes shared by several categories (Figure 4e). Moreover, our GO analysis also identified several enriched categories related to the activation of the immune system (Figure 4d; Supporting Information: Table S16), including "positive regulation of NF-kappaB transcription factor activity" (GO:0051092; Padjust = 9×10^{-4}), "cytokine production" (GO:0001816; Padjust = 7×10^{-7}), "macrophage activation" (GO:0042116; Padjust = 2×10^{-3}), "response to tumor necrosis factor" (GO:0034612; 4×10^{-2}), and "leukocyte activation" (GO:0045321; Padjust = 2×10^{-7}). Gene-concept analysis on these terms again revealed a cooperative network (Figure 4f), indicating that activation of the immune system is a common feature in the regressed testes of both species.

3 | DISCUSSION

We have previously reported the seasonal changes that the testes of *T. occidentalis* undergo at the histological, immunohistological, and hormonal level (Dadhich et al., 2010, 2011, 2013). To deepen in the molecular mechanisms underlying these changes, we have analyzed here the transcriptome of testes at different time points in the reproductive cycle of this species. We reported previously that, during the nonbreeding season, male moles have reduced levels of serum testosterone and regressed testes in which spermatogenesis is arrested, expression of cell adhesion molecules is disrupted and the BTB is not functional (Dadhich et al., 2013). Consistent with this, our transcriptome study shows that biological processes such as "cell-cell adhesion" and "cell junction assembly" as well as several molecular pathways including MAPK, ERK1/2, TGF-β, Cytosolic Ca^{2+}, PI3K, GTPase, and TNF (which operate in SCs and are necessary for spermatogenesis), and the dynamics of tight and adherens junctions forming the BTB, are altered in the inactive testes of *T. occidentalis*. The mitogen-activated protein kinases (MAPKs) comprise a family of regulators involved in the control of many physiological processes (Y. Sun et al., 2015). There are three classical subfamilies of MAPKs, (a) the extracellular signal-regulated kinases (ERKs), (b) the c-Jun N-terminal kinases (JNKs), and (c) the p38 MAPKs, all of which are known to regulate several aspects of the testicular function, including cell division and differentiation during spermatogenesis and junctional restructuring of the seminiferous epithelium (Ni et al., 2019; Q. Y. Sun et al., 1999; C.-H. Wong & Yan Cheng, 2005). The MAPK/ERK1/2 pathway plays essential roles in modulating cell adhesion and motility in several epithelia, including adhesion-mediated signaling (Howe et al., 2002), cytoskeleton dynamics (Stupack et al., 2000), and junction disassembly (Y. Wang et al., 2004). In the testis, the components of MAPK/ERK1/2 are found in SCs and all classes of germ cells in the seminiferous epithelium (C.-H. Wong & Yan Cheng, 2005), and regulates the formation of Sertoli–Sertoli and Sertoli–matrix anchoring junctions and the tight junction forming the BTB (Crépieux et al., 2001, 2002). This MAPK cascade also regulates the formation of ectoplasmic specialization (ES), structures that contribute to the adhesion between SCs at the BTB, and between Sertoli and developing spermatids at the adluminal compartment (Ni et al., 2019; Q. Y. Sun et al., 1999; C.-H. Wong & Yan Cheng, 2005). We found 132 and 52 genes belonging to the MAPK and ERK1/2 pathways, respectively, upregulated in the inactive mole testes (Supporting Information: Table S6, GO:0000165, and GO:0070371), and our gene-concept analysis showed that many of them are shared by these two pathways and by other processes, including cell junction assembly and regulation and cAMP-mediated signaling (Figure 1f). As mentioned above, MAPK can also act through the p38 MAPK cascade (Engelberg, 2004). This subfamily is activated by different pathways, including GTPases, usually resulting in inflammatory responses or apoptosis. Members of the p38 MAPK pathway have been found in SCs and elongate spermatids, and play a role in controlling cell junction dynamics in the seminiferous epithelium (C.-H. Wong & Yan Cheng, 2005). In SCs, this pathway

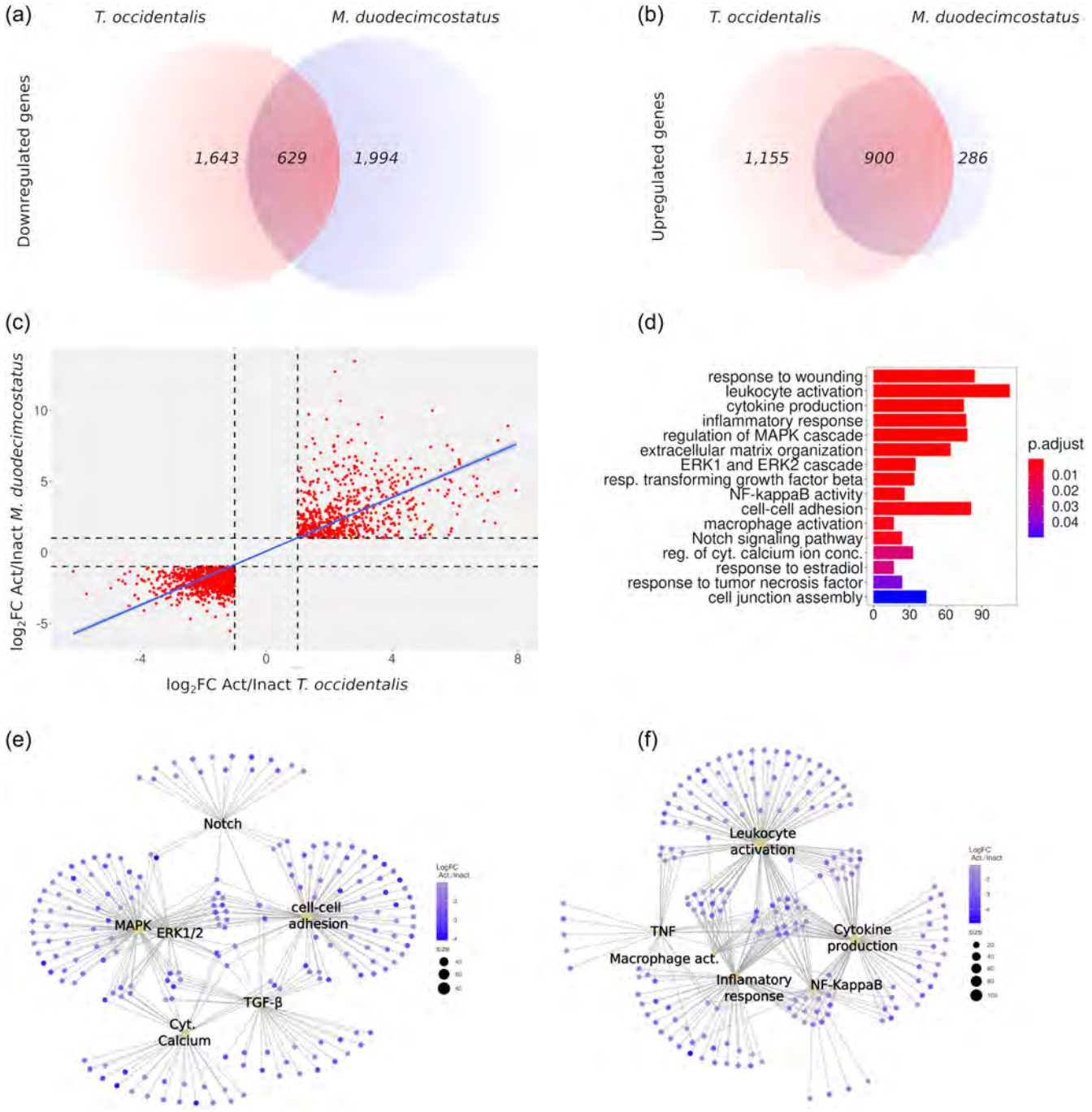

FIGURE 4 Biological functions altered in the inactive testes of both *Talpa occidentalis* and *Microtus duodecimcostatus*. (a,b) Venn-diagram representing the numbers of common genes downregulated (a) and upregulated (b) during testis regression. (c) Log_2 fold change scatterplot representing the differential gene expression between active and inactive testes of *T. occidentalis* against the same data from *M. duodecimcostatus*. (d) Gene ontology analysis of DEGs shared by both *T. occidentalis* and *M. duodecimcostatus*. (e) Gene-concept analysis of several significantly enriched GO terms associated with known molecular pathways acting in the testes of both species. (f) Gene-concept analysis of several significantly enriched GO terms associated with the activation of the immune response in both species. In pictures (e,f), red color indicates downregulation and bluish color upregulation of genes during testis regression, and the size of sepia circles is proportional to the number of deregulated genes they represent.

is activated in the presence of TGF-β3, leading to disruption of the tight-junction proteins in the BTB (Lui et al., 2003a, 2003b; C. Wong et al., 2004). Our transcriptomic analysis also revealed that the TGF-β and the GTPase pathways are altered in the mole inactive testes (Figure 1f; Supporting Table S4). The different MAPK cascades are likely to act in concert to regulate the BTB dynamics that facilitate germ cell migration throughout the seminiferous epithelium during the spermatogenic cycle (C.-H. Wong & Yan Cheng, 2005), and

several observations confirmed that these pathways are hormonally regulated. Testosterone can stimulate the MAPK/ERK signaling (Cheng et al., 2007; Fix et al., 2004) and low levels of this hormone, together with increased levels of TGF-β3, leads to the loss of cell adhesion molecules in the seminiferous epithelium, a process that seems to be mediated by different MAPK cascades (Y. Wang et al., 2004; C.-H. Wong & Yan Cheng, 2005). In light of this knowledge, our current transcriptomic data strongly suggest that the reduced levels of testosterone that the Iberian mole undergoes during the inactive season lead to the activation of different MAPK signaling cascades in the testes, a fact that in concert with other molecular pathways, including GTPase, PI3-K and TGF-β signaling, deregulates the cell adhesion function in the seminiferous epithelium, leading to BTB disruption and spermatogenic arrest.

As mentioned above, seasonal testis regression implies the massive depletion of meiotic and postmeiotic germ cells of the tetis. In *T. occidentalis*, this process occurs by desquamation of live, non-apoptotic germ cells. We found that most of the genes deregulated during this period do remain deregulated during the nonbreeding period, although at a less significant level. Among them, we found genes involved in the regulation of pathways that control cell adhesion such as MAPK, ERK1/2, GTPase, and TGF-β, indicating that deregulation of these pathways is likely to be also involved in the massive germ cell desquamation that accompanies seasonal testis regression in the mole.

A special immunological environment referred to as "immune privilege" operates in functional testes and protect germ cells from autoimmune attack. There are three main factors contributing to this immune privilege: (a) the existence of the BTB, which isolates meiotic and postmeiotic germ cells from the cells of the immune system, (b) the reduced capacity of the testicular macrophages to mount an inflammatory response, and (c) the production of anti-inflammatory cytokines by somatic cells (reviewed in (Fijak & Meinhardt, 2006; Li et al., 2012; Zhao et al., 2014). Our transcriptomic analysis revealed that categories related to immunological processes including "inflammatory response" "leukocyte activation" "macrophage activation" and "response to cytokine," were altered in the inactive testes of *T. occidentalis*, as well as molecular pathways that regulate the immune system, such as NF-kappaB and TNF, denoting the activation of the immune system in the inactive testes of *T. occidentalis*. Under normal physiological conditions, testicular macrophages present a reduced capability to mount inflammatory responses and to produce cytokines, when compared with macrophages from other tissues. Our RNA-seq data revealed both the activation of the macrophage population and cytokine production in the inactive testes of the Iberian mole and that TNF and NF-KappaB, two molecular pathways involved in the regulation of inflammatory cytokines production (Hayden & Ghosh, 2014), operate in the inactive testis. Several studies evidence an immunosuppressive role of testosterone on different components of the immune system (Foo et al., 2017; Trigunaite et al., 2015), so that testicular testosterone induces a reduction of pro-inflamatory cytokines in macrophages (D'agostino et al., 1999). Taking all these observations into account, we suggest that low levels of testosterone in the regressed testes of *T. occidentalis* may lead to the loss of the "immune privilege", which is manifested by BTB permeation and increased cytokine production by the macrophage population (and perhaps other somatic cells). Altogether, these processes might contribute to maintain the quiescent status of the mole gonads during the nonbreeding period.

We also analyzed the expression profile of genes belonging to the genetic expression signature of early spermatogenic cell populations (Supporting Information: Table S11) and found that several biological processes are altered in the regressed testes of the Iberian mole, particularly protein ubiquitination at the spermatogonia stage (Figure 3d; Supporting Information: Tables S12 and S13). Ubiquitination is essential for the establishment of both spermatogonial stem cells and differentiating spermatogonia and it is also involved in the regulation of several key events during meiosis, including homologous recombination and sex chromosome silencing (Bose et al., 2014). Indeed, mutations in the ubiquitin specific protease 26 (USP26), which is expressed in Leydig cells and early spermatogonia (Wosnitzer et al., 2014), are associated with defective spermatogenesis and infertility in both human and mice (Paduch et al., 2005; Sakai et al., 2019). Testosterone supports spermatogenesis through three mechanisms: (a) maintaining the BTB integrity (Meng et al., 2011), (b) regulating SC-spermatid adhesion (Holdcraft & Braun, 2004), and (c) controlling the release of mature sperm (Holdcraft & Braun, 2004). All these actions are mediated by SCs, as germ cells do not express the androgen receptor (AR) and, thus, are not direct targets of testosterone. In this study, we reveal that gene expression seems to be altered in the spermatogonial cells of the inactive mole testes, although it is difficult to know whether this is caused either by the particular testicular environment of quiescent testes, in which both the BTB and the cell adhesion function are disrupted, or by currently unknown mechanisms directly affecting germ cell expression, or both.

Finally, we have compared the mole testicular transcriptomic data with those we recently reported for the Mediterranean pine vole. We found a large number of genes that are deregulated in the regressed testes of both species, with two remarkable coincidences: (1) many of these genes are involved in the control of cell adhesion (Figure 4b,c; Supporting Information: Tables S14 and S15) and, accordingly, molecular pathways such as MAPK, ERK1/2, TGF-β, GTPase, and TNF, which control cell junctions in the seminiferous epithelium, are deregulated in the two species; (2) we also found a shared set of genes involved in the regulation of the immune response. These coincidences are relevant if we consider that the inactive testes of these two species do not show identical features. For example, meiosis initiation by spermatogonia is completely abolished in the inactive testes of *M. duodecimcostatus* (Lao-Pérez et al., 2021), but not in those of *T. occidentalis*, where meiosis entry continues and spermatogenesis progresses until the early primary spermatocyte stages (Dadhich et al., 2010, 2013). Moreover, the inactive seminiferous tubules of *M. duodecimcostatus* remain adjacent to each other (Lao-Pérez et al., 2021), whereas those of *T. occidentalis* become widely separated from each other by intervening Leydig cells

(Dadhich et al., 2013; Lao-Pérez et al., 2021). Despite these differences, here we report that two important testicular functions, cell adhesion, and immune response, are altered in the inactive testes of these two species, indicating that these are common molecular mechanisms operating in the regressed testes of seasonally breeding mammals.

4 | MATERIAL AND METHODS

4.1 | Animals

Six adult males of Iberian mole were captured alive in poplar groves near the locality of Chauchina (Granada province, south-eastern Spain) at three key stages of the reproductive cycle, using the methods developed in our laboratory (Barrionuevo et al., 2004). Two animals were captured in December (reproductive season), two more in April (transition period when testis regression occurs), and the last two in July (nonreproductive season). Animals were dissected, and the testes were removed under sterile conditions. The gonads were weighed, and frozen in liquid nitrogen for mRNA purification and further RNA-seq studies. A 5-mm thick slice of one of the testis of every animal was fixed in 50 volumes of 4% paraformaldehyde overnight at 4°C, embedded in paraffin, and processed for histology and immunofluorescence. Animals were captured with the permission of the Andalusian environmental authorities (Consejería de Agricultura, Pesca y Medio Ambiente) following the guidelines and approval of both the Ethical Committee for Animal Experimentation of the University of Granada and the Andalusian Council of Agriculture and Fisheries and Rural Development (Registration number: 450-19131; June 16th, 2014).

4.2 | Immunofluorescence

Testis sections were deparaffinized and incubated with primary antibodies overnight, washed, incubated with suitable conjugated secondary antibodies at room temperature for 1 h and counter-stained with 4′,6-diamino-2-phenylindol (DAPI). We used a Nikon Eclipse Ti microscope equipped with a Nikon DS-Fi1c digital camera (Nikon Corporation) to take photomicrographs. In negative controls, the primary antibody was omitted. The primary antibodies used were goat-anti-DMC1 (Santa Cruz Biotechnology, CA, sc-8973; 1:100) and rabbit-anti-DMRT1 (a kind gift from Sivana Guioli, 1:200). The secondary antibodies used were: green—donkey anti-rabbit IgG Alexa Fluor 488 (A32790); red—donkey anti-goat igG Alexa Fluor 555 (A32816).

4.3 | RNA-seq

Total RNA was isolated from both testes of the two males captured in every time point using the Qiagen RNeasy Midi kit following the manufacturer's instructions. After successfully passing quality check (RIN value > 7 measured in a Bioanalyzer, Agilent Technologies), the RNAs samples were paired-end sequenced separately in an Illumina HiSeq. 2500 platform at the Max Planck Institute for Molecular Genetics facilities in Berlin, Germany.

4.4 | Bioinformatics

The quality of the resulting sequencing reads was assessed using FastQC (http://www.bioinformatics.bbsrc.ac.uk/projects/fastqc/). The RNA-seq reads were mapped to the recently published genome of *T. occidentalis* (Real et al., 2020) with the *align* and featureCounts function from the R subread package (Liao et al., 2019). As mentioned above, most meiotic and postmeiotic germ cell types (from primary spermatocyte to spermatozoa) are exclusive of the active testes, being completely absent in inactive ones. Thus, many genes expressed in germ cells would appear as overexpressed in sexually active testes as such results would not reflect changes in gene expression but only differences in cell contents between active and inactive testes. Such an over-representation of germ-cell-specific transcripts in active testes would mask changes in gene expression of somatic cells, which do exert the control of the spermatogenic cycle, in particular SCs. Hence, to normalize the data and focus on the study of gene expression in somatic cells, we decided to remove transcripts expressed in germ cells from the General Feature Format (GFF) file of the Iberian mole that we have recently generated (Real et al., 2020). For this, we used previously published cell signatures in single-cell RNA sequencing studies (scRNA-seq) (Green et al., 2018; Hermann et al., 2018), as described in Lao-Pérez et al. (2021). We removed all genes included in clusters 1–13 and 16 from the Hermann et al. (2018) study, belonging to different germ cell types, and those from spermatogonia, spermatocyte, round spermatid, and elongating spermatid from the Green et al. (2018) one. After doing this, the number of genes analyzed decreased from 13,474 (Supporting Information: Table S1) to 8300 (Supporting Information: Table S3). Analysis of differential gene expression was performed with edgeR (Robinson et al., 2010). Genes were filtered by expression levels with the filterByExpr function, and the total number of reads per sample was normalized with the calcNormFactors function. Genes were considered to be differentially expressed at Padjust < 0.05 and |logFC | > 1. GO analysis was performed with the enrich GO function of the clusterProfiler bioconductor package (Yu et al., 2012). General terms and terms not related with testicular functions were not displayed.

AUTHOR CONTRIBUTIONS

Conceptualization: Rafael Jiménez, Francisco J. Barrionuevo, Francisca M. Real, Darío G. Lupiáñez, Stefan Mundlos; *Methodology*: Francisca M. Real, Miguel Lao-Pérez; *Software*: Francisco J. Barrionuevo, Miguel Burgos; *Formal analysis*: Francisca M. Real, Miguel Lao-Pérez, Francisco J. Barrionuevo, Rafael Jiménez; *Investigation*: Rafael Jiménez, Francisco J. Barrionuevo, Francisca M. Real, Darío G. Lupiáñez, Miguel Lao-Pérez; *Writing–original draft*: Francisco J.

Barrionuevo, Rafael Jiménez; *Writing–review & editing*: Rafael Jiménez, Francisco J. Barrionuevo, Francisca M. Real, Darío G. Lupiáñez, Stefan Mundlos; *Visualization*: Francisco J. Barrionuevo, Francisca M. Real, Darío G. Lupiáñez; *Funding acquisition*: Rafael Jiménez, Francisco J. Barrionuevo, Francisca M. Real, Darío G. Lupiáñez, Stefan Mundlos.

ACKNOWLEDGMENTS

The authors thank Dr. Slivana Guioli for kindly providing us with the DMRT1 antibody used in this study. This study was funded by the following sources: Spanish Secretaría de Estado de Investigación, Desarrollo e Innovación, Ministerio de Economía y Competitividad (grant number CGL-2015-67108-P), Junta de Andalucía (grant number BIO109), Deutsche Forschungsgemeinschaft (grant numbers MU 880/15-1 and MU 880/27-1), and Helmholtz ERC Recognition Award grant from the Helmholtz-Gemeinschaft (ERC-RA-0033).

CONFLICTS OF INTEREST

The authors declare no conflicts of interest.

DATA AVAILABILITY STATEMENT

The data that support the findings of this study are openly available in ArrayExpress at https://www.ebi.ac.uk/arrayexpress/, reference number E-MTAB-10836.

ORCID

Francisca M. Real http://orcid.org/0000-0003-0692-2260
Miguel Lao-Pérez http://orcid.org/0000-0001-6707-6825
Miguel Burgos http://orcid.org/0000-0003-4446-9313
Stefan Mundlos http://orcid.org/0000-0002-9788-3166
Darío G. Lupiáñez http://orcid.org/0000-0002-3165-036X
Rafael Jiménez http://orcid.org/0000-0003-4103-8219
Francisco J. Barrionuevo http://orcid.org/0000-0003-2651-1530

PEER REVIEW

The peer review history for this article is available at https://publons.com/publon/10.1002/jez.b.23142

REFERENCES

Barrionuevo, F. J., Zurita, F., Burgos, M., & Jiménez, R. (2004). Testis-like development of gonads in female moles. New insights on mammalian gonad organogenesis. *Developmental Biology*, *268*(1), 39–52. https://doi.org/10.1016/j.ydbio.2003.11.025

Bogacka, I., Paukszto, Ł., Jastrzębski, J. P., Czerwińska, J., Chojnowska, K., Kamińska, B., Kurzyńska, A., Smolińska, N., Giżejewski, Z., & Kamiński, T. (2017). Seasonal differences in the testicular transcriptome profile of free-living European beavers (*Castor fiber* L.) determined by the RNA-Seq method. *PLoS One*, *12*(7), e0180323. https://doi.org/10.1371/journal.pone.0180323

Bose, R., Manku, G., Culty, M., & Wing, S. S. (2014). Ubiquitin–proteasome system in spermatogenesis. In P. Sutovsky (Ed.), *Posttranslational protein modifications in the reproductive system* (pp. 181–213). Springer. https://doi.org/10.1007/978-1-4939-0817-2_9

Bronson, F. H., & Heideman, P. D. (1994). *The physiology of reproduction* (2nd ed.). Raven Press.

Cheng, J., Watkins, S. C., & Walker, W. H. (2007). Testosterone activates mitogen-activated protein kinase via Src kinase and the epidermal growth factor receptor in sertoli cells. *Endocrinology*, *148*(5), 2066–2074. https://doi.org/10.1210/en.2006-1465

Crépieux, P., Marion, S., Martinat, N., Fafeur, V., Vern, Y. L., Kerboeuf, D., Guillou, F., & Reiter, E. (2001). The ERK-dependent signalling is stage-specifically modulated by FSH, during primary Sertoli cell maturation. *Oncogene*, *20*(34), 4696–4709. https://doi.org/10.1038/sj.onc.1204632

Crépieux, P., Martinat, N., Marion, S., Guillou, F., & Reiter, E. (2002). Cellular adhesion of primary sertoli cells affects responsiveness of the extracellular signal-regulated kinases 1 and 2 to follicle-stimulating hormone but not to epidermal growth factor. *Archives of Biochemistry and Biophysics*, *399*(2), 245–250. https://doi.org/10.1006/abbi.2002.2773

Dadhich, R. K., Barrionuevo, F. J., Lupiañez, D. G., Real, F. M., Burgos, M., & Jiménez, R. (2011). Expression of genes controlling testicular development in adult testis of the seasonally breeding Iberian mole. *Sexual Development*, *5*(2), 77–88. https://doi.org/10.1159/000323805

Dadhich, R. K., Barrionuevo, F. J., Real, F. M., Lupiañez, D. G., Ortega, E., Burgos, M., & Jiménez, R. (2013). Identification of live germ-cell desquamation as a major mechanism of seasonal testis regression in mammals: A study in the Iberian mole (*Talpa occidentalis*)[1]. *Biology of Reproduction*, *88*(4), 1–12. https://doi.org/10.1095/biolreprod.112.106708

Dadhich, R. K., Real, F. M., Zurita, F., Barrionuevo, F. J., Burgos, M., & Jiménez, R. (2010). Role of apoptosis and cell proliferation in the testicular dynamics of seasonal breeding mammals: A study in the Iberian mole, Talpa occidentalis[1]. *Biology of Reproduction*, *83*(1), 83–91. https://doi.org/10.1095/biolreprod.109.080135

D'agostino, P., Milano, S., Barbera, C., Bella, G. D., Rosa, M. L., Ferlazzo, V., Farruggio, R., Miceli, D. M., Miele, M., Castagnetta, L., & Cillari, E. (1999). Sex hormones modulate inflammatory mediators produced by macrophagesa. *Annals of the New York Academy of Sciences*, *876*(1), 426–429. https://doi.org/10.1111/j.1749-6632.1999.tb07667.x

Dardente, H., Lomet, D., Robert, V., Decourt, C., Beltramo, M., & Pellicer-Rubio, M.-T. (2016). Seasonal breeding in mammals: From basic science to applications and back. *Theriogenology*, *86*(1), 324–332. https://doi.org/10.1016/j.theriogenology.2016.04.045

Das, G. K., & Khan, F. A. (2010). Summer anoestrus in buffalo—A review. *Reproduction in Domestic Animals = Zuchthygiene*, *45*(6), e483–e494. https://doi.org/10.1111/j.1439-0531.2010.01598.x

Engelberg, D. (2004). Stress-activated protein kinases—Tumor suppressors or tumor initiators? *Seminars in Cancer Biology*, *14*(4), 271–282. https://doi.org/10.1016/j.semcancer.2004.04.006

Fijak, M., & Meinhardt, A. (2006). The testis in immune privilege. *Immunological Reviews*, *213*(1), 66–81. https://doi.org/10.1111/j.1600-065X.2006.00438.x

Fix, C., Jordan, C., Cano, P., & Walker, W. H. (2004). Testosterone activates mitogen-activated protein kinase and the cAMP response element binding protein transcription factor in Sertoli cells. *Proceedings of the National Academy of Sciences USA*, *101*(30), 10919–10924. https://doi.org/10.1073/pnas.0404278101

Foo, Y. Z., Nakagawa, S., Rhodes, G., & Simmons, L. W. (2017). The effects of sex hormones on immune function: A meta-analysis. *Biological Reviews*, *92*(1), 551–571. https://doi.org/10.1111/brv.12243

Garcia, T. X., DeFalco, T., Capel, B., & Hofmann, M.-C. (2013). Constitutive activation of NOTCH1 signaling in Sertoli cells causes gonocyte exit from quiescence. *Developmental Biology*, *377*(1), 188–201. https://doi.org/10.1016/j.ydbio.2013.01.031

González, C. R., Isla, M. L. M., & Vitullo, A. D. (2018). The balance between apoptosis and autophagy regulates testis regression and recrudescence in the seasonal-breeding South American plains

vizcacha, *Lagostomus maximus*. *PLoS One*, *13*(1), e0191126. https://doi.org/10.1371/journal.pone.0191126

Gorczynska, E., & Handelsman, D. J. (1995). Androgens rapidly increase the cytosolic calcium concentration in Sertoli cells. *Endocrinology*, *136*(5), 2052–2059. https://doi.org/10.1210/endo.136.5.7720654

Green, C. D., Ma, Q., Manske, G. L., Shami, A. N., Zheng, X., Marini, S., Moritz, L., Sultan, C., Gurczynski, S. J., Moore, B. B., Tallquist, M. D., Li, J. Z., & Hammoud, S. S. (2018). A comprehensive roadmap of murine spermatogenesis defined by single-cell RNA-seq. *Developmental Cell*, *46*(5), 651–667.e10. https://doi.org/10.1016/j.devcel.2018.07.025

Hayden, M. S., & Ghosh, S. (2014). Regulation of NF-κB by TNF family cytokines. *Seminars in Immunology*, *26*(3), 253–266. https://doi.org/10.1016/j.smim.2014.05.004

Hermann, B. P., Cheng, K., Singh, A., Roa-De La Cruz, L., Mutoji, K. N., Chen, I.-C., Gildersleeve, H., Lehle, J. D., Mayo, M., Westernströer, B., Law, N. C., Oatley, M. J., Velte, E. K., Niedenberger, B. A., Fritze, D., Silber, S., Geyer, C. B., Oatley, J. M., & McCarrey, J. R. (2018). The mammalian spermatogenesis single-cell transcriptome, from spermatogonial stem cells to spermatids. *Cell Reports*, *25*(6), 1650–1667.e8. https://doi.org/10.1016/j.celrep.2018.10.026

Holdcraft, R. W., & Braun, R. E. (2004). Androgen receptor function is required in Sertoli cells for the terminal differentiation of haploid spermatids. *Development*, *131*(2), 459–467. https://doi.org/10.1242/dev.00957

Howe, A. K., Aplin, A. E., & Juliano, R. L. (2002). Anchorage-dependent ERK signaling—Mechanisms and consequences. *Current Opinion in Genetics & Development*, *12*(1), 30–35. https://doi.org/10.1016/S0959-437X(01)00260-X

Jiménez, R., Burgos, M., & Barrionuevo, F. J. (2015). Circannual testis changes in seasonally breeding mammals. *Sexual Development: Genetics, Molecular Biology, Evolution, Endocrinology, Embryology, and Pathology of Sex Determination and Differentiation*, *9*(4), 205–215. https://doi.org/10.1159/000439039

Jimenez, R., Burgos, M., Sanchez, A., Sinclair, A. H., Alarcon, F. J., Marin, J. J., Ortega, E., & de la Guardia, R. D. (1993). Fertile females of the mole *Talpa occidentalis* are phenotypic intersexes with ovotestes. *Development*, *118*(4), 1303–1311. https://doi.org/10.1242/dev.118.4.1303

Lao-Pérez, M., Massoud, D., Real, F. M., Hurtado, A., Ortega, E., Burgos, M., Jiménez, R., & Barrionuevo, F. J. (2021). Mediterranean pine vole, *Microtus duodecimcostatus*: A paradigm of an opportunistic breeder. *Animals: An Open Access Journal from MDPI*, *11*(6), 1639. https://doi.org/10.3390/ani11061639

Li, N., Wang, T., & Han, D. (2012). Structural, cellular and molecular aspects of immune privilege in the testis. *Frontiers in Immunology*, *3*, https://doi.org/10.3389/fimmu.2012.00152

Liao, Y., Smyth, G. K., & Shi, W. (2019). The R package Rsubread is easier, faster, cheaper and better for alignment and quantification of RNA sequencing reads. *Nucleic Acids Research*, *47*(8), e47. https://doi.org/10.1093/nar/gkz114

Liu, M., Cao, G., Zhang, Y., Qu, J., Li, W., Wan, X., Li, Y., Zhang, Z., Wang, Y., & Gao, F. (2016). Changes in the morphology and protein expression of germ cells and Sertoli cells in plateau pikas testes during non-breeding season. *Scientific Reports*, *6*(1), 1–12. https://doi.org/10.1038/srep22697

Luaces, J. P., Rossi, L. F., Merico, V., Zuccotti, M., Redi, C. A., Solari, A. J., Merani, M. S., & Garagna, S. (2013). Spermatogenesis is seasonal in the large hairy armadillo, *Chaetophractus villosus* (Dasypodidae, Xenarthra, Mammalia). *Reproduction, Fertility, and Development*, *25*(3), 547–557. https://doi.org/10.1071/RD12127

Luaces, J. P., Rossi, L. F., Sciurano, R. B., Rebuzzini, P., Merico, V., Zuccotti, M., Merani, M. S., & Garagna, S. (2014). Loss of sertoli-germ cell adhesion determines the rapid germ cell elimination during the seasonal regression of the seminiferous epithelium of the large hairy armadillo *Chaetophractus villosus*[1]. *Biology of Reproduction*, *90*(3), 48. https://doi.org/10.1095/biolreprod.113.113118

Lui, W., Lee, W. M., & Cheng, C. Y. (2003a). Sertoli-germ cell adherens junction dynamics in the testis are regulated by RhoB GTPase via the ROCK/LIMK signaling pathway[1]. *Biology of Reproduction*, *68*(6), 2189–2206. https://doi.org/10.1095/biolreprod.102.011379

Lui, W., Lee, W. M., & Cheng, C. Y. (2003b). Transforming growth factor β3 regulates the dynamics of sertoli cell tight junctions via the p38 mitogen-activated protein kinase pathway[1]. *Biology of Reproduction*, *68*(5), 1597–1612. https://doi.org/10.1095/biolreprod.102.011387

Martin, G. B., Tjondronegoro, S., & Blackberry, M. A. (1994). Effects of nutrition on testicular size and the concentrations of gonadotrophins, testosterone and inhibin in plasma of mature male sheep. *Journal of Reproduction and Fertility*, *101*(1), 121–128. https://doi.org/10.1530/jrf.0.1010121

Martínez-Hernández, J., Seco-Rovira, V., Beltrán-Frutos, E., Ferrer, C., Serrano-Sánchez, M. I., & Pastor, L. M. (2020). Proliferation, apoptosis, and number of Sertoli cells in the Syrian hamster during recrudescence after exposure to short photoperiod[†‡]. *Biology of Reproduction*, *102*(3), 588–597. https://doi.org/10.1093/biolre/ioz198

Massoud, D., Lao-Pérez, M., Hurtado, A., Abdo, W., Palomino-Morales, R., Carmona, F. D., Burgos, M., Jiménez, R., & Barrionuevo, F. J. (2018). Germ cell desquamation-based testis regression in a seasonal breeder, the Egyptian long-eared hedgehog, *Hemiechinus auritus*. *PLoS One*, *13*(10), e0204851. https://doi.org/10.1371/journal.pone.0204851

Massoud, D., Lao-Pérez, M., Ortega, E., Burgos, M., Jiménez, R., & Barrionuevo, F. J. (2021). Divergent seasonal reproductive patterns in syntopic populations of two murine species in southern Spain, *Mus spretus* and *Apodemus sylvaticus*. *Animals: An Open Access Journal from MDPI*, *11*(2), 243. https://doi.org/10.3390/ani11020243

Maywood, E. S., Chahad-Ehlers, S., Garabette, M. L., Pritchard, C., Underhill, P., Greenfield, A., Ebling, F. J. P., Akhtar, R. A., Kyriacou, C. P., Hastings, M. H., & Reddy, A. B. (2009). Differential testicular gene expression in seasonal fertility. *Journal of Biological Rhythms*, *24*(2), 114–125. https://doi.org/10.1177/0748730409332029

Meng, J., Greenlee, A. R., Taub, C. J., & Braun, R. E. (2011). Sertoli cell-specific deletion of the androgen receptor compromises testicular immune privilege in mice. *Biology of Reproduction*, *85*(2), 254–260. https://doi.org/10.1095/biolreprod.110.090621

Nelson, R. J., Gubernick, D. J., & Blom, J. M. (1995). Influence of photoperiod, green food, and water availability on reproduction in male California mice (*Peromyscus californicus*). *Physiology and Behavior*, *57*(6), 1175–1180. https://doi.org/10.1016/0031-9384(94)00380-n

Ni, F.-D., Hao, S.-L., & Yang, W.-X. (2019). Multiple signaling pathways in Sertoli cells: Recent findings in spermatogenesis. *Cell Death & Disease*, *10*(8), 541. https://doi.org/10.1038/s41419-019-1782-z

Paduch, D., Mielnik, A., & Schlegel, P. N. (2005). Novel mutations in testis-specific ubiquitin protease 26 gene may cause male infertility and hypogonadism. *Reproductive BioMedicine Online*, *10*(6), 747–754. https://doi.org/10.1016/S1472-6483(10)61119-4

Pastor, L. M., Zuasti, A., Ferrer, C., Bernal-Mañas, C. M., Morales, E., Beltrán-Frutos, E., & Seco-Rovira, V. (2011). Proliferation and apoptosis in aged and photoregressed mammalian seminiferous epithelium, with particular attention to rodents and humans. *Reproduction in Domestic Animals*, *46*(1), 155–164. https://doi.org/10.1111/j.1439-0531.2009.01573.x

Real, F. M., Haas, S. A., Franchini, P., Xiong, P., Simakov, O., Kuhl, H., Schöpflin, R., Heller, D., Moeinzadeh, M.-H., Heinrich, V., Krannich, T., Bressin, A., Hartmann, M. F., Wudy, S. A., Dechmann, D. K. N., Hurtado, A., Barrionuevo, F. J., Schindler, M., Harabula, I., … Lupiáñez, D. G. (2020). The mole genome reveals

regulatory rearrangements associated with adaptive intersexuality. *Science*, *370*(6513), 208–214. https://doi.org/10.1126/science.aaz2582

Robinson, M. D., McCarthy, D. J., & Smyth, G. K. (2010). edgeR: A Bioconductor package for differential expression analysis of digital gene expression data. *Bioinformatics*, *26*(1), 139–140. https://doi.org/10.1093/bioinformatics/btp616

Sakai, K., Ito, C., Wakabayashi, M., Kanzaki, S., Ito, T., Takada, S., Toshimori, K., Sekita, Y., & Kimura, T. (2019). Usp26 mutation in mice leads to defective spermatogenesis depending on genetic background. *Scientific Reports*, *9*(1), 13757. https://doi.org/10.1038/s41598-019-50318-6

Seco-Rovira, V., Beltrán-Frutos, E., Ferrer, C., Saez, F. J., Madrid, J. F., Canteras, M., & Pastor, L. M. (2015). Testicular histomorphometry and the proliferative and apoptotic activities of the seminiferous epithelium in Syrian hamster (*Mesocricetus auratus*) during regression owing to short photoperiod. *Andrology*, *3*(3), 598–610. https://doi.org/10.1111/andr.12037

Stupack, D. G., Cho, S. Y., & Klemke, R. L. (2000). Molecular signaling mechanisms of cell migration and invasion. *Immunologic Research*, *21*(2), 83–88. https://doi.org/10.1385/IR:21:2-3:83

Sun, Q. Y., Breitbart, H., & Schatten, H. (1999). Role of the MAPK cascade in mammalian germ cells. *Reproduction, Fertility, and Development*, *11*(8), 443–450. https://doi.org/10.1071/rd00014

Sun, Y., Liu, W.-Z., Liu, T., Feng, X., Yang, N., & Zhou, H.-F. (2015). Signaling pathway of MAPK/ERK in cell proliferation, differentiation, migration, senescence and apoptosis. *Journal of Receptors and Signal Transduction*, *35*(6), 600–604. https://doi.org/10.3109/10799893.2015.1030412

Temple, J. L. (2004). The musk shrew (*Suncus murinus*): A model species for studies of nutritional regulation of reproduction. *Institute for Laboratory Animal Research Journal*, *45*(1), 25–34. https://doi.org/10.1093/ilar.45.1.25

Trigunaite, A., Dimo, J., & Jørgensen, T. N. (2015). Suppressive effects of androgens on the immune system. *Cellular Immunology*, *294*(2), 87–94. https://doi.org/10.1016/j.cellimm.2015.02.004

Tsubota, T., Howell-Skalla, L., Nitta, H., Osawa, Y., Mason, J. I., Meiers, P. G., Nelson, R. A., & Bahr, J. M. (1997). Seasonal changes in spermatogenesis and testicular steroidogenesis in the male black bear *Ursus americanus*. *Journal of Reproduction and Fertility*, *109*(1), 21–27. https://doi.org/10.1530/jrf.0.1090021

Wang, X., Adegoke, E. O., Ma, M., Huang, F., Zhang, H., Adeniran, S. O., Zheng, P., & Zhang, G. (2019). Influence of Wilms' tumor suppressor gene WT1 on bovine Sertoli cells polarity and tight junctions via non-canonical WNT signaling pathway. *Theriogenology*, *138*, 84–93. https://doi.org/10.1016/j.theriogenology.2019.07.007

Wang, Y., Zhang, J., Yi, X., & Yu, F.-S. X. (2004). Activation of ERK1/2 MAP kinase pathway induces tight junction disruption in human corneal epithelial cells. *Experimental Eye Research*, *78*(1), 125–136. https://doi.org/10.1016/j.exer.2003.09.002

Wang, Y.-J., Jia, G.-X., Yan, R.-G., Guo, S.-C., Tian, F., Ma, J.-B., Zhang, R.-N., Li, C., Zhang, L.-Z., Du, Y.-R., & Yang, Q.-E. (2019). Testosterone-retinoic acid signaling directs spermatogonial differentiation and seasonal spermatogenesis in the Plateau pika (*Ochotona curzoniae*). *Theriogenology*, *123*, 74–82. https://doi.org/10.1016/j.theriogenology.2018.09.033

Wong, C., Mruk, D. D., Lui, W., & Cheng, C. Y. (2004). Regulation of blood-testis barrier dynamics: An in vivo study. *Journal of Cell Science*, *117*(5), 783–798. https://doi.org/10.1242/jcs.00900

Wong, C.-H., & Yan Cheng, C. (2005). Mitogen-activated protein kinases, adherens junction dynamics, and spermatogenesis: A review of recent data. *Developmental Biology*, *286*(1), 1–15. https://doi.org/10.1016/j.ydbio.2005.08.001

Wosnitzer, M. S., Mielnik, A., Dabaja, A., Robinson, B., Schlegel, P. N., & Paduch, D. A. (2014). Ubiquitin specific protease 26 (USP26) expression analysis in human testicular and extragonadal tissues indicates diverse action of USP26 in cell differentiation and tumorigenesis. *PLoS One*, *9*(6), e98638. https://doi.org/10.1371/journal.pone.0098638

Young, K. A., & Nelson, R. J. (2001). Mediation of seasonal testicular regression by apoptosis. *Reproduction*, *122*(5), 677–685.

Yu, G., Wang, L.-G., Han, Y., & He, Q.-Y. (2012). clusterProfiler: An R package for comparing biological themes among gene clusters. *OMICS: A Journal of Integrative Biology*, *16*(5), 284–287. https://doi.org/10.1089/omi.2011.0118

Zhang, H., Yin, Y., Wang, G., Liu, Z., Liu, L., & Sun, F. (2014). Interleukin-6 disrupts blood-testis barrier through inhibiting protein degradation or activating phosphorylated ERK in Sertoli cells. *Scientific Reports*, *4*(1), 4260. https://doi.org/10.1038/srep04260

Zhao, S., Zhu, W., Xue, S., & Han, D. (2014). Testicular defense systems: Immune privilege and innate immunity. *Cellular & Molecular Immunology*, *11*(5), 428–437. https://doi.org/10.1038/cmi.2014.38

SUPPORTING INFORMATION

Additional supporting information can be found online in the Supporting Information section at the end of this article.

How to cite this article: Real, F. M., Lao-Pérez, M., Burgos, M., Mundlos, S., Lupiáñez, D. G., Jiménez, R., & Barrionuevo, F. J. (2023). Cell adhesion and immune response, two main functions altered in the transcriptome of seasonally regressed testes of two mammalian species. *Journal of Experimental Zoology Part B: Molecular and Developmental Evolution*, 340, 231–244. https://doi.org/10.1002/jez.b.23142

Nilsson et al. BMC Genomics 2013, 14:496
http://www.biomedcentral.com/1471-2164/14/496

BMC Genomics

RESEARCH ARTICLE Open Access

Gene bionetworks that regulate ovarian primordial follicle assembly

Eric Nilsson[1], Bin Zhang[2] and Michael K Skinner[1*]

Abstract

Background: Primordial follicle assembly is the process by which ovarian primordial follicles are formed. During follicle assembly oocyte nests break down and a layer of pre-granulosa cells surrounds individual oocytes to form primordial follicles. The pool of primordial follicles formed is the source of oocytes for ovulation during a female's reproductive life.

Results: The current study utilized a systems approach to detect all genes that are differentially expressed in response to seven different growth factor and hormone treatments known to influence (increase or decrease) primordial follicle assembly in a neonatal rat ovary culture system. One novel factor, basic fibroblast growth factor (FGF2), was experimentally determined to inhibit follicle assembly. The different growth factor and hormone treatments were all found to affect similar physiological pathways, but each treatment affected a unique set of differentially expressed genes (signature gene set). A gene bionetwork analysis identified gene modules of coordinately expressed interconnected genes and it was found that different gene modules appear to accomplish distinct tasks during primordial follicle assembly. Predictions of physiological pathways important to follicle assembly were validated using ovary culture experiments in which ERK1/2 (MAPK1) activity was increased.

Conclusions: A number of the highly interconnected genes in these gene networks have previously been linked to primary ovarian insufficiency (POI) and polycystic ovarian disease syndrome (PCOS). Observations have identified novel factors and gene networks that regulate primordial follicle assembly. This systems biology approach has helped elucidate the molecular control of primordial follicle assembly and provided potential therapeutic targets for the treatment of ovarian disease.

Keywords: Ovary, Primordial follicle, Assembly, Ovarian development, PCO, POI, Transcriptome, Female fertility, Genomics, System biology

Background

Complex and interconnected networks of gene expression, cellular signaling and other processes within cells and organs are what control biological processes. This raises the concern that the common reductionist experimental approach to biomedical research may not be adequate to fully understand the systems that control these processes. Reductionist experiments will commonly impose single treatments onto the biological entity under study and measure a single response parameter compared to controls. A relevant example from the authors' own laboratory is the study of the effect that treatment of neonatal rat ovaries with anti-Müllerian hormone (AMH) has on the proportion of primordial follicles formed [1]. Results from these types of experiments can provide clear information about candidate regulatory factors, but typically do not elucidate the network of factors or signals that are required for a normal biological process. A systems biology experimental approach to studying normal development can be a powerful tool that is complementary to the more reductionist methods. The goal of the current study is to use a systems biology approach to identify gene expression networks involved in the formation of ovarian primordial follicles (primordial follicle assembly), and to identify putative regulatory factors involved in this developmental process.

Primordial follicle assembly is the process by which ovarian primordial follicles are formed. A primordial

* Correspondence: skinner@wsu.edu
[1]Center for Reproductive Biology, School of Biological Sciences, Washington State University, Pullman, WA 99164-4236, USA
Full list of author information is available at the end of the article

follicle is composed of an oocyte arrested in prophase of the first meiotic division and surrounded by a single layer of pre-granulosa cells [2]. Follicle assembly in mammals occurs either during gestation (e.g. cattle and humans) or shortly after birth (e.g. rodents). The pool of assembled primordial follicles is the source of oocytes for follicle growth and ovulation over the course of a female's reproductive life [3]. When the primordial follicle pool is depleted reproduction ceases and women enter menopause [2-7]. Prior to follicle assembly, mitotic proliferation of germ cells creates groups of cells linked by intracellular bridges and surrounded by an epithelial/mesenchymal cell layer and the structures are called oocyte nests and when the surrounding stromal cells are considered ovigerous cords [8-10]. The mitotically arrested germ cells within the nests enter meiosis and progress to the diplotene stage of prophase one of meiosis and arrest at that stage until such time as ovulation occurs [5,6,11].

During the follicle assembly process oocyte nests break down and a single layer of pre-granulosa cells surrounds individual oocytes to form primordial follicles [3]. The majority of oocytes in each nest undergo apoptosis during follicle assembly [3,6,12,13]. Abnormalities in the follicle assembly process can lead to a reduced primordial follicle pool size and reproductive capacity. Abnormal pool size may lead to some types of infertility such as Primary Ovarian Insufficiency (POI) in which the follicle pool is depleted early in life and women undergo early menopause [14,15]. Previous research has shown that several extracellular signaling molecules (e. g. growth factors and hormones) can regulate follicle assembly [3,5-7]. These studies have primarily used a reductionist approach to test candidate factors one at a time for their ability to affect the assembly process. Growth factors and hormones that have been shown to regulate primordial follicle assembly include anti-Müllerian hormone (AMH) (decrease) [1], connective tissue growth factor (CTGF) (increase) [16], estradiol (E2) (increase) [17-21], activin A (increase) [21], progesterone (P4) (decrease) [17,18,22,23], tumor necrosis factor alpha (TNFa) (decrease) [23-25], members of the notch/jagged signaling pathway (increase) [26], members of the brain derived neurotrophic factor (BDNF) / NTRK2 neurotrophin signaling pathway [27,28] and kit ligand (KITL) and growth differentiation factor-9 (GDF9) (increase) [29]. Evidence suggests fibroblast growth factor-2 (FGF2) may also be a regulator of follicle assembly [1,30], although this has not been confirmed experimentally.

A systems biology experimental approach was employed in the current study to expand upon the results of these previous experiments that examined single gene effects on the follicle assembly process. A similar systems biology approach has been used previously to identify coordinately and interconnected expressed gene modules and gene networks that regulate the primordial to primary follicle transition which is the subsequent stage of ovarian follicle development [31]. This previous study used a systems approach to elucidate the suite of genes involved in initiating the development of arrested primordial follicles to initiate folliculogenesis. In the current investigation, whole rat ovaries from zero-day old rats were cultured *in vitro* in a manner that allows primordial follicle assembly to occur. The ovaries were treated with one of several different extracellular signaling factors that have been shown to regulate follicle assembly. Messenger RNA was isolated from the ovaries and used for microarray transcriptome analysis to globally survey gene expression under these different treatment conditions. The effects of each signaling factor treatment were analyzed to determine similarities and differences in gene expression between the treatments. A gene bionetwork analysis subjected all the differentially expressed genes across all treatments to a weighted co-expression cluster analysis to identify groups of genes (i.e. modules) whose expression was regulated in a coordinated and interconnected manner [32-35]. In this type of analysis biological systems are surveyed with microarrays multiple times with and without perturbations that cause the system to change. The coordinately and interconnected expressed gene modules identified are often associated with specific physiological processes and have been used to identify potential therapeutic targets [32,36,37]. In addition, the various groups and modules of genes identified were subjected to an unbiased gene network analysis that compared gene lists to databases of known gene binding and/or functional relationships. The gene expression analyses can then be interpreted from the standpoint of physiological function and important regulatory gene networks. The objective of the investigation was to use a systems biology experimental approach to identify gene expression networks involved in regulating primordial follicle assembly. Novel regulatory factors and potential therapeutic targets were identified that correlate with normal follicle assembly and associated ovarian disease.

Results

Actions on primordial follicle assembly

In the selection of regulatory factors to be used in the current study one novel factor was considered. Previous research [1,30] indicated that FGF2 might be a regulatory growth factor for the follicle assembly process. In order to determine if FGF2 would be included as a treatment in the current study, organ culture experiments were performed to empirically test the effects of FGF2 on follicle assembly. Ovaries from zero-day old rats containing un-assembled oocytes in nests (Figure 1A) were placed into an organ culture system and cultured for two days with or without FGF2. After culture ovaries

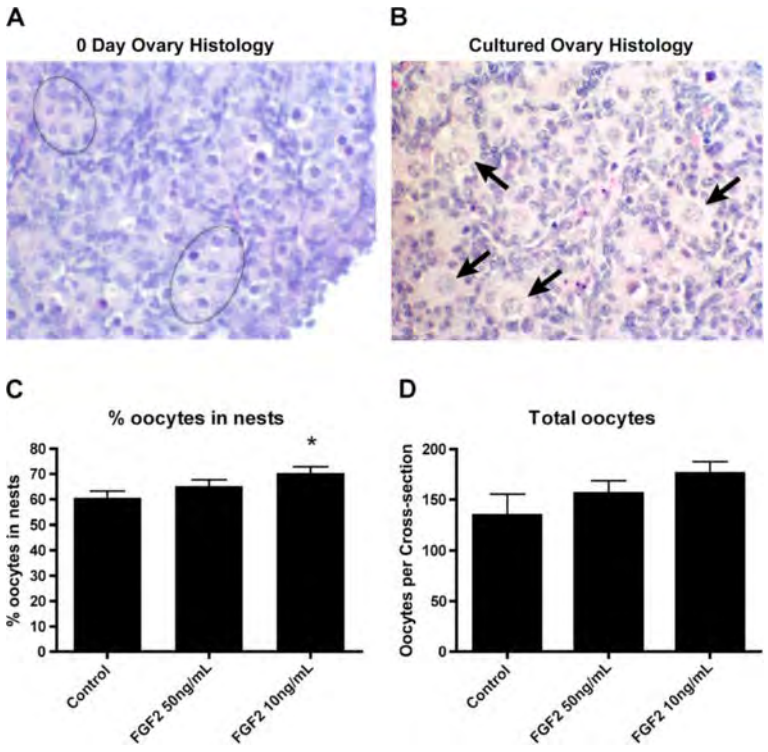

Figure 1 Validation of FGF2 as a growth factor that affects primordial follicle assembly. A) Representative image of a 0-day old rat ovary, showing oocytes in nests (circle nests). **B)** Representative image of an ovary after two days in culture, showing some oocytes assembled into primordial follicles (arrows). **C)** Proportion of oocytes still retained in nests after two days of culture with or without FGF2 treatment. **D)** Total number of oocytes per ovarian cross-section after culture. * = $p<0.05$ compared to untreated Control by Student's *t*-test.

were fixed, sectioned, stained and evaluated morphologically (Figure 1B). The number of oocytes in oocyte nests and assembled into primordial follicles was observed (see Methods). Results indicate that treatment with 10ng/ml FGF2 resulted in a modest but statistically significant increase in the proportion of oocytes retained in unassembled nests (Figure 1C). A larger duration culture of four days promotes a greater magnitude response, but is a combined effect of oocyte survival and follicle assembly, such that the shorter duration culture was used to focus on follicle assembly. A 50 ng/ml dose did not have an effect in comparison with the 10 ng/ml dose which is assumed to be due to negative feedback regulation during the 2 day culture period required. There was no statistical difference in the total number of oocytes per ovarian cross-section with FGF2 treatment (Figure 1D), although there was a trend for oocyte numbers to rise. Observations suggest FGF2 acts to inhibit the follicle assembly process. Based on these results it was decided that FGF2 be included as a treatment in the follicle assembly network experiments.

Growth factor and hormone regulation of the ovarian transcriptome

To determine the gene networks and processes involved in follicle assembly ovaries from zero-day old rats were placed into an organ culture system and exposed to different regulatory factors. The ovaries were treated for 24 hours with one of each of the following regulatory extracellular signaling factors: AMH, CTGF, E2, FGF2, activin A, P4, TNFa, or were untreated as Controls. CTGF, activin A, estradiol have been shown the increase assembly, while AMH, progesterone and TNFa decrease assembly. A 24 hour culture period was used to minimize the impact of differences in follicle numbers (morphological impact), due to the required 2 days of culture to observe detectable morphological differences. After culture the ovaries receiving the same treatment from one culture well were pooled and RNA isolated. There were three different experiments involving different ovaries for each of the seven treatment compounds, and seven different experiments with different ovaries for the controls, for a total of 28 samples (see Methods). Gene expression in the RNA samples was evaluated using Affymetrix© Rat Gene 1.0 ST microarrays. Array data pre-processing and evaluation determined that one array (P4-treated) was abnormal and an outlier, so that array was eliminated from further analysis (Additional file 1: Figure S1).

The sets of differentially expressed genes, defined as signature lists, in the treated ovary groups compared to

controls were identified using criteria as described in Methods. A total of 1081 genes were differentially expressed in ovaries treated with these known regulators of follicle assembly, suggesting these genes are involved in the ovarian primordial follicle assembly process. Whether the specific genes have an increase or decrease in expression is shown in Additional file 2: Table S1. Each treatment resulted in 50 to 303 genes being differentially expressed compared to controls. Interestingly, there were relatively few (5-10%) differentially expressed genes in common between the different treatments (Figure 2) as indicated for specific genes in Additional file 2: Table S1. Only one gene, the growth factor staniocalcin 1, was differentially expressed in as many as four different treatments, and no other genes were differentially expressed in more than three treatments (Additional file 2: Table S1). These genes in these signature lists were categorized into gene functional categories. The metabolism and transport, signaling, and receptors and binding proteins were predominant categories for all treatments (Figure 3 and Additional file 1: Table S1).

Primordial follicle assembly pathway analysis

The complete list of 1081 differentially expressed genes from the signature lists were correlated to curated cellular pathway and process gene lists from the KEGG database (see Methods) to identify physiological processes and pathways that may be regulated during follicle assembly. Pathways that were statistically over-represented within the differentially expressed gene lists included focal adhesion, chemokine signaling, cytochrome P450 metabolism, glutathione metabolism, ECM-receptor interaction and ribosomal components (Additional file 3: Table S2). There was a high degree of overlap of affected pathways between different treatments (Figure 2). The statistical analysis used both a hypergeometric probability calculation and Fishers exact test calculation to identify statistical likelihood of over-representation of differentially expressed genes in pathways (Additional file 3: Table S2). This analysis reduces the variable of data set size and potential for artifact generation by identifying those pathways with over-representation having differentially expressed genes from several treatments. As can be seen, not all pathways had statistical significance while others consistently did (Additional file 4: Figure S2). From 44% to 87% of affected pathways were common between treatments. According to Fisher's Exact test the probability that our list of differentially expressed genes randomly overlaps with the pathways is negligible (~1/2000 chance), particularly since we had many genes falling in more than one pathway. As can be seen in Additional file 3: Table S2 and Figure 4, most affected pathways contained differentially expressed genes from several different treatments. As shown in the focal adhesion pathway, five of the factors affected genes in the same pathway (Figure 4). Therefore, each of these extracellular signaling factors that were used as treatments affected similar pathways via different genes. There were isolated exceptions to this trend. For example, all of the genes present in the ribosome process pathway were induced by activin A treatment, and four of five genes in the GABAergic synapse pathway were induced by FGF2 (Additional file 3: Table S2).

Primordial follicle assembly bionetwork analysis

Gene expression level data from the entire set of 1081 differentially expressed genes was subjected to a cluster analysis to identify groups (i.e. modules) of genes whose expression is regulated in a coordinated and interconnected manner (see Methods). The cluster analysis scores each gene according to how well across different

		AMH	CTGF	E2	FGF2	Activin	P4	TNFa
	# genes	#PW 73	9	79	115	83	85	63
AMH	158		4	45	63	43	41	29
CTGF	50	2		7	8	7	7	5
E2	120	10	0		69	49	49	38
FGF2	303	13	4	9		71	70	50
ActivinA	287	11	1	4	14		52	40
P4	167	5	3	8	11	14		43
TNFa	116	6	4	4	7	9	3	

Number (#) of pathways overlapped

Number (#) of genes overlapped

Figure 2 Number of genes and physiological pathways overlapped between treatment group (signature) lists. Total number of differentially expressed genes for each treatment is shown in dark yellow column, while numbers of genes in common between each pair of treatment groups are in light yellow columns. Total number of KEGG pathways affected by each treatment is shown in dark green row; numbers of KEGG pathways in common for each pair of treatment groups are shown in light green rows. A KEGG pathway is considered affected if ≥ 3 differentially expressed genes are present in the pathway.

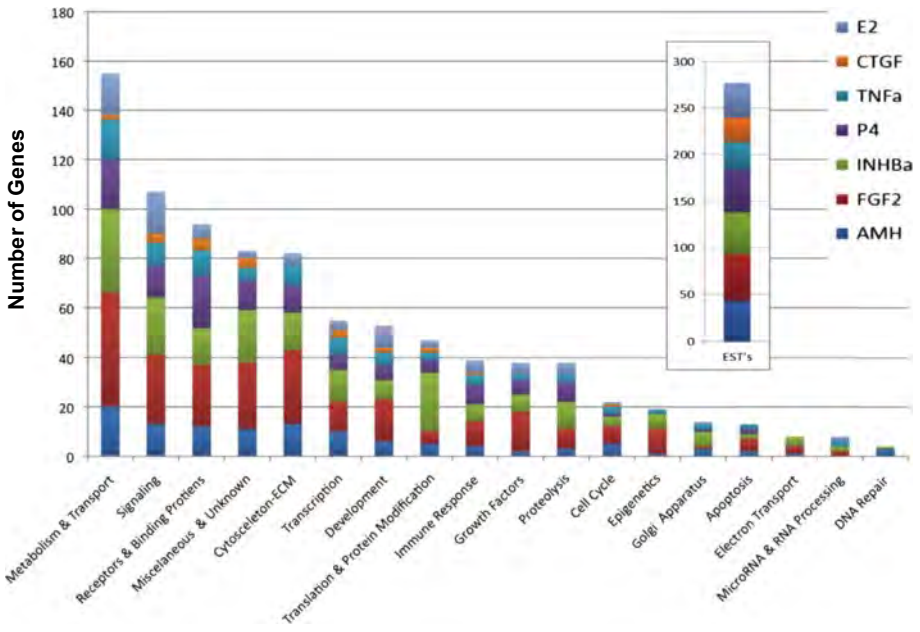

Figure 3 Numbers of genes with mRNA expression levels significantly different between Control and treated ovaries after two days of culture. Genes are placed into functional categories.

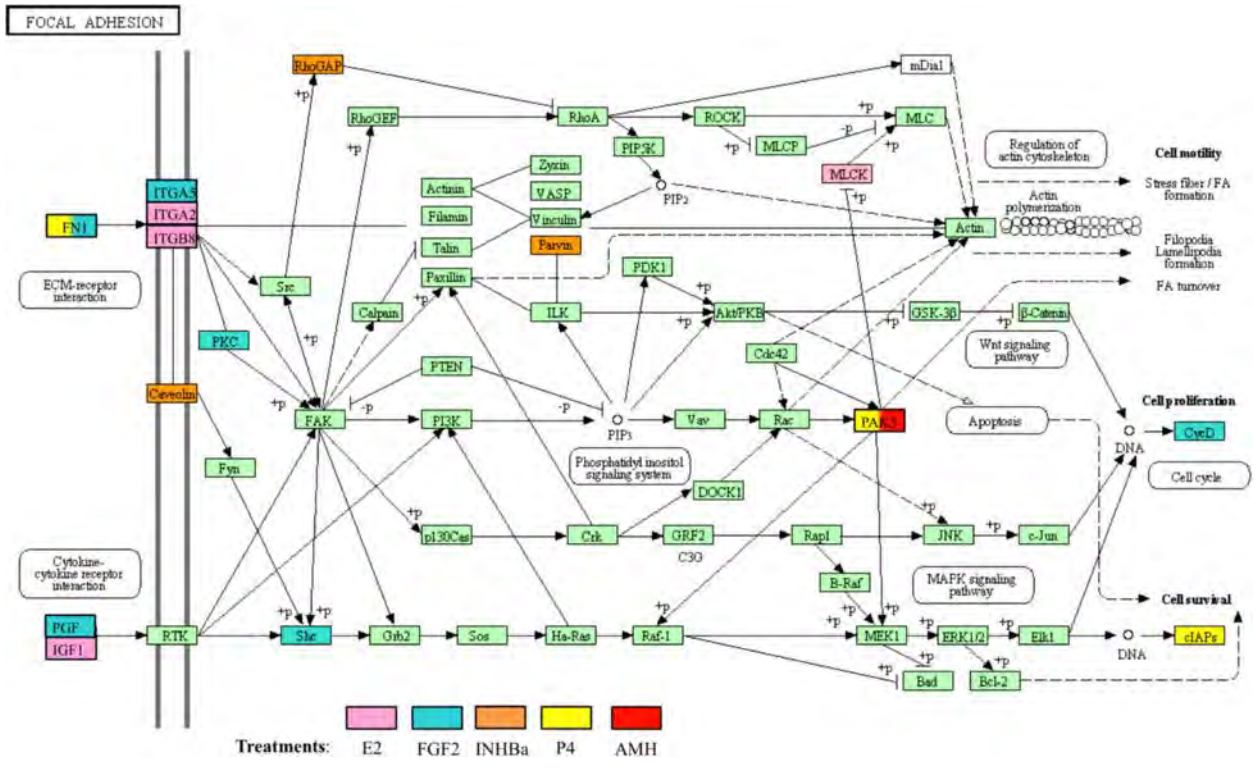

Figure 4 Focal adhesion signaling pathway highlighting those genes that are differentially expressed compared to untreated control ovaries and identifying by color the treatment group(s) from which the differentially expressed genes came. Adapted from KEGG pathway rno04510, Kanehisa Laboratories, Kyoto University, Japan.

treatments its changes in gene expression are correlated with the changes in expression of every other gene. High connectivity scores indicate that expression of a particular gene changes in concert with that of many other genes. In addition, the cluster expression analysis identifies gene modules in which the member genes have similar changes in expression in response to the various experimental treatments. Such gene modules are often associated with specific biological processes [32]. To identify gene modules, a topological overlap matrix [37] was generated that reflected connectivity scores and sorted genes based on an agglomerative hierarchical clustering algorithm (see Methods). The topological overlap matrix map with gene modules color-coded for the nine modules identified is shown in Figure 5. The module to which each gene belongs can be found in Additional file 2: Table S1. The nine modules contained collectively 851 genes with the remaining 230 genes (colored as grey) not falling into any module. The list of differentially expressed genes in each module was correlated to signaling pathway and cellular process databases to determine if specific physiological processes were associated with particular modules (see Methods). Those pathways and processes statistically over-represented for each module are shown in Table 1.

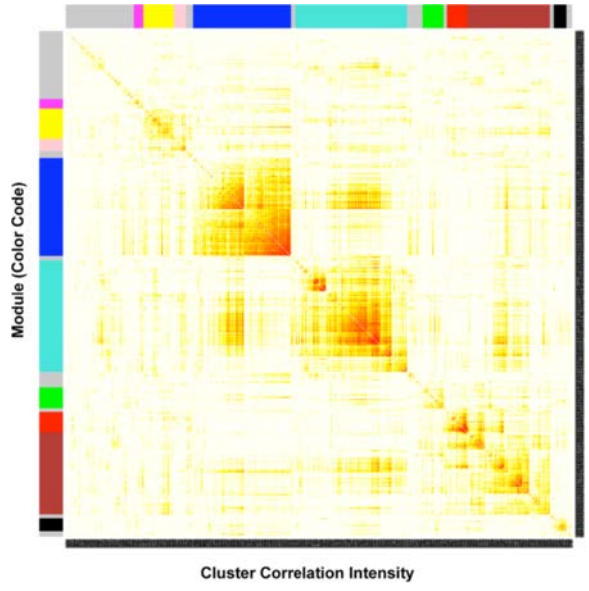

Figure 5 Gene cluster analysis and corresponding gene modules. A topological overlap matrix of the gene co-expression network consisting of the 1081 genes regulated by the various ovary treatments is shown. Genes in the rows and columns are sorted by an agglomerative hierarchical clustering algorithm (see Methods). The different shades of color signify the strength of the connections between the nodes (from white signifying not significantly correlated to red signifying highly significantly correlated). The hierarchical clustering and the topological overlap matrix indicate highly interconnected subsets of genes (modules). Modules identified are colored along both column and row and are boxed.

Table 1 Gene category overlap with modules

Module	Gene category	Gene number module overlap*	Over representation fisher P-value†
Turquoise	Ribosome	10	7.52E-08
Turquoise	cytosolic ribosome	7	2.40E-06
Turquoise	Neural tube closure	4	0.00041
Turquoise	Negative regulation of binding	5	0.00045
Turquoise	Primary neural tube formation	4	0.00056
Turquoise	Protein biosynthesis	15	0.00071
Turquoise	Glutathione metabolism	5	0.0011
Blue	Response to oxidative stress	12	1.30E-06
Blue	Regulation of anatomical structure morphogenesis	13	2.20E-06
Blue	Mesoderm development	18	1.90E-05
Blue	Angiogenesis	6	2.20E-05
Blue	Response to carbohydrate stimulus	6	3.60E-05
Blue	Regulation of axonogenesis	6	5.00E-05
Blue	Membrane raft	9	7.80E-05
Blue	negative chemotaxis	3	1.00E-04
Blue	Axon guidance	6	3.70E-03
Blue	Glutathione metabolism	3	3.10E-02
Blue	Focal adhesion	6	3.20E-02
Blue	Fc gamma R-mediated phagocytosis	4	3.60E-02
Blue	MAPK signaling pathway	6	8.50E-02
Brown	Germ cell nucleus	3	7.00E-04
Brown	Male meiosis	3	0.0015
Brown	Neurite regeneration	3	0.0031
Brown	Condensed nuclear chromosome	3	0.0041
Brown	Other oncogenesis	3	0.0074
Brown	Cell cycle	4	0.026
Brown	Olfactory transduction	12	0.065
Yellow	Hematopoietic cell lineage	3	0.0027
Yellow	Positive regulation of apoptosis	5	0.009
Yellow	Coenzyme and prosthetic group metabolism	3	0.015
yellow	Mitochondrial lumen	3	0.018
Green	proteinaceous extracellular matrix	3	0.0072
Black	Extracellular matrix	4	0.00015
Black	extracellular region	7	0.00042
Black	Response to stress	8	0.002
Black	Cell communication	6	0.0029
Black	Negative regulation of apoptosis	4	0.0029
Pink	Apical plasma membrane	3	0.0011
Pink	Protein glycosylation	3	0.0018
Magenta	Calcium mediated signaling	2	0.0066

*Gene Number Module Overlap is the number of genes from that module that are in common with those in the listed physiological process or pathway (see Methods).
†Fisher's Exact test was used to calculate a p-value reflecting the probability that the specified module and pathway/process would have listed number of overlapped genes.

The turquoise module predominately contains genes coding for ribosomal components and genes involved in protein and glutathione metabolism. The blue module contains genes involved in processes related to tissue morphogenesis. The red module has genes involved with germ cells and meiosis. Some physiological processes, such as apoptosis and extracellular matrix function, were over-represented in several modules. However, in general the genes of different modules were over-represented in different cellular pathways and processes (Table 1).

Genes whose expression altered in response to treatments were correlated with the genes assigned to each module to determine if specific modules were heavily influenced by particular regulatory factors (Figure 6). In most cases, differentially expressed genes from each treatment group could be found in each of the modules. However, some modules had strikingly high numbers of genes in common with specific treatments. For example, among the 240 genes of the turquoise module and the 287 genes of the activin A treatment group, 184 genes were in common. Interestingly, these included 10 of the 11 differentially expressed genes that populated the ribosomal component process. In addition, among the 209 genes of the blue module and the 303 genes of the FGF2 treatment group, 169 genes were in common. Similarly, there were 58 genes in common between the brown module and the P4 treatment group, and these included 8 of the 19 genes that populated the olfactory transduction pathway (Figure 6).

Primordial follicle assembly gene network analysis

In order to determine what functional relationships and gene networks exist between the differentially expressed genes identified, the complete list of 1081 genes was subjected to an automated unbiased analysis of published literature using Pathway Studio software (Elsevier Inc. Rockville, MD USA), (see Methods). A total of 326 genes were found to form a gene network that linked neighboring genes together with regulatory or binding relationships. While this network was too large and complex for easy visual interpretation (Additional file 4: Figure S2), inferences about the genes involved can be obtained. Genes with the greatest number of putative regulatory connections to neighbors in the network were considered to be important in controlling the follicle assembly process, either as upstream regulators of the assembly network or as downstream targets of the network. The genes with the most connections to neighbors in the network of 326 genes were *Il1b* (interleukin 1 beta; 144 connections), *Fn1* (fibronectin 1; 100 connections) and *Igf1* (insulin-like growth factor 1; 99 connections) (Additional file 4: Figure S2).

Each module of coordinately regulated genes was subjected to gene network analysis to determine which genes within a module formed a gene network as shown in Figure 7. A network for the turquoise module identified *Fn1, Stat1* (signal transducer and activator of transcription 1) and *Vcam* (vascular cell adhesion molecule 1) as having many connections, suggesting they may play a role in controlling the physiological processes mediated by the turquoise module. For the blue module (Additional file 5: Figure S3A) *Cav1* (caveolin), *Anxa2* (annexin A2), *F3* (coagulation factor 3, thromboplastin) and *Ccnd1* (cyclin D1) have the most neighbor connections. *F3* and *Ccnd1* are seen to be primarily the recipients of the regulatory relationships suggesting their regulation may be an important output of the blue module network. Although relatively small, the black module also formed a network of connected genes (Additional file 5: Figure S3B). The growth factors *Igf1* and *Il1b* have the most neighbor connections. The remaining modules did not form significant networks of genes related to each other, even though many of these modules had more genes than were present in the black module.

Each treatment signature list of differentially expressed genes was analyzed to determine which genes formed a gene network of regulatory relationships. For the genes of the E2 treatment group, *Igf1* is seen to have many

		turquoise	blue	brown	yellow	green	red	black	pink	magenta
	# genes	240	209	176	65	45	43	27	26	20
AMH	158	14	7	28	19	**25**	0	0	7	3
CTGF	50	0	4	8	1	1	5	2	3	4
E2	120	1	6	3	20	8	**14**	**15**	9	4
FGF2	303	4	**169**	44	28	9	1	0	2	4
INHBa	287	**184**	24	26	5	2	**15**	0	**14**	1
P4	167	16	5	**58**	11	0	8	6	7	4
TNFa	116	**36**	10	19	6	4	2	4	0	6

Figure 6 Numbers of genes found to be in common when comparing genes differentially expressed in various ovary culture treatment groups (left column) with differentially expressed genes assigned to co-expression modules (top row). Numbers in bold type indicate a high number of genes in common with a treatment compared to others for that module (column). Underlined numbers indicate a high number of genes in common with a module compared to others for that treatment (row).

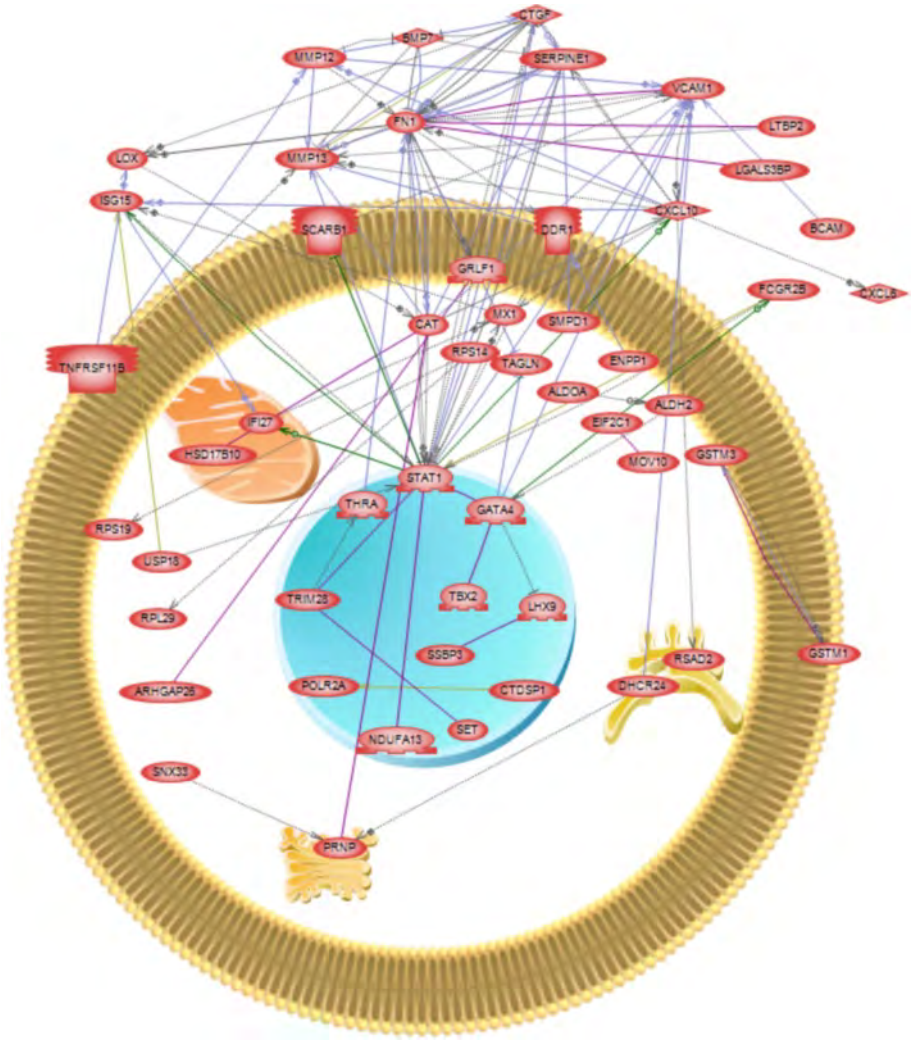

Figure 7 Gene network of known relationships among those differentially expressed genes assigned to the turquoise module. Node shapes code: oval – protein; diamond – ligand; irregular polygon – phosphatase; circle/oval on tripod platform – transcription factor; ice cream cone – receptor. Grey arrows represent regulation, lilac – expression, green – promoter binding, olive – protein modification, purple - binding. Plasma membrane, cell nucleus, mitochndria, golgi apparatus and endoplasmic reticulum are indicated for gene expression localization.

neighbor connections (Additional file 6: Figure S4A). For the FGF2 treatment network *Vcam, Vim* (vimentin) and *Tgfb2* (transforming growth factor beta 2) have many neighbor connections, while *Ccnd1* and *F3* appear to be outputs of the network (Additional file 6: Figure S4B). For the activin A treatment group, the transcription factor *Stat1* and the growth factor *Cxcl10* have many connections, while *Fn1* appears to be an output (Additional file 6: Figure S4C).

In order to determine those genes whose actions are likely to be the most important in regulating the control of primordial follicle assembly, a combined approach was taken that determined the gene network associated with the most highly interconnected genes. For each module, the top 10% of genes with the highest connectivity index (k.in.) (i.e., those that are the most tightly co-regulated within their module) were selected. These genes were then screened for whether they were present in the large network of 326 genes with known regulatory connections derived from the entire list of 1081 differentially expressed genes (Additional file 4: Figure S2). Those genes from the top 10% of each module (tightly co-expressed) that also had the most neighbor connections (regulatory relationships) are presented in Table 2. These included the transcriptions factors *Ppargc1a* and *Gata4*, the growth factor *Tgfb2*, the transferrin receptor (*Tfrc*), *Mdm2* and *Prkcb* (protein kinase C beta). These genes formed a regulatory network among themselves, and were associated with specific pathways and cellular processes. As can be seen in Figure 8, these genes have been previously shown to influence the processes of apoptosis, vascularization, contraction, cell migration, proliferation and differentiation.

Table 2 Gene connectivity ranking information

Name / symbol gene	Gene description	Local connectivity *
TNFRSF1A	Tumor necrosis factor receptor superfamily, member 1A	37
TGFB2	Transforming growth factor, beta 2	36
MDM2	Mdm2 p53 binding protein homolog (mouse)	27
GATA4	GATA binding protein 4	27
PPARGC1A	Peroxisome proliferator-activated receptor gamma, coactivator 1 alpha	26
PRKCB	Protein kinase C, beta	25
TFRC	Transferrin receptor (p90, CD71)	23
ANXA5	Annexin A5	20
ANXA2	Annexin A2	20
SDC4	Syndecan 4	16
LRP2	Low density lipoprotein-related protein 2	16
GRLF1	Glucocorticoid receptor DNA binding factor 1	15
GSTP1	Glutathione S-transferase pi 1	14
HSD11B1	Hydroxysteroid (11-beta) dehydrogenase 1	13
UCP2	Uncoupling protein 2 (mitochondrial, proton carrier)	12
THRA	Thyroid hormone receptor, alpha (erythroblastic leukemia viral (v-erb-a) oncogene homolog, avian)	10
ANPEP	Alanyl (membrane) aminopeptidase	10
IL1R1	Interleukin 1 receptor, type I	9
EPHA2	EPH receptor A2	9
CTSK	Cathepsin K	8
SMPD1	Sphingomyelin phosphodiesterase 1, acid lysosomal	8

*Local connectivity is the number of regulatory connections which that gene has with other genes, identified in published literature, within the gene network of 326 genes derived from the complete set of 1081 differentially expressed genes (see Additional file 4: Figure S2).

Other groups of differentially expressed genes examined were the growth factor, hormone and receptor families. These genes provide novel regulatory factors to be investigated in future studies in their role in controlling ovarian primordial follicle assembly. A subset of the entire set of 1081 differentially expressed genes, comprised of growth factors, hormones and their receptors was evaluated for their ability to form a sub-network of regulatory connections. A sub-network of 52 genes was identified showing the regulatory connections between these growth factors and receptors (Figure 9).

Primordial follicle assembly signaling pathway modulation and validation

As described above, specific physiological processes and pathways are over-represented in the lists of differentially expressed genes identified in these studies (Table 1 and Additional file 3: Table S2), and so are predicted to be important in regulating follicle assembly. The MAPK signaling, focal adhesion and chemokine signaling pathways are over-represented in particular gene modules or in the global set of all 1081 differentially expressed genes. ERK1/2 (MAPK1) is a kinase that plays a prominent role in these pathways (Figure 4). ERK1/2 activity is inhibited by Dusp6 (dual specificity phosphatase 6; MKP-3) [38]. In order to test if these physiological pathways are in fact important to the assembly process, ovaries from 0-day old rats were treated in vitro for 2 days with the inhibitor of DUSP6: BCI ((E)-2-benzylidene-3-(cyclohexylamino)-2,3-dihydro-1H-inden-1-one [39,40]. Dusp6 inhibition resulted in a significant increase in the proportion of assembled follicles at the end of ovary culture with no effect on oocyte numbers (Figure 10). Therefore, alteration of ERK1/2 signaling in physiological pathways predicted to be important for follicle assembly resulted in a change in the rate of assembly of primordial follicles.

Primordial follicle assembly regulated gene correlation with ovarian disease

The final analysis identified those differentially expressed genes associated with ovarian disease. The genes within the differentially expressed gene lists (Additional file 2: Table S1) that have previously been shown to be linked in the literature with primary ovarian insufficiency (POI) and polycystic ovarian syndrome (PCOS) were identified (Figure 11). Seventeen genes associated with POI and PCOS were identified and two genes, Igf1 and Tgfbr3 were common to both POI and PCOS.

Discussion

A systems biology approach was used to elucidate how regulatory factors alter gene expression to influence ovarian primordial follicle assembly. Neonatal rat ovaries were treated with different growth factors or hormones and changes in gene expression at the transcriptome level were assayed and analyzed. The strength of a systems biology approach is that it is unbiased and examines the genome wide complexity of gene expression to elucidate regulatory networks that control developmental processes. These genes are identified regardless of whether they have known functions consistent with the follicle assembly process or whether they have known functions at all. The unbiased systems analysis allows the complexity of the biology to be considered to elucidate the developmental process. Future investigations can now target identified genes to further characterize their specific actions in the networks regulating follicle assembly.

Primordial follicle assembly growth factors and hormones investigated

Ovaries were treated with several different growth factors or hormones that affect the assembly process to get a more complete view of the gene expression changes

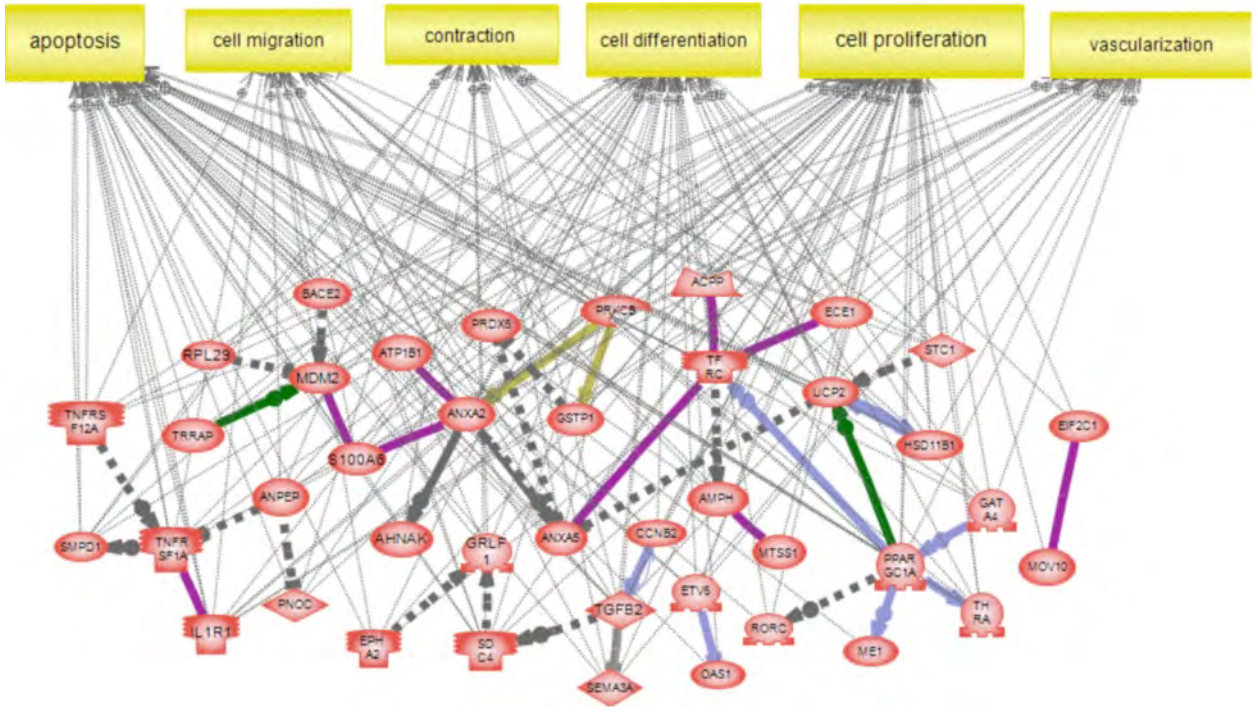

Figure 8 Gene network of known relationships and associations with specific cell processes for those differentially expressed genes from the top 10% of each module that also had the most neighbor connections (see Table 2 for list). Node shapes code: oval and circle – protein; diamond – ligand; irregular polygon – phosphatase; circle/oval on tripod platform – transcription factor; ice cream cone – receptor. Grey rectangles represent cell processes; arrows with plus sign show positive regulation/activation, arrows with minus sign – negative regulation/inhibition. Grey arrows represent regulation, lilac – expression, green – promoter binding, olive – protein modification.

accompanying primordial follicle assembly. A number of growth factors and hormones previously shown to influence primordial follicle assembly were selected including: AMH [1], CTGF [16], estradiol [17-21], progesterone [18,22,23], activin A [21], and TNFa [23,24]. The combined actions of factors on assembly has not been thoroughly investigated, but studies on follicle transition have shown combined stimulatory or inhibitory factors does not provide an additional response different from the individual factors [3]. All of the growth factors and corresponding receptors, as well as hormone receptors, associated with the factors used have been shown to be expressed in the ovary during primordial follicle assembly. For example, AMH is expressed in the stromal/interstitial cells of the 0 day ovary followed by expression later in development by the secondary and developing follicles [1]. Interestingly, some of the factors promote follicle assembly (CTGF, activin A, estradiol), while others (AMH, progesterone, TNFa, FGF2) inhibit follicle assembly. Therefore, both positive and negative regulation of follicle assembly is considered when characterizing the regulatory gene networks. Comparison of the stimulatory versus inhibitory factors did not show any major differences in regards to regulated genes or gene networks.

In addition to these known regulatory agents, a novel factor was examined and included in the analysis. Previous research suggested FGF2 may be a regulator of follicle assembly. A receptor for FGF2, FGFR2B, has previously been shown to be differentially expressed in 0-day old rat ovaries with oocyte nests compared to 4-day old ovaries that had completed assembly [30]. Treatment of neonatal rat ovaries with the known inhibitor of follicle assembly AMH resulted in differential expression of *Nudt6* (*nudix 6*) [41], which acts as an antisense inhibitor of *Fgf2* expression [42]. In order to determine if FGF2 would be included as a treatment in the current investigations, organ culture experiments were performed to empirically test the effects of FGF2 on follicle assembly. It was found that FGF2 acts as an inhibitor of follicle assembly (Figure 1). The magnitude of the inhibitory actions can be increased with an extended culture duration (four days), but then alterations in follicle number and ovarian morphology become confounders influencing data interpretation. A short 2-day culture was used to reduce these confounder effects. The optimal dose for the analysis of in vitro follicle assembly analysis was lower than that for the short-term 24-hour culture gene expression analysis, in part due to the negative feedback of the extended culture duration.

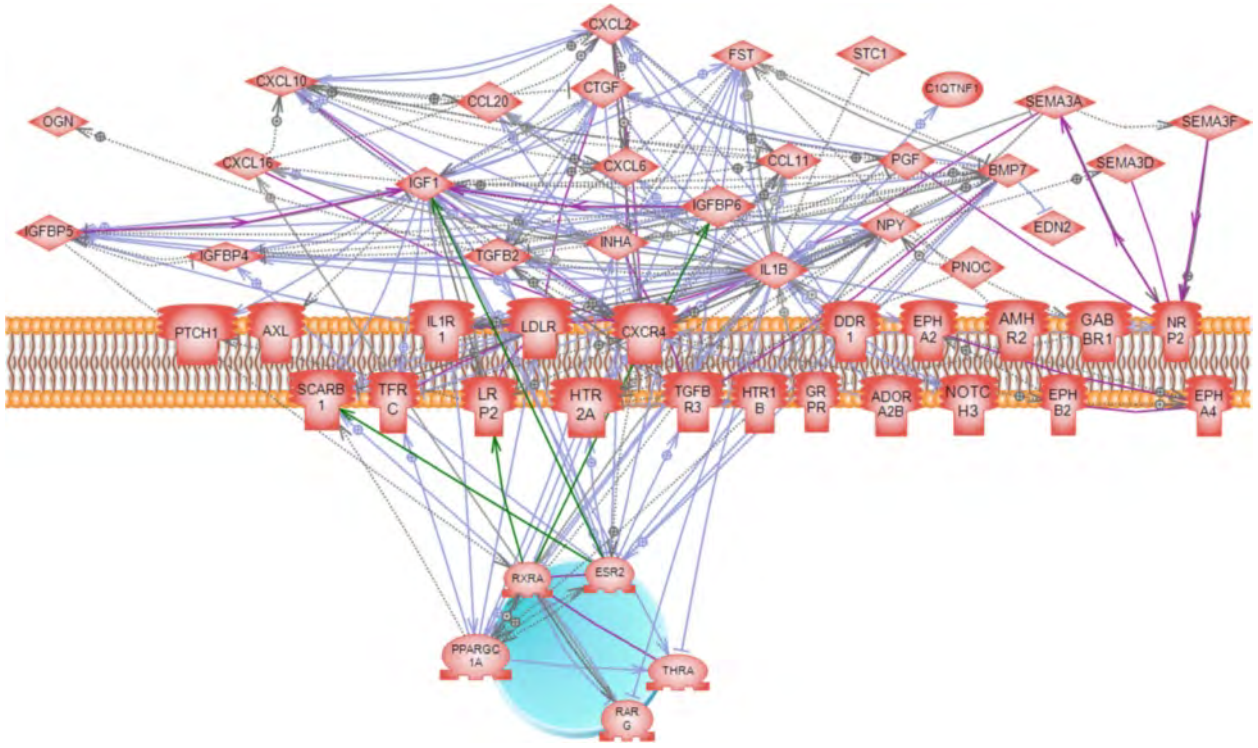

Figure 9 Gene network of known relationships among those differentially expressed genes that were extracellular signaling factors, growth factors, growth factor binding proteins, growth factor receptors or hormone receptors (see Additional file 2: Table S1: categories 'Growth Factors' and 'Receptors & Binding Proteins'). Node shapes code: oval – protein; diamond – ligand; circle/oval on tripod platform – transcription factor/hormone receptor; ice cream cone – receptor. Grey arrows represent regulation, lilac – expression, green – promoter binding, olive – protein modification, purple - binding. Plasma membrane and cell nucleus are indicated for gene expression localization.

The FGF2 was found to alter the expression of 303 genes with approximately 10% of these genes in common with the differentially expressed gene sets of the other features. Although the differentially expressed genes influenced by FGF were unique, 50–70 different pathways were affected and in common with other factors investigated, (Figure 2). Therefore FGF2 was included as one of the seven treatments used to perturb the neonatal rat ovary experimental system.

Primordial follicle assembly differentially expressed genes

One thousand and eight-one genes were found to be differentially expressed compared to controls when results were combined across the different treatment groups. These genes were predominantly from the functional categories of metabolism and transport, signaling proteins and receptors. The genes differentially expressed in response to each growth factor or hormone treatment were compared across the different treatments. Interestingly, only a small proportion of differentially expressed genes (<10%) were found to be common between any two treatments (Figure 2). This is somewhat surprising in light of the fact that all the treatments affect the same process of follicle assembly. However, this same finding was observed in a systems biology investigation of genes regulating ovarian primordial to primary follicle transition [31]. In that study different treatments, all known to regulate the transition of arrested primordial follicles to developing primary follicles, were found to have few differentially expressed genes in common. Although neither this previous study nor the current study found a high degree of overlap between the specific treatment signature gene lists, there was a high degree of overlap among the specific signaling pathways and cellular processes impacted by the differentially expressed genes of each treatment (Figures 2 and 3). This indicates that all the treatments affect similar cellular pathways and processes as follicle assembly occurs (44% to 87%), but that each treatment affects different genes in those pathways. As shown in Additional file 2: Table S2, some pathways had a highly statistically significant over-representation of differentially expressed genes while others did not, suggesting the analysis was not unduly influenced by data set size or simply an artifact of the analysis. An example of this is shown in Figure 4 where five of the different factors affected different genes in the focal adhesion pathway. Similar observations have shown this phenomena in other biological systems [43]. Multiple

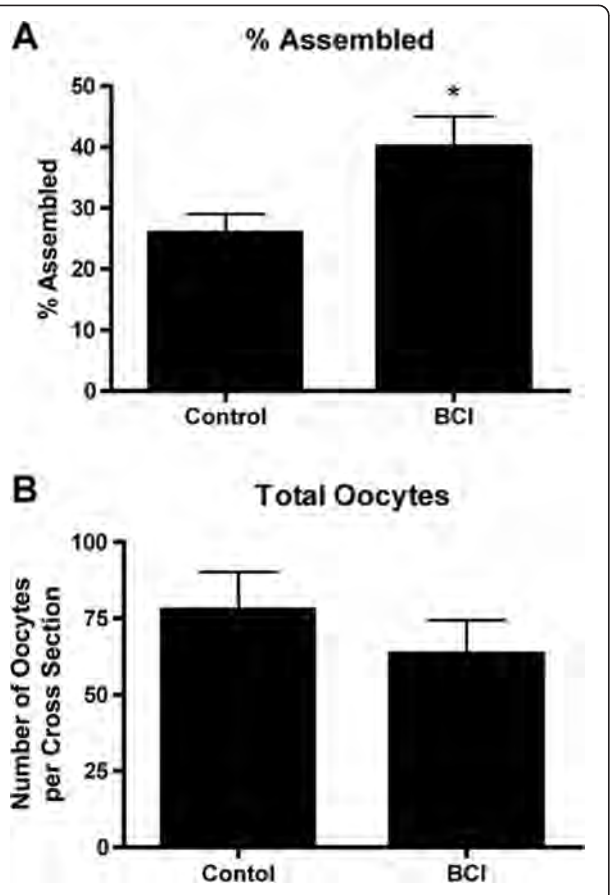

Figure 10 Results of experiments in which 0-day old ovaries were cultured two days with or without BCI (an inhibitor of DUSP6 that results in increased ERK12/MAPK1 activity). A) Proportion of oocytes still assembled into follicles. **B)** Total number of oocytes per ovarian cross-section after culture. * = $p<0.05$ compared to untreated vehicle-treated Control by Student's *t*-test. Mean ± SEM from three different experiments is presented.

input points into these cellular pathways and processes may allow for more precise regulation and for a more robust regulatory network in the face of disruptions.

A cluster analysis of coordinated gene expression grouped the differentially expressed genes into gene modules containing genes whose expression responded in concert to the different growth factor and hormone treatments. This approach of generating a weighted gene network and then clustering genes making use of a topological overlap matrix has been used extensively for uncovering biologically meaningful gene modules [31,32,44-46]. The gene modules identified in the current study were, on the whole, each enriched with genes associated with differing cellular pathways and processes (Table 1). For example, the turquoise module contains genes coding for ribosomal components, while the blue module contains genes involved in processes related to tissue morphogenesis, and the red module has genes associated with meiosis. This suggests that these modules of genes are each responsible for controlling distinct functions necessary for primordial follicle assembly. In contrast, most modules were enriched for genes involved in apoptosis and extracellular matrix function, perhaps underscoring the importance of these processes to follicle assembly. Oocyte apoptosis is known to have a vital role in the assembly of primordial follicles [3,6,12,13]. Identification and examination of the gene modules helps elucidate the molecular control of follicle assembly.

When genes whose expression changed in response to treatments were cross-matched with the genes assigned to each module, it was found that in most cases differentially expressed genes from each treatment group could be found in all the gene modules (Figure 6). This is consistent with the idea that all the treatments affect the same cellular processes, but that each treatment affects different genes within those pathways. However, it should be noted that in some cases a particular treatment shared a disproportionate number of genes within a specific module. For example, the activin A treatment resulted in differential expression of 287 genes, of which 184 were in common with the 240 genes assigned to the turquoise module, and these included almost all the genes that coded for ribosomal components. Therefore, in some cases signaling from a particular growth factor will induce a suite of genes that may be targeted toward specific physiological tasks.

Primordial follicle assembly gene networks

In order to identify functional relations among differentially expressed genes, an analysis of published literature was used to detect connections among listed genes to form gene networks of putative regulatory relationships. Examination of these networks can yield inferences about how genes interact to regulate primordial follicle assembly, and can identify potentially important control points within these regulatory networks. When the entire list of genes found to be differentially expressed during follicle assembly was analyzed in this way it was found that the genes *Il1b* (interleukin 1 beta), *Fn1* (fibronectin 1) and *Igf1* (insulin-like growth factor 1) had the most regulatory connections to neighbors. These genes are considered important in controlling the follicle assembly process as either regulators of the assembly network or as downstream effectors of the network. However, it should be kept in mind that genes that have been extensively studied are more likely to have relationships with other genes in the published literature, and that un-studied genes may in fact be important. Nonetheless, gene networks of regulatory connections provide a good starting point toward understanding the control of processes such as follicle assembly.

Since the genes of each module may act in concert to accomplish distinct cellular processes during follicle

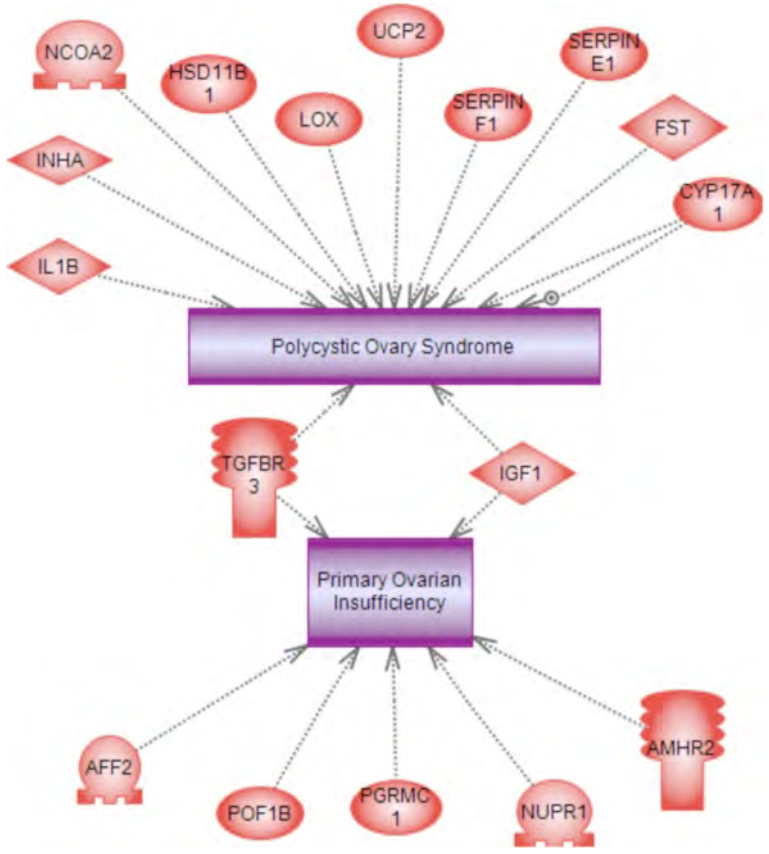

Figure 11 Genes differentially expressed during follicle assembly that are also known to be associated with the adult-onset diseases primary ovarian insufficiency and polycystic ovarian syndrome. Node shapes code: oval – protein; diamond – ligand; circle/oval on tripod platform – transcription factor; ice cream cone – receptor.

assembly, each module was analyzed separately for gene networks of putative regulatory relationships. The genes of the turquoise, blue and black modules each formed distinct gene networks (Figure 7 and Additional file 5: Figure S3), implicating the genes *Fn1*, *Stat1* (signal transducer and activator of transcription 1), *Vcam* (vascular cell adhesion molecule 1), *Cav1* (caveolin), *Anxa2* (annexin A2), *F3* (coagulation factor 3), *Ccnd1* (cyclin D1), *Igf1* and *Il1b* as being important within their respective modules. Interestingly, genes of the brown, yellow, green, red, pink and magenta modules did not contain gene networks of known regulatory relationships, even though some of these modules contained many more genes than the black module, which did have such a network. This suggests that the genes within each of these modules may have as yet un-characterized regulatory relationships with each other. Furthermore, the genes of the red module were not found to be over-represented in association with any particular known cellular pathways or processes, and many of the red module genes are poorly characterized expressed sequence tags (ESTs). However, genes of the red module had relatively high connectivity scores (k. in.), indicating that this group of genes was quite tightly co-regulated (Figure 5). Observations suggest that groups of poorly characterized genes are likely playing important roles in primordial follicle assembly. Further research is needed to uncover the functions of these genes and their roles in developmental processes such as follicle assembly.

The most highly interconnected (k. in.) genes from each module were compared to databases of genes present in specific cellular pathways and processes. This group of highly interconnected genes was found to be over-represented in the processes of apoptosis, cell migration, cell differentiation and cell proliferation (Figure 8). This is consistent with the activities that occur during follicle assembly and supports the idea that these highly interconnected genes contribute to follicle assembly. Genes were also over-represented in the process of vascularization which is not known to be a part of follicle assembly. Investigations into the role vascularization plays in follicle assembly are suggested in future studies.

Analysis of a specific gene sub-network of differentially expressed genes in the growth factor, hormone and

receptor functional gene categories identified a large number of such regulatory signaling factors that appear to regulate ovarian primordial follicle assembly (Figure 9). Many of these growth factors and receptors in this sub-network have multiple connections with each other, indicating that these genes are known to regulate other signaling factors within the sub-network. The growth factors IL1B, IGF1 and CXCL10, and the receptor CXCR4 have the most connections to other genes, so these are candidates in the regulation of follicle assembly to investigate in future studies. The CXCR4 and IGF1 genes have been shown to be involved in primordial follicle transition [47,48], but not previously been associated with assembly.

Primordial follicle assembly modulation and pathway validation

Analyses of the differentially expressed genes of the current study implicate specific physiological pathways and gene networks as being important to the follicle assembly process. In order to test the validity of some of these predictions, organ culture experiments were preformed in which neonatal rat ovaries were treated with BCI. BCI has the effect of increasing ERK1/2 (MAPK1) activity *via* inhibition of DUSP6 [38,39]. ERK1/2 plays a prominent role in the MAPK signaling, focal adhesion and chemokine signaling pathways, all of which were implicated as important to follicle assembly (Figure 4, Additional file 3: Table S2, Table 1). BCI-treated ovaries with increased ERK1/2 activity were shown to have an increase in assembled follicles (Figure 10), supporting the predicted role of these physiological pathways in primordial follicle assembly. This experiment helps validate the systems biology approach used in the current study.

Primordial follicle assembly and ovarian disease

Since follicle assembly provides each female mammal with the pool of primordial follicles from which their ovulated eggs are derived, abnormal follicle assembly could result in defective primordial follicles that may lead to a reduced follicle pool size. This in turn can lead to infertility and the cessation of reproduction early in life, as is seen in women with primary ovarian insufficiency (POI). Women with POI deplete their pool of primordial follicles prior to age 40 and undergo early menopause [14,15]. Forty-nine genes that have been implicated in POI in humans have been compiled and are listed with the Ovarian Kaleidoscope Database (http://ovary.stanford.edu/). Seven of these genes were found to be in common with the 1081 differentially expressed genes found in the current study to be associated with follicle assembly (significant at $p<0.05$ by Fisher's Exact test). These genes were *Tgfbr3* (transforming growth factor beta receptor type 3), *Amhr2* (anti-Müllerian hormone receptor type 2), *Pgrmc1* (progesterone receptor membrane component 1), *Nupr1* (nuclear protein transcriptional regulator 1), *Pof1b* (premature ovarian failure 1b), IGF1 and AFF2 (AF4/FMR2 family, member 20). AMH, progesterone and *Pgrmc1* are known to play roles in follicle assembly [1,17,18,22,23]. It is notable that *Pof1b*, the gene named for its association with premature ovarian failure (i.e. POI), is linked to follicle assembly in the current study. These observations suggest that some cases of POI may have abnormal follicle assembly as an underlying cause. In addition to specific gene links with POI, a number of links were also made to polycystic ovarian syndrome (PCOS) (Figure *11*). PCOS is the most predominant female reproductive disease affecting 7-18% of the female population [49]. A number of the differentially expressed genes identified in the current study correlated to previously known genes linked to PCOS (Figure *11*). Observations suggest abnormal ovarian primordial follicle assembly may be a component of POI and PCOS later in life as some of the genes involved are in common. Future analysis of these genes and the gene networks identified is anticipated to help elucidate the molecular etiology of POI and PCOS, as well as provide novel therapeutic targets.

Conclusions

In summary, a systems biology experimental approach can provide an unbiased global view of the relationships important to a particular developmental process. For the primordial follicle assembly process the systems approach evaluated genes that were differentially expressed in response to growth factor and hormone treatments. It was found that different treatments all affected similar cellular pathways and processes, but that each treatment affected expression of different genes within those pathways. Cluster analyses identified modules of coordinately regulated genes and the different modules appear to accomplish distinct cellular functions during follicle assembly. The regulatory gene networks identified provide predictions about important regulatory genes, signaling pathways and cellular processes involved in ovarian primordial follicle assembly. An organ culture experiment in which ovaries were treated to increase ERK1/2 activity confirmed some of the predicted physiological pathways were in fact important in follicle assembly regulation. The regulatory genes and gene networks identified as controlling primordial follicle assembly, when disrupted or altered, were suggested to be linked to the etiology of ovarian diseases such as primary ovarian insufficiency POI and polycystic ovarian syndrome PCOS. Future investigations can now utilize the observations from this systems approach to further elucidate the molecular control of ovarian primordial follicle development and associated diseases.

Methods

Ovarian organ culture

Zero-day old female Sprague–Dawley rats (Harlan Laboratories, Inc., USA) were euthanized within six hours after birth according to Washington State University IACUC approved (#02568) protocols and the ovaries removed and cultured whole as described previously [50]. Zero-day old rat ovaries contain primarily oocytes in nests, prior to being assembled into follicles. For ovary culture experiments in which ovarian RNA was collected, 2–3 ovaries per well were cultured for one day in the absence (controls) or presence (treated) of either AMH (human Anti-Müllerian hormone)(50 ng/ml, R&D Systems Inc., USA), FGF2 (rat Fibroblast growth factor 2)(50 ng/ml, R&D Systems Inc., USA), CTGF (human Connective Tissue Growth Factor)(500 ng/ml, PeproTech Inc., NJ USA), TNFa (rat Tumor Necrosis Factor alpha)(1ng/ml, R&D Systems Inc., USA), activin A (human/mouse/rat activin beta-A homodimer)(100 ng/ml, R&D Systems Inc., USA), E2 (Estradiol)(1×10^{-6}M, Sigma-Aldrich, USA), or P4 (Progesterone)(1×10^{-6}M, Sigma-Aldrich, USA). After only one day of culture there are few morphological differences between control and treated ovaries, so measurements of whole-ovary gene expression reflect differences in RNA transcription, rather than differing proportions of cell types due to differing cell proliferation between treatments. After culture the 2–3 ovaries receiving the same treatment from one culture well were pooled and homogenized in one ml Trizol™ reagent (Sigma-Aldrich, USA), then stored at −70°C. There were three different biological experiments (biological replicates) for each of the seven treatment compounds, and seven replicates of the controls, for a total of 28 RNA samples.

In order to determine the effect of FGF2 on primordial follicle assembly, ovaries were cultured as above for two days in the absence or presence of FGF2 (50 ng/ml). Similarly, in order to determine the effect of increased ERK1/2 signaling on follicle assembly, ovaries were cultured in the presence or absence of BCI (1μM; Sigma-Aldrich #B4313). After 2 days culture ovaries were fixed with Bouin's solution, paraffin embedded, sectioned onto microscope slides and stained with hematoxylin and eosin as described previously [50].

Morphometric analysis

The number of oocytes at each developmental stage was counted and averaged in two serial sections from the largest cross-section through the center of the ovary. Oocytes in ovarian cross sections were classified as unassembled, or as assembled into primordial (stage 0), or developing follicles (stages 1–4: early primary, primary, transitional and preantral) as previously described [1,51]. Oocytes in nests are contiguous with other oocytes, without intervening stromal cells. An oocyte was still considered to be part of a nest if, for any region of its perimeter, one quarter of its circumference or more was contiguous with other oocytes. Primordial follicles consist of an oocyte arrested in prophase I of meiosis that is encapsulated by squamous (i.e. flattened) pregranulosa cells. Early transition primary follicles have initiated development (i.e., undergone primordial to primary follicle transition) and contain at least two cuboidal granulosa cells. Primary and preantral follicles exhibit one or more complete layers of cuboidal granulosa cells [30,52]. Hematoxylin/eosin stained ovarian sections were analyzed at 400× magnification using light microscopy. Degenerating red eosin-stained oocytes were not counted. Oocytes in which the cell nucleus was not clearly visible in the plane of section were not counted.

RNA preparation

RNA was isolated from whole rat ovaries after homogenization in one ml Trizol™ reagent (Sigma-Aldrich, USA), according to manufacturer's instructions. Two or three ovaries from the same culture well (from different rat pups) and receiving the same treatment were pooled and homogenized together. Homogenized samples were stored at −70°C until the time of RNA isolation. After isolation from Trizol, RNA was further purified using RNeasy MinElute Cleanup Kits (Qiagen, USA) and stored in aqueous solution at −70°C.

Microarray analysis

The microarray analysis was performed by the Genomics Core Laboratory, Center for Reproductive Biology, Washington State University, Pullman, WA using standard Affymetrix reagents and protocol. Briefly, mRNA was transcribed into cDNA with random primers, cRNA was transcribed, and single-stranded sense DNA was synthesized which was fragmented and labeled with biotin. Biotin-labeled ssDNA was then hybridized to the Rat Gene 1.0 ST microarrays containing 27,342 transcripts (Affymetrix, Santa Clara, CA, USA). Hybridized chips were scanned on Affymetrix Scanner 3000. CEL files containing raw data were then pre-processed and analyzed with Partek Genomic Suite 6.3 software (Partek Incorporated, St. Louis, MO) using an RMA GC-content adjusted algorithm. Comparison of all array histogram graphs demonstrated that the data for 27 of 28 chips were similar and appropriate for further analysis. One chip, from a P4-treated sample, was an outlier and so was discarded (Additional file 1: Figure S1). In addition, a batch effect associated with RNA processing date was noted and incorporated into the analysis. The data from the remaining 27 chips were again pre-processed and analyzed as a group, with the RNA processing batch used as a blocking factor.

The microarray quantitative data involves over 10 different oligonucleotides arrayed for each gene and the hybridization must be consistent to allow for a statistically significant quantitative measure of gene expression and regulation. In contrast, a quantitative PCR procedure only uses two oligonucleotide primers, and primer bias is a major factor in this type of analysis. Therefore, we did not attempt to use PCR based approaches as we feel the microarray analysis is more accurate and reproducible without the primer bias of PCR based approaches.

All microarray CEL files (MIAME compliant raw data) from this study have been deposited with the NCBI gene expression and hybridization array data repository (GEO, http://www.ncbi.nlm.nih.gov/geo) (GEO Accession number: Pending), all arrays combined with one accession number, and can be also accessed through www.skinner.wsu.edu. For gene annotation, Affymetrix annotation file RaGene-1_0-st-v1.na32.rn4.transcript.csv was used unless otherwise specified.

Gene bionetwork analysis

The cluster coordinated expression analysis was restricted to genes differentially expressed between the control and the treatment groups based on previously established criteria: (1) fold change of group means ≥1.2 or ≤0.83; (2) *T* test p-value ≤0.05 compared to control; and (3) absolute difference of group means ≥10. The less stringent cutoff for fold change avoids loss of important genes at such an early stage of analysis since these candidate genes will go through subsequent systems-level coexpression network and pathway analyses that can further filter noisy signal, as we have shown in the previous study [53]. The union of the differentially expressed genes from the different treatments resulted in 1081 genes (i.e. Affymetrix probesets) being identified and used for constructing a weighted gene co-expression network [32,44]. Unlike traditional un-weighted gene co-expression networks in which two genes (nodes) are either connected or disconnected, the weighted gene co-expression analysis assigns a connection weight to each gene pair using soft-thresholding and thus is robust to parameter selection. The weighted network analysis begins with a matrix of the Pearson correlations between all gene pairs, then converts the correlation matrix into an adjacency matrix using a power function $f(x) = x^{\beta}$. The parameter β of the power function is determined in such a way that the resulting adjacency matrix (i.e., the weighted co-expression network), is approximately scale-free. To measure how well a network satisfies a scale-free topology, we use the fitting index proposed by Zhang & Horvath [32] (i.e., the model fitting index R^2 of the linear model that regresses $log(p(k))$ on $log(k)$ where k is connectivity and $p(k)$ is the frequency distribution of connectivity). The fitting index of a perfect scale-free network is 1. For this dataset, we select the smallest β (= 7) which leads to an approximately scale-free network with the truncated scale-free fitting index R^2 greater than 0.75. The distribution $p(k)$ of the resulting network approximates a power law: $p(k) \sim k^{-1.29}$.

To explore the modular structures of the co-expression network, the adjacency matrix is further transformed into a topological overlap matrix [37]. The topological overlap between two genes reflects not only their direct interaction, but also their indirect interactions through all the other genes in the network. Previous studies [32,37] have shown that topological overlap leads to more cohesive and biologically meaningful modules. To identify modules of highly co-regulated genes, we used average linkage hierarchical clustering to group genes based on the topological overlap of their connectivity, followed by a dynamic cut-tree algorithm to dynamically cut clustering dendrogram branches into gene modules [54]. A total of nine modules were identified and the module size was observed to range from 20 to 240 genes.

To distinguish between modules, each module was assigned a unique color identifier, with the remaining, poorly connected genes colored grey. In this type of map, the rows and the columns represent genes in a symmetric fashion, and the color intensity represents the interaction strength between genes (Figure 5). This connectivity map highlights the fact that differentially expressed genes fall into distinct network modules, where genes within a given module are more interconnected with each other (blocks along the diagonal of the matrix) than with genes in other modules. There are several network connectivity measures, but one particularly important one is the within module connectivity (k.in). The k.in of a gene was determined by taking the sum of its connection strengths (co-expression similarity) with all other genes in the module to which the gene belonged.

In order to compile a shorter list of the most tightly co-regulated genes from each module, the top 10% of genes from each module with highest k.in. scores (connectivity within module) were selected. Additional genes were added from each module, above 10%, if those genes had k. in. scores >8. If the list for any module did not include enough named genes (i.e. genes that were not EST's) to equal 10% of the module size, then additional genes with the highest k.in. scores were added until 10% named genes was achieved.

Pathway analysis

Lists of differentially expressed genes for each regulatory factor treatment, as well as for each module generated in the network analysis, were analyzed for KEGG (Kyoto Encyclopedia for Genes and Genome, Kyoto University, Japan) pathway enrichment using Pathway-Express, a web-based tool freely available as part of the Onto-Tools

(http://vortex.cs.wayne.edu) [55]. Additionally, gene lists were analyzed using the KEGG website (http://www.genome.jp/kegg/pathway.html). KEGG pathways were considered 'impacted' and were included in analyses for this manuscript if three or more differentially expressed genes were present within a KEGG pathway. Statistical over-representation of differentially expressed genes within a pathway was determined by Fischer's exact test for two by two contingency tables, and by calculating hypergeometric probability of obtaining exactly the listed number of genes in common with that pathway.

Global literature analysis of various gene lists was performed using Pathway Studio (Ariadne, Genomics Inc. Rockville MD) software, which performs pathway and interaction analysis and identifies genes that have regulatory or binding relationships. Pathway Studio was also used to identify cellular functions and diseases (including polycystic ovarian syndrome) linked in the published literature to the genes in these lists. In addition, Pathway Studio was used to determine over-represented physiological processes for gene lists based on KEGG, PANTHER (Protein ANalysis THrough Evolutionary Relationships) and NCBI GO (National Center for Biotechnology Information Gene Ontology) databases.

Additional files

Additional file 1: Figure S1. Sample histograms and box plots for ovary RNA sample microarray signal values prior to pre-processing and normalization. Note that one of the P4-treated samples was an outlier, and was discarded. X-axis shows hybridization intensity value. Y-axis (Hybridization Frequency) shows the number of genes having a given hybridization intensity.

Additional file 2: Table S1. Differentially expressed genes: A) Genes influenced by treatment with anti-Müllerian hormone (AMH). B) Genes influenced by treatment with CTGF. C) Genes influenced by treatment with FGF2. D) Genes influenced by treatment with ActivinA. E) Genes influenced by treatment with P4. F) Genes influenced by treatment with TNFa. G) Genes influenced by treatment with E2.

Additional file 3: Table S2. Treatment and module differentially expressed genes correlated to cellular pathways and processes.

Additional file 4: Figure S2. Gene network of known relationships among all 1081 genes found to be differentially expressed in treated *versus* Control ovaries. Genes with the greatest number of connections (relationships) to other genes have enlarged gene symbols. Network is derived from an un-biased search of literature using Pathway Studio™. Node shapes code: oval – protein; diamond – ligand; irregular polygon – phosphatase; circle/oval on tripod platform – transcription factor; ice cream cone – receptor. Grey arrows represent regulation, lilac – expression, green – promoter binding, olive – protein modification, purple - binding.

Additional file 5: Figure S3. Gene network of known relationships among differentially expressed genes assigned to specific co-expression modules. A) Blue module. B) Black module. Network is derived from an un-biased search of literature using Pathway Studio™. Node shapes code: oval – protein; diamond – ligand; irregular polygon – phosphatase; circle/oval on tripod platform – transcription factor; ice cream cone – receptor. Grey arrows represent regulation, lilac – expression, green – promoter binding, olive – protein modification, purple - binding.

Additional file 6: Figure S4. Gene network of known relationships among genes differentially expressed in ovaries receiving specific treatments, compared to controls. A) E2 (estrogen). B) FGF2. C) Activin A. Network is derived from an un-biased search of literature using Pathway Studio™. Node shapes code: oval – protein; diamond – ligand; irregular polygon – phosphatase; circle/oval on tripod platform – transcription factor; ice cream cone – receptor. Grey arrows represent regulation, lilac – expression, green – promoter binding, olive – protein modification, purple - binding.

Abbreviations

POI: Primary ovarian insufficiency; PCOS: Polycystic ovarian disease syndrome; AMH: Anti-Müllerian hormone; CTGF: Connective tissue growth factor; E2: Estradiol; P4: Progesterone; TNFa: Tumor necrosis factor alpha; BDNF: Brain derived neurotrophic factor; KITL: Kit ligand; GDF9: Growth differentiation factor-9; FGF2: Fibroblast growth factor-2; k.in.: Connectivity index.

Competing interest

The authors declare that no competing interests exist.

Authors' contribution

MKS designed the study. EN performed the ovary cultures and microarray analysis and network design. BZ performed the bionetwork analysis and bioinformatics. EN wrote the manuscript and all authors edited the manuscript. All authors read and approved the final manuscript.

Acknowledgements

We thank the expert technical assistance of Ms. Rebecca Tracey, Ms. Renee Espinosa Najera, Ms. Jessica Shiflett, Ms. Chrystal Bailey, Ms. Colleen Johns, and Mr. Md. Haque. We thank Ms. Heather Johnson for assistance in preparation of the manuscript.

Financial disclosure

This study was supported by a grant from the NIH, NIEHS to MKS.
The funders had no role in study design, data collection and analysis, decision to publish, or preparation of the manuscript.

Author details

[1]Center for Reproductive Biology, School of Biological Sciences, Washington State University, Pullman, WA 99164-4236, USA. [2]Department of Genetics & Genomic Sciences, Mount Sinai School of Medicine, New York, NY, USA.

Received: 4 February 2013 Accepted: 4 July 2013
Published: 23 July 2013

References

1. Nilsson EE, Schindler R, Savenkova MI, Skinner MK: **Inhibitory actions of Anti-Mullerian Hormone (AMH) on ovarian primordial follicle assembly.** *PLoS One* 2011, **6**(5):e20087.
2. Hirshfield AN: **Development of follicles in the mammalian ovary.** *Int Rev Cytol* 1991, **124:**43–101.
3. Skinner MK: **Regulation of primordial follicle assembly and development.** *Hum Reprod Update* 2005, **11**(5):461–471.
4. Rajah R, Glaser EM, Hirshfield AN: **The changing architecture of the neonatal rat ovary during histogenesis.** *Dev Dyn* 1992, **194**(3):177–192.
5. Sarraj MA, Drummond AE: **Mammalian foetal ovarian development: consequences for health and disease.** *Reproduction* 2012, **143**(2):151–163.
6. Pepling ME: **Follicular assembly: mechanisms of action.** *Reproduction* 2012, **143**(2):139–149.
7. Richards JS, Pangas SA: **The ovary: basic biology and clinical implications.** *J Clin Invest* 2010, **120**(4):963–972.
8. Pepling ME, Spradling AC: **Female mouse germ cells form synchronously dividing cysts.** *Development* 1998, **125**(17):3323–3328.
9. Gondos B: **Germ cell degeneration and intercellular bridges in the human fetal ovary.** *Z Zellforsch Mikrosk Anat* 1973, **138**(1):23–30.
10. Byskov AG: **Differentiation of mammalian embryonic gonad.** *Physiol Rev* 1986, **66**(1):71–117.
11. Borum K: **Oogenesis in the mouse. A study of the meiotic prophase.** *Exp Cell Res* 1961, **24:**495–507.

12. McGee EA, Hsu SY, Kaipia A, Hsueh AJ: **Cell death and survival during ovarian follicle development.** *Mol Cell Endocrinol* 1998, **140**(1–2):15–18.
13. Pepling ME, Sundman EA, Patterson NL, Gephardt GW, Medico L Jr, Wilson KI: **Differences in oocyte development and estradiol sensitivity among mouse strains.** *Reproduction* 2010, **139**(2):349–357.
14. De Vos M, Devroey P, Fauser BC: **Primary ovarian insufficiency.** *Lancet* 2010, **376**(9744):911–921.
15. Maclaran K, Panay N: **Premature ovarian failure.** *J Fam Plann Reprod Health Care* 2011, **37**(1):35–42.
16. Schindler R, Nilsson E, Skinner MK: **Induction of ovarian primordial follicle assembly by connective tissue growth factor CTGF.** *PLoS One* 2010, **5**(9):e12979.
17. Chen Y, Jefferson WN, Newbold RR, Padilla-Banks E, Pepling ME: **Estradiol, progesterone, and genistein inhibit oocyte nest breakdown and primordial follicle assembly in the neonatal mouse ovary in vitro and in vivo.** *Endocrinology* 2007, **148**(8):3580–3590.
18. Yang MY, Fortune JE: **The capacity of primordial follicles in fetal bovine ovaries to initiate growth in vitro develops during mid-gestation and is associated with meiotic arrest of oocytes.** *Biol Reprod* 2008, **78**(6):1153–1161.
19. Wang C, Roy SK: **Development of primordial follicles in the hamster: role of estradiol-17beta.** *Endocrinology* 2007, **148**(4):1707–1716.
20. Zachos NC, Billiar RB, Albrecht ED, Pepe GJ: **Developmental regulation of baboon fetal ovarian maturation by estrogen.** *Biol Reprod* 2002, **67**(4):1148–1156.
21. Bristol-Gould SK, Kreeger PK, Selkirk CG, Kilen SM, Cook RW, Kipp JL, Shea LD, Mayo KE, Woodruff TK: **Postnatal regulation of germ cells by activin: the establishment of the initial follicle pool.** *Dev Biol* 2006, **298**(1):132–148.
22. Nilsson EE, Skinner MK: **Progesterone regulation of primordial follicle assembly in bovine fetal ovaries.** *Mol Cell Endocrinol* 2009, **313**(1–2):9–16.
23. Nilsson EE, Stanfield J, Skinner MK: **Interactions between progesterone and tumor necrosis factor-alpha in the regulation of primordial follicle assembly.** *Reproduction* 2006, **132**(6):877–886.
24. Marcinkiewicz JL, Balchak SK, Morrison LJ: **The involvement of tumor necrosis factor-alpha (TNF) as an intraovarian regulator of oocyte apoptosis in the neonatal rat.** *Front Biosci* 2002, **7**:d1997–d2005.
25. Morrison LJ, Marcinkiewicz JL: **Tumor necrosis factor alpha enhances oocyte/follicle apoptosis in the neonatal rat ovary.** *Biol Reprod* 2002, **66**(2):450–457.
26. Trombly DJ, Woodruff TK, Mayo KE: **Suppression of Notch signaling in the neonatal mouse ovary decreases primordial follicle formation.** *Endocrinology* 2009, **150**(2):1014–1024.
27. Spears N, Molinek MD, Robinson LL, Fulton N, Cameron H, Shimoda K, Telfer EE, Anderson RA, Price DJ: **The role of neurotrophin receptors in female germ-cell survival in mouse and human.** *Development* 2003, **130**(22):5481–5491.
28. Kerr B, Garcia-Rudaz C, Dorfman M, Paredes A, Ojeda SR: **NTRK1 and NTRK2 receptors facilitate follicle assembly and early follicular development in the mouse ovary.** *Reproduction* 2009, **138**(1):131–140.
29. Wang J, Roy SK: **Growth differentiation factor-9 and stem cell factor promote primordial follicle formation in the hamster: modulation by follicle-stimulating hormone.** *Biol Reprod* 2004, **70**(3):577–585.
30. Kezele PR, Ague JM, Nilsson E, Skinner MK: **Alterations in the ovarian transcriptome during primordial follicle assembly and development.** *Biol Reprod* 2005, **72**(1):241–255.
31. Nilsson EE, Savenkova MI, Schindler R, Zhang B, Schadt EE, Skinner MK: **Gene bionetwork analysis of ovarian primordial follicle development.** *PLoS One* 2010, **5**(7):e11637.
32. Zhang B, Horvath S: **A general framework for weighted gene co-expression network analysis.** *Stat Appl Genet Mol Biol* 2005, **4**:17.
33. Lum PY, Chen Y, Zhu J, Lamb J, Melmed S, Wang S, Drake TA, Lusis AJ, Schadt EE: **Elucidating the murine brain transcriptional network in a segregating mouse population to identify core functional modules for obesity and diabetes.** *J Neurochem* 2006, **97**(Suppl 1):50–62.
34. Millstein J, Winrow CJ, Kasarskis A, Owens JR, Zhou L, Summa KC, Fitzpatrick K, Zhang B, Vitaterna MH, Schadt EE, *et al*: **Identification of causal genes, networks, and transcriptional regulators of REM sleep and wake.** *Sleep* 2011, **34**(11):1469–1477.
35. Wang IM, Zhang B, Yang X, Zhu J, Stepaniants S, Zhang C, Meng Q, Peters M, He Y, Ni C, *et al*: **Systems analysis of eleven rodent disease models reveals an inflammatome signature and key drivers.** *Mol Syst Biol* 2012, **8**:594.
36. Schadt EE, Lamb J, Yang X, Zhu J, Edwards S, Guhathakurta D, Sieberts SK, Monks S, Reitman M, Zhang C, *et al*: **An integrative genomics approach to infer causal associations between gene expression and disease.** *Nat Genet* 2005, **37**(7):710–717.
37. Ravasz E, Somera AL, Mongru DA, Oltvai ZN, Barabasi AL: **Hierarchical organization of modularity in metabolic networks.** *Science* 2002, **297**(5586):1551–1555.
38. Arkell RS, Dickinson RJ, Squires M, Hayat S, Keyse SM, Cook SJ: **DUSP6/MKP-3 inactivates ERK1/2 but fails to bind and inactivate ERK5.** *Cell Signal* 2008, **20**(5):836–843.
39. Molina G, Vogt A, Bakan A, Dai W, de Queiroz Oliveira P, Znosko W, Smithgall TE, Bahar I, Lazo JS, Day BW, *et al*: **Zebrafish chemical screening reveals an inhibitor of Dusp6 that expands cardiac cell lineages.** *Nat Chem Biol* 2009, **5**(9):680–687.
40. Li G, Yu M, Lee WW, Tsang M, Krishnan E, Weyand CM, Goronzy JJ: **Decline in miR-181a expression with age impairs T cell receptor sensitivity by increasing DUSP6 activity.** *Nat Med* 2012, **18**(10):1518–1524.
41. Nilsson E, Rogers N, Skinner MK: **Actions of anti-Mullerian hormone on the ovarian transcriptome to inhibit primordial to primary follicle transition.** *Reproduction* 2007, **134**(2):209–221.
42. MacFarlane LA, Murphy PR: **Regulation of FGF-2 by an endogenous antisense RNA: effects on cell adhesion and cell-cycle progression.** *Mol Carcinog* 2010, **49**(12):1031–1044.
43. Yang D, Li Y, Xiao H, Liu Q, Zhang M, Zhu J, Ma W, Yao C, Wang J, Wang D, *et al*: **Gaining confidence in biological interpretation of the microarray data: the functional consistence of the significant GO categories.** *Bioinformatics* 2008, **24**(2):265–271.
44. Zhu J, Wiener MC, Zhang C, Fridman A, Minch E, Lum PY, Sachs JR, Schadt EE: **Increasing the power to detect causal associations by combining genotypic and expression data in segregating populations.** *PLoS Comput Biol* 2007, **3**(4):e69.
45. Gargalovic PS, Imura M, Zhang B, Gharavi NM, Clark MJ, Pagnon J, Yang WP, He A, Truong A, Patel S, *et al*: **Identification of inflammatory gene modules based on variations of human endothelial cell responses to oxidized lipids.** *Proc Natl Acad Sci U S A* 2006, **103**(34):12741–12746.
46. Horvath S, Zhang B, Carlson M, Lu KV, Zhu S, Felciano RM, Laurance MF, Zhao W, Qi S, Chen Z, *et al*: **Analysis of oncogenic signaling networks in glioblastoma identifies ASPM as a molecular target.** *Proc Natl Acad Sci U S A* 2006, **103**(46):17402–17407.
47. Holt JE, Jackson A, Roman SD, Aitken RJ, Koopman P, McLaughlin EA: **CXCR4/SDF1 interaction inhibits the primordial to primary follicle transition in the neonatal mouse ovary.** *Dev Biol* 2006, **293**(2):449–460.
48. Slot KA, Kastelijn J, Bachelot A, Kelly PA, Binart N, Teerds KJ: **Reduced recruitment and survival of primordial and growing follicles in GH receptor-deficient mice.** *Reproduction* 2006, **131**(3):525–532.
49. Dunaif A: **Polycystic ovary syndrome in 2011: Genes, aging and sleep apnea in polycystic ovary syndrome.** *Nat Rev Endocrinol* 2012, **8**(2):72–74.
50. Dole G, Nilsson EE, Skinner MK: **Glial-derived neurotrophic factor promotes ovarian primordial follicle development and cell-cell interactions during folliculogenesis.** *Reproduction* 2008, **135**(5):671–682.
51. Oktay K, Schenken RS, Nelson JF: **Proliferating cell nuclear antigen marks the initiation of follicular growth in the rat.** *Biol Reprod* 1995, **53**(2):295–301.
52. Parrott JA, Skinner MK: **Kit-ligand/stem cell factor induces primordial follicle development and initiates folliculogenesis.** *Endocrinology* 1999, **140**(9):4262–4271.
53. Skinner MK, Manikkam M, Haque MM, Zhang B, Savenkova M: **Epigenetic Transgenerational Inheritance of Somatic Transcriptomes and Epigenetic Control Regions.** *Genome Biol* 2012, **13**(10):R91.
54. Langfelder P, Horvath S: **Eigengene networks for studying the relationships between co-expression modules.** *BMC Syst Biol* 2007, **1**:54.
55. Draghici S, Khatri P, Tarca AL, Amin K, Done A, Voichita C, Georgescu C, Romero R: **A systems biology approach for pathway level analysis.** *Genome Res* 2007, **17**(10):1537–1545.

doi:10.1186/1471-2164-14-496
Cite this article as: Nilsson *et al.*: Gene bionetworks that regulate ovarian primordial follicle assembly. *BMC Genomics* 2013 **14**:496.